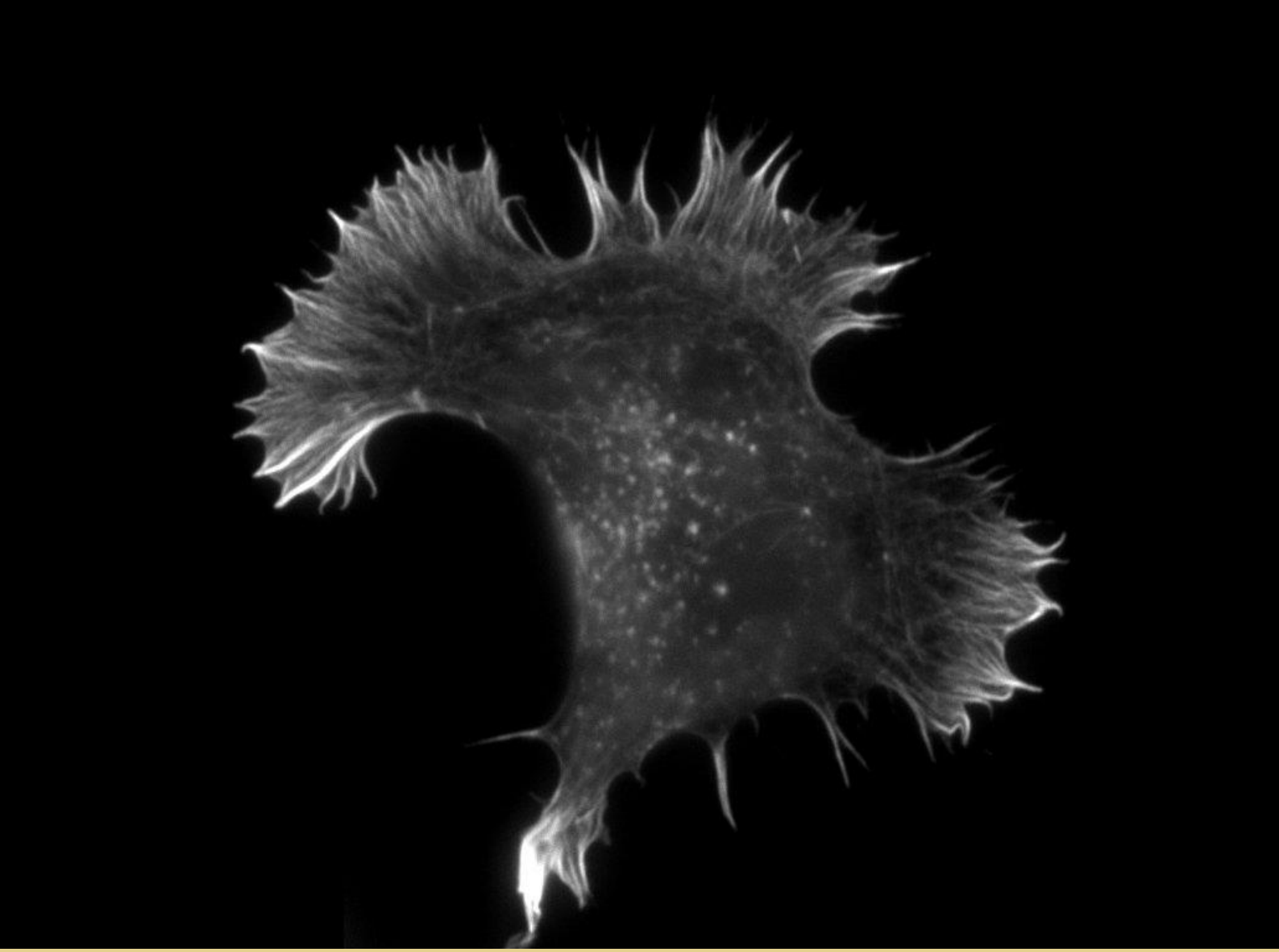

Laura Nunes Soares Sequeira Salavessa

Endocytic trafficking mechanisms in Alzheimer's disease: role of the actin regulators Bin1 and CD2AP

Tese de Mestrado em Investigação Biomédica

Junho/2015

· U C ·

UNIVERSIDADE DE COIMBRA

Laura Nunes Soares Sequeira Salavessa

Endocytic trafficking mechanisms in Alzheimer's disease: role of the actin regulators Bin1 and CD2AP.

Dissertação de mestrado em Investigação Biomédica, orientada por Cláudia G. Almeida e co-orientada por Cláudia Fragão Pereira, e apresentada à Faculdade de Medicina da Universidade de Coimbra para obtenção do grau de Mestre.

Junho, 2015

UNIVERSIDADE DE COIMBRA

O trabalho apresentado nesta dissertação foi realizado no Centro de Estudos de Doenças Crónicas (CEDOC), da Faculdade de Medicina da Universidade Nova de Lisboa, Portugal.

Para os meus pais
que lutaram tanto por isto quanto eu.

Acknowledgments

Este trabalho não seria possível de concretizar sem a ajuda de uma série de pessoas que, de uma maneira ou de outra, contribuíram para o trabalho em si ou para a minha motivação ao longo do mesmo.

Cláudia, não sei como agradecer toda a ajuda e motivação que me deste ao longo deste ano. Numa das muitas boleias que me deste de Oeiras para Lisboa disseste-me que, para ti, ser orientadora era um pouco como ser mãe. Obrigada pela especial preocupação que tens com as pessoas no laboratório, pelo teu entusiasmo constante pelo trabalho e por quereres sempre transmitir esse entusiasmo a quem te rodeia. Foram inúmeras as vezes que fui ter contigo com mais uma das minhas (muitas) experiências falhadas, e tu conseguias sempre encontrar alguma coisa positiva para me animar e manter motivada. Obrigada por toda a paciência, pelo conhecimento, pelo espírito crítico, e por toda a confiança que me deste e que, no meio das minhas muitas incertezas, me fez considerar o meu futuro como investigadora.

Florent, thank you for everything you have taught me. You are an amazing scientist, I could hardly find someone so passionate about science like you. I wish to have that passion, someday. I'm sure you will have a brilliant future ahead. Thank you for your patient with me, for not just answering the endless questions I asked you but for motivating me to find the answer by myself. I still think it is because of you that I ended up doing my masters with Cláudia, it was you that convinced her to let me stay. Obrigado por tudo, por toda a simpatia desde o primeiro dia em que me levaste ao CEDOC e me apresentaste a toda as pessoas que passaram por nós. (I think, after all the times I helped you with your homework, your portuguese should be good enough to understand that… let's see.)

Tatiana, podia escrever páginas e páginas para agradecer todas as coisas nas quais me ajudaste. Foste uma companhia fantástica durante este ano, mais do que uma colega de laboratório, foste uma grande amiga. Obrigada por toda a ajuda que me deste, especialmente nesta última fase do trabalho, por partilhares o meu stress e por tentares sempre manter-me calma. Tenho a certeza que vais ter mais sucesso nesta área do que aquilo que julgas, acredita em mim.

Obrigada também ao Ricardo, ao Cláudio, à Francisca, à Ana (com as suas visitas de médico), apesar do pouco tempo que passei com a maior parte deles, todos contribuíram de alguma forma para o meu trabalho e, claro, para uma vivência fantástica no lab.

Um obrigada à Cláudia Pereira e ao Henrique Girão por estarem sempre dispostos a ajudar no que for preciso.

Um grande obrigada à Covilhã e aos amigos eternos que, mesmo estando longe, estão sempre comigo. Em especial a ti, Festas, obrigada por todas as vezes que me foste "salvar" à biblioteca do IGC para mais uma partilha de m&m's.

Obrigada a Coimbra, à Ana, à Filipa, à Ritinha, à Rita Gouveia e ao Rafa, por toda a felicidade nas tardes de finos no café e por partilharem comigo toda a angústia deste último mês e ainda assim me fazerem rir. São o melhor que levo de Coimbra.

Aos meus putos em casa, João e David, obrigada pela vossa boa disposição sempre que entro em casa cansada depois de mais um dia. Serão sempre os de sempre, para sempre.

Aos meus pais (e à Indy, é claro!), nunca será possível agradecer o apoio incondicional em tudo aquilo que eu faço, mesmo que isso implique um esforço enorme para vocês. E ao meu irmão, obrigada por me ligares todos os fins-de-semana em que estive fechada em casa a escrever só para me dizeres que estavas na praia.

Por fim, ao Rufo, obrigada por ouvires todas as minhas birras quando estou em pânico (e quando não estou…), e ainda assim, depois de tantas vezes, me dizeres sempre "vai correr tudo bem, tu consegues".

Index

Index of Figures

Index of Tables

Abbreviations

3xTg-AD	Triple transgenic AD mouse model
αCTF	α-cleaved C-terminal fragment
βCTF	β-cleaved C-terminal fragment
Aβ	Amyloid β
$Aβ_{40}$	Amyloid β (40 amino acids)
$Aβ_{42}$	Amyloid β (42 amino acids)
AD	Alzheimer's disease
ADF	Actin depolymerizing factor
ADP	Adenosine diphosphate
AICD	APP intracellular domain
Amph1	Amphiphysin 1
Amph2	Amphiphysin 2
AnxA2	Annexin A2
AP-2	Adaptor protein-2
APOE	Apolipoprotein E
APP	Amyloid precursor protein
Arp2/3	Actin-related proteins 2/3
ATP	Adenosine triphosphate
BACE1	Beta-site APP-cleavage enzyme 1
BAR	Bin/Amphiphysin/RVS
BIN1	Bridging integrator 1
C83	α-carboxyl-terminal fragment containing 83 amino acids
C99	β-carboxyl-terminal fragment containing 99 amino acids
CD2AP	CD2-associated protein
CIN85	c-Cbl interacting protein of 85 kDa
CMS	Cas ligand with multiple SH3 domains
CP	Capping protein
CytoD	Cytochalasin D
EEA1	Early endosome antigen 1
EOAD	Early-onset Alzheimer's disease
F-actin	Filamentous actin
G-actin	Globular actin
GluR1	Glutamate receptor subunit 1
GWAS	Genome-wide association study
JMY	Junction-mediating and -regulatory protein
LOAD	Late-onset Alzheimer's disease
M6PR	Mannose-6-phosphate receptor
MVBs	Multivesicular bodies
Myo1b	Myosin 1b
NFTs	Neurofibrillary tangles
NPFs	Nucleation promoting factors
N-WASP	Neuronal Wiskott–Aldrich Syndrome protein
PDGF	Platelet-derived growth factor

PM	Plasma membrane
PS-1	Presenilin 1 protein
PSD-95	Postsynaptic density protein 95
PSEN1	Presenilin 1
PSEN2	Presenilin 2
sαAPP	Amyloid precursor protein (soluble α-cleaved fragment)
sβAPP	Amyloid precursor protein (soluble β-cleaved fragment)
SH3	Src homology 3
SNP	Single nucleotide polymorphism
SNX4	Sorting nexin 4
TGN	Trans-Golgi network
VEGF	Vascular endothelial growth factor
WASH	Wiskott–Aldrich syndrome protein and SCAR homologue
WASp	Wiskott–Aldrich Syndrome family of proteins
WASP	Wiskott–Aldrich Syndrome protein
WAVE	WASP-family verprolin homologous protein
WHAMM	WAS protein homolog associated with actin, Golgi membranes and microtubules

Abstract

Alzheimer's disease (AD) is the most common neurodegenerative disorder and, despite the intensive research, there is still no treatment. Excessive neuronal production of beta-amyloid (Aβ) leads to synaptic dysfunction and cognitive impairment. Thus, it is urgent to develop new therapeutic strategies, targeting the mechanisms that initiate Aβ production in late-onset AD, the most prevalent form of the disease.

Several susceptibility gene variants, conferring higher risk for late-onset AD, were identified, among them *CD2AP* and *BIN1*. Whether Bin1 and CD2AP impact Aβ generation and thus increase the risk of developing AD is not known. Bin1 and CD2AP regulate endocytic trafficking and actin dynamics. Aβ is generated in endosomes from the proteolytic cleavage of amyloid precursor protein (APP) by its secretases, mainly BACE1. Thus, Aβ production depends on the endocytic trafficking of APP and BACE1. We previously established that Bin1 and CD2AP loss of function exacerbate Aβ generation in neurons. Our previous results implicate Bin1 in BACE1 recycling, whereas CD2AP appears to regulate multivesicular body (MVB) sorting of APP for degradation.

Actin dynamics' role in AD is not well established. Nevertheless, actin dynamics controls intracellular trafficking mainly by shaping cellular membranes, assisting in membrane invagination for endocytosis and membrane tubulation, in the secretory and endocytic pathway. However it is not known if actin controls Aβ generation. Both Bin1 and CD2AP are implicated in actin remodelling, directly or through actin-regulatory proteins. We hypothesize that Bin1 and CD2AP control Aβ generation by regulation of the actin-dependent endocytic trafficking of APP and BACE1.

Our data supports the role of Bin1 and CD2AP as regulators of actin dynamics. Bin1 and CD2AP appear to regulate the actin pool associated with early endosomes. We explore the mechanisms by which Bin1 and CD2AP may impact the endocytic trafficking of APP and BACE1. Moreover we found that actin depolymerization can increase Aβ levels. We also found CD2AP depletion to affect synapse. However, further investigations are needed to unravel how Bin1 and Cd2ap regulate actin dynamics to control the endocytic trafficking involved in ab generation to contribute to AD development.

Resumo

A doença de Alzheimer (DA) é a causa mais comum de demência para a qual ainda não existe um tratamento efectivo, apesar da investigação intensiva. Na DA, a produção excessiva de beta-amilóide (Aβ), nos neurónios, leva à disfunção sináptica e ao défice cognitivo. Assim, é essencial o desenvolvimento de novas estratégias terapêuticas, tendo como alvo os mecanismos que iniciam a produção de Aβ na DA de início tardio, a forma mais prevalente da doença.

Foram já identificadas diversas variações genéticas associadas à DA de início tardio, que conferem um maior risco de desenvolvimento da doença. Entre esses factores de risco genético encontram-se o *BIN1* e o *CD2AP*. No entanto, não se sabe ainda se o *BIN1* e o *CD2AP* influenciam a produção de Aβ, aumentando o risco de desenvolvimento da DA. O Bin1 e o CD2AP regulam o tráfego endocítico e a dinâmica do citoesqueleto de actina. O Aβ é produzido nos endossomas, através da clivagem proteolítica da proteína precursora de amilóide (APP) pelas suas secretases, principalmente pela BACE1. Assim, a produção de Aβ depende do tráfego endocítico da APP e da BACE1. Anteriormente, estabelecemos que a perda de função do Bin1 e do CD2AP leva a um aumento na produção de Aβ nos neurónios. Os nossos resultados prévios indicam que o Bin1 regula a reciclagem da BACE1 para a membrana plasmática, enquanto o CD2AP parece regular o transporte de APP para os corpos multivesiculares e a sua subsequente degradação.

O papel da dinâmica de actina na DA não está ainda bem estabelecido. No entanto, a dinâmica de actina controla o tráfego intracelular, principalmente através da deformação de membranas celulares, ajudando na invaginação da membrana durante a endocitose e na tubulação da membrana, na via secretora e endocítica. Porém, não se sabe se a actina controla a produção de Aβ. O Bin1 e o CD2AP estão associados à remodelação da actina, directamente ou através da interacção com proteínas reguladoras de actina. A nossa hipótese é que o Bin1 e o CD2AP controlam o tráfego endocítico da APP e da BACE1, através da regulação do citoesqueleto de actina, influenciado assim a produção de Aβ.

Os nossos resultados apoiam a função do Bin1 e do CD2AP como reguladores da dinâmica de actina. O Bin1 e o CD2AP parecem regular a actina associada aos endossomas. Nós explorámos os mecanismos pelos quais o Bin1 e o CD2AP podem afectar o tráfego endocítico da APP e da BACE1. Além disso, descobrimos que a despolimerização do citoesqueleto de actina pode aumentar os níveis de Aβ, e que a perda de função do CD2AP pode afectar as sinapses. No entanto, são necessários estudos adicionais que permitam desvendar como é que o Bin1 e o CD2AP regulam a dinâmica de actina, controlando o tráfego endocítico envolvido na produção de Aβ e contribuindo para o desenvolvimento da DA.

Chapter 1

Introduction

1.1 Alzheimer's disease

1.1.1 Pathogenesis and etiology of the disease

Alzheimer's disease (AD) was first described in 1907 by the German physician Alois Alzheimer [1,2]. It is the most common cause of dementia in the elderly, contributing to 60–70% of cases [3], thus being a major socioeconomic burden as the average life expectancy increases [1,4]. AD is associated with progressive memory impairment and deterioration of general cognitive functions represented by clinical symptoms such as impaired judgment, decision-making and orientation; and, in late stages of the disease, erratic behavioural signs (aggression, psychosis) and loss of motor control[1,4]. The key tombstone hallmarks of AD are aggregates of amyloid beta (Aβ) peptide deposited extracellularly as senile plaques, and intraneuronal neurofibrillary tangles (NFTs) composed of paired helical filaments of hyperphosphorylated tau protein, a microtubule-binding protein. These pathological features are found in the medial temporal lobe and cortical areas of patients' brains, leading to progressive neurodegeneration with sequential loss of spines (post-synaptic compartment), of synapses and neurites, and, ultimately, loss of vulnerable neurons[1,4–6].

According to the age of onset, AD is classified as early-onset or familial AD (EOAD), with onset before 65 years-old and accounting for 1-5% of all cases[5]; and late-onset or sporadic AD (LOAD), with onset after age 65 years and accounting for >95% of patients[1,5]. EOAD is associated with mutations in three genes – amyloid precursor protein (APP), presenilin 1 (PSEN1) and presenilin 2 (PSEN2) – which are all involved in the Aβ generation process[1,5,7]. These mutations lead to increased Aβ production and thus to a more rapid rate of disease progression[1,5]. Importantly, ageing is still the major risk factor for LOAD, most likely due to deficient mechanisms to clear misfolded proteins and repair damaged cells, along with an higher prevalence of other risk factors (obesity, diabetes, hypertension, cerebrovascular diseases, …)[1,5,6].For many years genetic risk factors associated with LOAD accounted only the APOEε4 allele, one isoform of the lipid-binding protein apolipoprotein E (APOE) that acts as a cholesterol transporter in the brain. APOEε4 increases the risk for AD since it has less affinity for Aβ than the other APOE isoforms, making it less efficient in Aβ clearance hence promoting its aggregation. Even though APOEε4 allele represents the major genetic risk factor in LOAD, alone is not sufficient to develop the disease[1,5].

More recently, additional genetic risk factors were identified using large-scale meta-analysis of genome-wide association studies (GWAS) and currently more than twenty susceptibility loci are associated with AD, among them *BIN1* and *CD2AP*[5,8].

Over the last few years there has been considerable progress in the understanding of the disease. However there is still no cure for AD. Initially NFTs and amyloid plaques were the researchers' main focus[4]. Yet genetic studies have highlighted specific mechanistic pathways, from immune response and inflammation to lipid metabolism, intracellular endocytic

trafficking[5,8]. Most of the treatments developed until now focus on the symptomatic effects of advanced AD, slightly attenuating them[1]. Thereby it is crucial to understand the molecular mechanisms that initiate the pathology, and find new drug candidates for the pre-symptomatic disease.

1.1.2 APP processing and Aβ generation: how and where

APP is a type I transmembrane protein with a large N-terminal extracellular tail and with the Aβ domain partly embedded in the membrane[1]. APP can undergo a nonamyloidogenic or an amyloidogenic processing[1,4,7,9]. In the first, APP at the plasma membrane is cleaved within the Aβ domain by α-secretase and releases, to the extracellular space, a large soluble APP fragment (sαAPP) (Fig. 1.1a). The remaining C-terminal fragment (αCTF or C83) is then cleaved by a transmembrane γ-secretase complex, releasing a short peptide – p3[1,4,7], while the remaining APP intracellular domain (AICD) is transported to the nucleus[9,10]. In the amyloidogenic pathway (Fig. 1.1b), APP at the plasma membrane is internalized, by clathrin-mediated endocytosis[4,10], into endosomes where beta-site APP-cleavage enzyme 1 (BACE1, β-secretase) cleaves APP, just before the Aβ domain, and releases a soluble sβAPP (APP N-terminal β-fragment) that is secreted to the extracellular space. The remaining membrane associated βCTF (C99) is cleaved by the γ-secretase complex within the endosomal membrane, producing the Aβ peptide with commonly 40 ($A\beta_{40}$) or 42 ($A\beta_{42}$) amino acid residues[1,4,7,10]. The Aβ peptide can be secreted to the extracellular space or remain in the endosome[9,10].

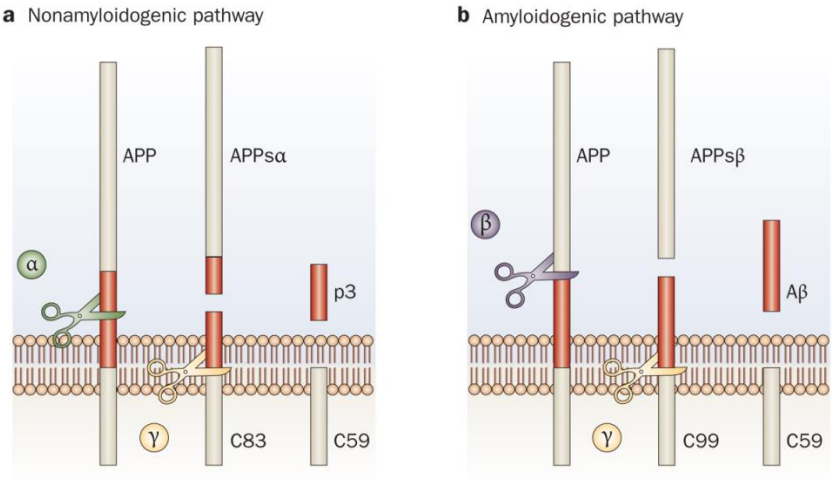

Figure 1.1 Processing of APP through the nonamyloidogenic and amyloidogenic pathway. **(a)** In the nonamyloidogenic pathway, APP at the cell surface is first cleaved by α-secretase, within the Aβ sequence, producing the soluble αAPP ectodomain (sαAPP) and the αC-terminal fragment (αCTF or C83). C83 is subsequently cleaved by γ-secretase producing the p3 fragment and a C-terminal fragment (C59), named APP intracellular domain (AICD). **(b)** In the amyloidogenic pathway, APP is cleaved by β-secretase (BACE1) at the amino terminus and releases sβAPP and the βCTF. Further processing of the βCTF (C99) by γ-secretase results in the production of Aβ and AICD. Aβ vary in length depending on the site of γ-cleavage. *Adapted from D. Strooper et al., 2010.*

APP processing can occur at different sites in the cell, according to which secretase is involved in its cleavage. α-cleavage takes place at the plasma membrane[9], whereas BACE1 activity (β-cleavage) has been predominantly associated with the endosomal compartment, where there is a low pH optimal for its enzymatic activity. γ-secretase has been shown to act in the Golgi, endosomes, and the plasma membrane[9]. Inhibition of APP endocytosis through expression of a mutant dynamin, a protein crucial in clathrin-mediated endocytosis, resulted in increased APP levels at the plasma membrane and in a reduction of Aβ release[11]. Moreover, neurons expressing a mutation in the APP-endocytosis domain show an impaired convergence of APP with BACE1-containing vesicles[12], suggesting that APP endocytosis is required for its β-cleavage.

Consistent with this, $A\beta_{42}$ accumulates specifically in multivesicular bodies (MVBs) of human AD brains, and in neurites and brains of APP mutant transgenic mice[13]. MVBs are compartments formed from early endosomes, hence considered late endosomes with inner vesicles produced by membrane invagination[14]. APP is also mostly observed within the lumen of endosomes that contain intraluminal vesicles, characteristic of MVBs[15]. Blocking the intraluminal sorting of APP retains it at the limiting membrane of endosomes and enhances its amyloidogenic processing[15]. Therefore, it is believed that Aβ production occurs within endosomes, and that the endosomal limiting membrane is an hotspot for APP processing.

1.1.3 Aβ and the amyloid cascade

Aβ is produced constitutively during normal cell metabolism and, under normal conditions, it is degraded by peptidases and cleared from the brain[1,16]. Gradual changes in the steady-state levels of Aβ are believed to initiate the amyloid cascade. This may be due to an imbalance between the production/clearance of Aβ in the brain or to mutations in genes associated to the familial form of the disease[1,6,17].

Aβ undergoes a conformational change to β-sheet, prone to aggregate into soluble oligomers and larger insoluble fibrils and, eventually, in plaques[1]. $A\beta_{40}$ is the most abundant form of the peptide, although $A\beta_{42}$ (approximately 10% of the Aβ produced) is more hydrophobic and prone to aggregate, thus being more neurotoxic[4,7,9]. Moreover, $A\beta_{42}$ is the predominant isoform in cerebral plaques[7]. At first, only Aβ plaques were assumed to be neurotoxic[1,4], however plaques correlate poorly with neuronal loss and currently Aβ oligomers are believed to be more harmful, inhibiting hippocampal long-term potentiation and disrupting synaptic plasticity, correlating better with disease progression[7,18,19].

The amyloid cascade hypothesis states that excessive Aβ accumulation and deposition in the brain initiates a sequence of downstream events, comprising synaptic alterations, and progressive neuronal loss with cognitive failure, ultimately leading to AD dementia[16,17].

One of the controversial questions in AD field was whether extracellular or intracellular Aβ accumulation initiates the disease process. Several studies in post-mortem AD patients,

transgenic mouse brains and cultured primary neurons have supported the idea that Aβ is generated within neurons, and that most of the intraneuronal Aβ is $Aβ_{42}$[4,7,20]. In the triple transgenic AD mouse model (3xTg-AD) Aβ accumulation begins intracellularly, when cognitive deficits are first detected in mice[7]. Similar results are seen in AD-vulnerable regions in human brain tissue[20], and in Down syndrome patients that invariably develop features of AD due to trisomy of chromosome 21, on which APP resides[7,20,21]. Furthermore, evidence indicate that accumulation of $Aβ_{42}$ within transgenic APP mutant is involved in alterations in pre- and post-synaptic compartments[22]. Overall, it is now accepted that the intraneuronal pool of Aβ may act as a focal point for Aβ deposition, and together with the extracellular Aβ oligomers it leads to disrupted neuronal function and plaque formation[4,7,20].

1.1.4 Neuronal transport of APP and BACE1

Neurons are complex polarized cells with a unique morphology and compartmentalization, and a network of endosomes scattered throughout the processes, which makes the trafficking pathways of both BACE1 and APP controversial between studies[9,23]. Selective transport ensures a polarized enrichment of specific membrane proteins at different neuronal domains (cell body, dendrites, axon)[9].

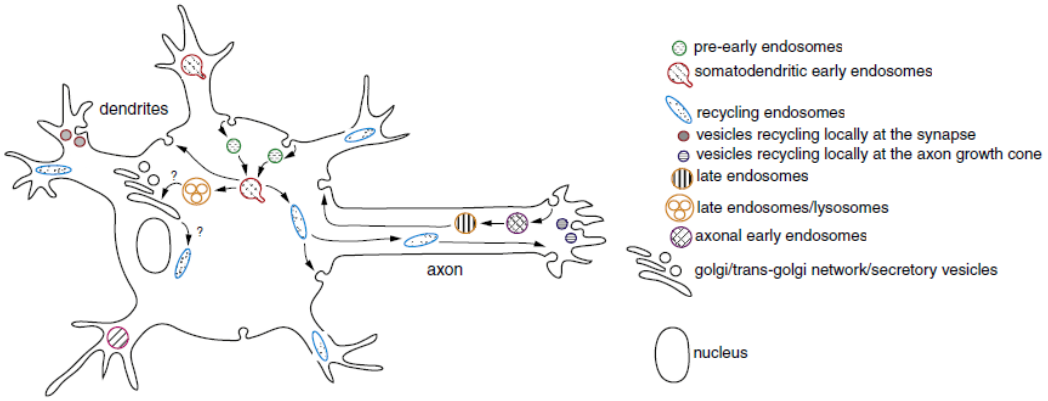

Figure 1.2 Schematic model of the neuronal endomembrane system. At the plasma membrane, proteins are endocytosed into pre-early endosomal compartments that mature and/or fuse into early endosomes containing regulators as EEA1 and rab5. Within early endosomes, proteins might be directly recycled back to the plasma membrane, or directed to specialized recycling endosomes that function in polarized sorting and recycling. Proteins can also be degraded, via sorting to late endosomes that mature to lysosomes. In the axons, endocytosed proteins accumulate in axonal early endosomes that likely mature into late endosomes, which travel retrogradely towards the cell soma. Recycling endosomal compartments are present at both axons and dendrites and traffic bidirectionally. There are also endosomal compartments at the axon growth cone and at the pre- and post-synaptic sites that are important for local protein recycling. *Adapted from Lasiecka et al., 2011.*

In neurons, the polarized organization of microtubules allows transport of carriers in two directions. Anterograde transport, from the neuronal cell body to axons/dendrites, and retrograde transport, from axons/dendrites to the cell body[9]. Bidirectional transport (anterograde and retrograde) occurs along both axons and dendrites[23], and APP and BACE1

can be transported to both the somatodendritic (cell body and dendrites) and the axonal compartments[9,24]. So, where does APP processing takes place in neurons?

Recently, Buggia-Prévot *et al.* showed that the internalized pool of BACE1 in dendrites undergoes exclusive retrograde transport towards the soma, while total and internalized BACE1 in axons undergoes bidirectional transport, in hippocampal neurons. Preventing BACE1 retrograde transport in dendrites induced a decrease in total and internalized BACE1 levels in axons, suggesting that internalized BACE1 in dendrites is ultimately targeted to axons, a process named transcytosis[25]. On the other hand, APP seems to undergo bidirectional transport in axons.[9,24] Evidence suggests that APP is cleaved by BACE1 during anterograde axonal transport, generating and releasing Aβ at or near presynaptic sites[9,25]. Several studies address the trafficking pathways of APP and BACE1 in non-neuronal cells. However, the sorting mechanisms of these proteins can be fundamentally different in polarized cells. Therefore, studies in neuronal cells are essential to gain new insights on the endocytic trafficking of APP and BACE1.

1.1.5 Regulation of Aβ generation by APP and BACE1 trafficking

Normal Aβ production occurs to a small extent because the neuronal trafficking pathways of APP and BACE1 are largely segregated (Fig. 1.3)[12,26]. APP and BACE1 are both transmembrane proteins that initiate their secretory pathway after exiting the trans-Golgi network (TGN), in distinct post-Golgi carriers[12], directed to the plasma membrane. At the cell surface, APP and BACE1 undergo endocytosis through different internalization mechanisms and are delivered to early endosomes[10,27]. APP is sorted to endosomal intraluminal vesicles, a process named multivesicular endosome (MVB) biogenesis, and is predominantly degraded in lysosomes[15,26]. BACE1 is sorted to the recycling pathway and returns to the cell surface[25,26]. Thus, β-cleavage only occurs when the two proteins come together in early endosomes. Deregulation of APP and BACE1 trafficking may potentiate their encounter in a common endosome, enhancing Aβ accumulation.

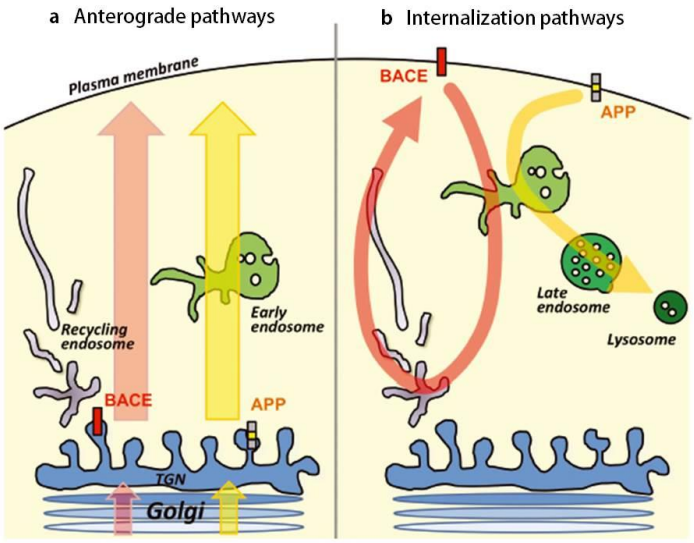

Figure 1.3 Model of the individual trafficking routes of BACE1 and APP. **(a)** Newly synthesized APP and BACE1 are transported from the trans-Golgi network (TGN) to the plasma membrane. **(b)** APP and BACE1 are internalized to early endosomes, where they are segregated by independent sorting events. BACE1 is transported predominantly to the recycling endosome and then to the cell surface, whereas APP is transported to late endosomes/lysosomes, likely being degraded. This normal traffic of APP and BACE1 may be protective against excessive production of Aβ. *Adapted from Chia et al., 2013.*

Two other AD risk factors, PICALM and SORL1, function as trafficking regulators, modulating Aβ accumulation[28]. PICALM, an adaptor protein involved in clathrin-mediated endocytosis, co-localizes with APP in vitro and in vivo, and controls APP internalization and Aβ generation. PICALM knockdown reduces APP internalization and Aβ generation, whereas its overexpression increases APP internalization and Aβ production. In vivo, overexpression of PICALM increases plaque deposition in AD transgenic mice[29]. SORL1 is involved in vesicle trafficking, and it controls APP transport between the TGN and early endosomes, thereby restricting APP deliver to endosomes and preventing its processing. Defects in SORL1 results in enhanced production of Aβ[30,31].

Moreover, evidence supports that synaptic activity triggers amyloidogenesis[32]. Studies report that upon synaptic activity in neurons APP is endocytosed via a clathrin-mediated process and routed into BACE1-containing recycling endosomes[12]. Synaptic activity induces an increase of APP anterograde transport and its β-cleavage, enhancing Aβ at activated synapses[33]. Therefore, the regulation of APP and BACE1 subcellular distribution, intracellular trafficking and localization are critical factors that impact APP processing and Aβ production.

1.2 The actin cytoskeleton in the regulation of endocytic trafficking

1.2.1 Actin

Actin is the most abundant intracellular protein in most eukaryotic cells, existing three main actin isoforms: α-actin, present in muscle cells, and β- and γ-actin, present in nonmuscle cells. Actin exists as a globular monomer (G-actin) and as a filamentous polymer (F-actin), which is a linear chain of G-actin monomers. Each actin molecule contains either ATP or ADP[34]. When G-actin assembles into F-actin ATP is hydrolysed to ADP, which reduces the stability of the filament, thereby promoting depolymerization[35].

In vitro polymerization of G-actin implicates three sequential phases (Fig. 1.4): the nucleation phase, in which G-actin aggregates into short and unstable oligomers that when reach a certain length can act as a nucleus; the elongation phase, in which more actin monomers are added to the nucleus, increasing its length; and the steady-state phase, in which, due to a decrease in G-actin concentration and F-actin filaments growing, it is reached an equilibrium between monomers and filaments. The ability of G-actin to polymerize into F-actin and depolymerize into G-actin is essential for the dynamics of the actin cytoskeleton. Actin filaments are continually forming and dissolving, and these variations in actin organization generate forces that are crucial to promote membrane shape changes[34].

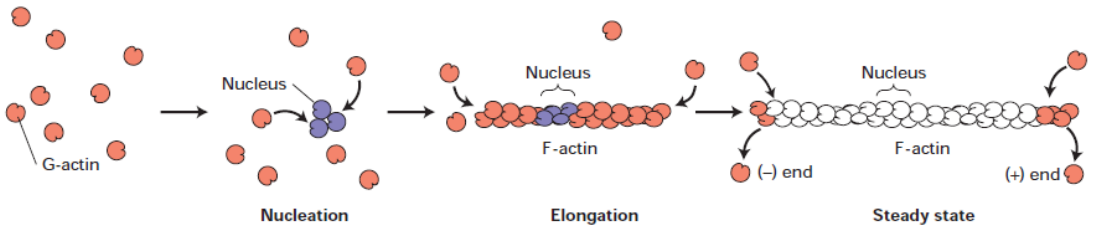

Figure 1.4 The three phases of G-actin polymerization *in vitro*. In the initial nucleation phase, monomers of ATP-G-actin (orange) slowly form a stable complex of actin – nucleus (blue). During the second phase, these nuclei are rapidly elongated through the addition of subunits to both ends of the filament. In the steady state phase, actin filaments have reached an equilibrium with monomers of G-actin. Subunits that were incorporated into a filament are now hydrolyzed, resulting in stable ADP-F-actin (white). In this last phase there is also an exchange of G-actin monomers with subunits at the filament's ends, without changing its total mass. Actin filaments can act as nuclei, skipping the nucleation process. *Adapted from Lodish et al., 2003*

Actin filaments assemble into stable networks and bundles with the help of several actin cross-linking proteins[34,35]. In a cell we can find different proteins that may promote or inhibit actin polymerization. For instance, severing proteins break actin filaments into shorter fragments, generating new filament ends for polymerization; while capping proteins cap the ends of actin filaments, preventing addition or loss of actin subunits and stabilizing them.

The Arp2/3 is a complex of actin-related proteins (Arps) that bind F-actin and promotes its assembly by nucleating a daughter filament[34]. This process is stimulated by nucleation promoting factors (NPFs) that are proteins of the Wiskott–Aldrich Syndrome (WASp) family

(WASP, N-WASP, WAVE, WHAMM, JMY and WASH), which localize to defined membrane microdomains[36]. The Arp2/3 complex creates a branched network of filaments[34], whereas formins, on the other hand, are actin-binding proteins that promote polymerization of linear actin filaments[35,36]. Actin filaments can also form tracks along which motor proteins, myosins, transport organelles or help shape endomembranes[35]. Actin is found throughout the cytoplasm but it is highly concentrated at the cell cortex. This cortical actin network controls the shape and mechanical properties of the cell surface, and can be organized into different structures. Lamellipodia, for instance, is a sheetlike structure that contains a dense meshwork of actin filaments, which polymerization is promoted by the Arp2/3 complex. Filopodia, on the other hand, are thin, stiff protrusions at the leading edge of the cell surface that depend on formins. Both are motile structures that form and retract with great speed[35].

Actin can be experimentally manipulated using toxins like cytochalasin D (CytoD), latrunculin or phalloidin that alter actin dynamics through different mechanisms. CytoD prevents actin polymerization by blocking the addition of actin subunits; latrunculin binds G-actin and inhibits its association to filaments. In contrast, phalloidin, which is widely used to stain actin filaments, binds at the interface between actin subunits and prevents depolymerization[34,35].

1.2.2 Actin and the endocytic pathway

The actin cytoskeleton and its associated motors are crucial to maintain the spatial distribution of endocytic compartments within the cell, and to assist in membrane remodeling, vesicle formation and cargo sorting[37].

Growing evidences indicate the requirement of actin dynamics in major cellular events (Fig. 1.5). For instances, in mammalian cells actin polymerization has been particularly explored in clathrin-mediated endocytosis. During invagination of clathrin-coated pits actin polymerizes towards the membrane, exerting force that may help stabilize and elongate the newly formed neck of a nascent vesicle, while also providing tension at the vesicle neck that, along with dynamin, promotes vesicle budding[36–38]. The large GTPase dynamin is responsible for the scission of the nascent vesicle[38]. In yeast, endocytosis absolutely requires F-actin, whereas it is not always essential in mammalian cells[36,39]. It is particularly needed to assist uptake when a larger force is required for budding, for example at plasma membrane locations with high membrane rigidity, or during uptake of larger cargoes[37].

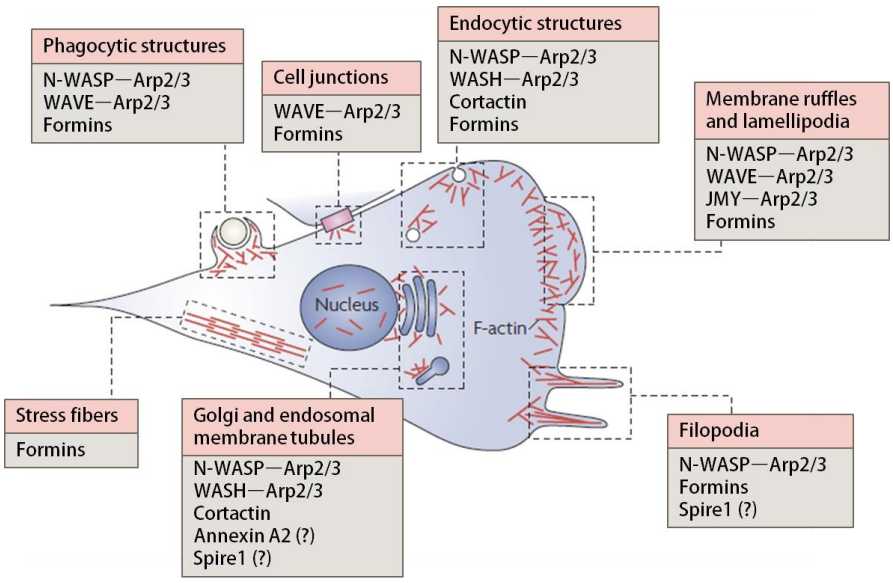

Figure 1.5 Localization of actin nucleation factors in mammalian cells. Filamentous actin (F-actin, in red) is nucleated into branched networks by the Arp2/3 complex and its nucleation promoting factors (NPFs). F-actin can also be polymerized into linear structures by formins. Some of the nucleation factors mentioned in this work are depicted, presenting several functional roles in cellular processes as phagocytosis, assembly of cell junctions, endocytosis, membrane ruffling and lamellipodia dynamics, filopodia formation, Golgi and endosomal tubuvesicular membrane dynamics, and stress fiber formation. Question marks indicate that the precise mechanism for the nucleation factor is still unclear. Other nucleation factors may exist. *Adapted from Campellone and Welch, 2010.*

The actin associated motor proteins, myosins, are also critical in carrier biogenesis. Membrane-bound myosins moving on pre-existing actin filaments may generate mechanical force and pull membranes, and/or control the organization of F-actin foci on organelles, perhaps through modulation of Arp2/3. Aditionally, mechanosensing properties of actin-based motors could overcome high membrane tension, assisting on membrane deformation and tubulation[36]. Besides myosins, other proteins can sense membrane shape and induce or stabilize membrane curvature. Proteins containing BAR (Bin/Amphiphysin/RVS) domains promote membrane invagination, coupled to actin polymerization and dynamin recruitment[36,38]. Indeed, many BAR domain proteins bind WASP family members, hence sustaining F-actin polymerization required for tubule elongation. Additionally they could also act as platforms that recruit key components, as dynamin, controlling subsequent steps of carrier biogenesis[36].

There is also evidence that actin polymerization generates actin comet tails that can support short-range movements of organelles[37]. In highly polarized cells, such as neurons, movement of endosomes and lysosomes is essential for several processes as dendritic branching, transport of survival factors and protection against toxicity[37]. Microtubules and their associated motors function in concert with actin and myosins to promote organelle movement and membrane shape changes during carrier biogenesis[36,37]. Microtubule motors generate a pulling force on the endosomal membrane, while the actin polymerization machinery generates a pushing force on the endosome. These two opposite forces likely

increase the tension of the membrane that will undergo fission, probably through recruitment of dynamin[40].

1.2.3 Regulation of endosomal trafficking by actin

The actin cytoskeleton has been implicated in the regulation of endosomal trafficking, which is an area of intensive research.

Initially, it was proposed, in *Xenopus* eggs, that movement of intracellular vesicles was driven by the assembly of actin comet tails, and that association of the actin comet tail to the vesicle's membrane was mediated by N-WASP. In HeLa cells, actin comet tails could be observed associated with a multivesicular/endosomal morphology, when cells were incubated with a diacylglycerol mimet[41]. Thus it was postulated that the force provided by actin assembly, via N-WASP and Arp2/3 nucleation, could propel endosomes through the cytoplasm.

More recently, studies propose that actin-based motility does not play a major role in endosomal transport, but rather that short actin filaments facilitate membrane remodeling required for endocytosis[39] and intracellular trafficking[42].

During endocytosis, different actin regulators, including the Arp2/3 complex, cortactin and N-WASP, are recruited to clathrin-coated pits at the time of membrane scission by dynamin[38,39]. Previously, it was reported that pharmacologically inhibiting actin dynamics, or disrupting the interaction between actin and clathrin, selectively stalls apical clathrin-coated pits at a late stage of assembly[39]. Thus, actin dynamics plays a role in clathrin-mediated endocytosis, likely assisting in vesicle budding through a constriction force generated by its polymerization.

At the endosome, evidence supports a role for actin dynamics in endosomal recycling mechanisms. The recycling pathway is highly regulated and specific cargo can be sorted into specialized subsets of tubules, in a single endosome, that are functionally distinct[43]. In HEK293 cells, actin was dynamically assembled and associated with endosomal recycling tubules. This localized actin cytoskeleton may be required to stabilize a subset of endosomal tubules, allowing the entry and concentration of cargo that is recycled in a regulated manner, through a specific sorting sequence[43]. The Arp2/3 complex, cortactin, WASH and WASP can be found at the base of endosomal tubules, where they generate actin-rich patches[43–45]. Previously, Derivery *et al.* described WASH associated with an actin network on restricted domains of sorting and recycling endosomes, being required for tubule scission depending on dynamin recruitment[40].

Actin dynamics is also associated with the maturation of early endosomes to late endosomes. Morel *et al.* observed that actin depolymerization by latrunculin treatment reduced the formation of MVBs and prevented the epidermal growth factor receptor (EGFR) to reach late endosomes, delaying its degradation in HeLa cells. This suggested that actin

polymerization is required for early-to-late endosome transport. Additionally, they could see that actin patches formed on early endosomes depended on annexin A2 (AnxA2), a protein present on early endosomes, Arp2/3 and Spire1, another actin nucleation factor. Knockdown of any of these proteins decreased the number of actin patches associated with early endosomes and inhibited transport to late endosomes[45]. Cortactin was also reported as a critical regulator of late endosomes/lysosomes trafficking and Golgi homeostasis. Cortactin knockdown induced the accumulation of the endosome-to-Golgi retrograde cargo mannose-6-phosphate receptor (M6PR), in enlarged late endosomes/lysosomes in HeLa cells. This is consistent with a block in late endosome maturation and/or trafficking[46].

Moreover, it was described that actin filaments, along with the actin-based motor myosin 1b (Myo1b), contribute for the modulation of multivesicular endosome morphology, regulating the transport of protein cargo to the internal vesicles of these endosomes[47]. In addition, Almeida *et al.* also described a function for Myo1b and the actin cytoskeleton in the formation of tubular-carrier precursors at the TGN. Myo1b or Arp2/3 knockdown in HeLa cells led to a decrease in F-actin at the TGN and to a reduction in the formation of tubular precursors, preventing the exit of M6PR from the Golgi. They hypothesized that Myo1b tethers polymerized actin to the TGN membrane. Actin would generate force leading to membrane deformation and creation of tubular precursors that allow protein exit from the TGN[48]. Therefore actin dynamics is crucial for membrane deformation, regulating several trafficking events within the cell (Fig. 1.5).

1.2.4 Cross-talk between AD and the actin cytoskeleton

In neurons, the actin cytoskeleton is critical for dendritic spine dynamics, working as a structural scaffold that anchors neurotransmitter receptors at the synapse[49,50]. Dendritic spines are small protrusions along dendrites that constitute postsynaptic sites for synaptic transmission[51]. A small fraction of actin in spines is stable, conferring the structural and functional integrity of the glutamatergic synapse, whereas the dynamic fraction of actin is required for structural remodeling of spines, contributing to synaptic plasticity and memory formation[50,51]. Synaptic strength and neuronal function are greatly influenced by dendritic spine size and number[50].

A loss or alteration in spines has been described in patients with AD and in mouse models of the disease[51]. AD transgenic mice present decreased spine density and decreased levels of PSD-95 and glutamate receptors in hippocampal neurons, along with cognitive decline at the time spines become depleted. The remaining dendritic spines have increased size, perhaps as a putative compensatory mechanism[22,50]. In addition it was recently reported, in 3xTg-AD mice, that hippocampal regions with a greater accumulation of Aβ present lower levels of cortactin and a decrease in F-actin at post-synaptic sites[52]. It is believed that alterations in spines dynamics are responsible for the cognitive defects observed in AD, before neuronal loss[51].

Other defects in the organization of the actin cytoskeleton are seen in AD. Two common actin-containing structures are Hirano bodies and actin depolymerizing factor (ADF)/cofilin-actin rods[53,54]. Hirano bodies are intracytoplasmic inclusions that consist of large aggregates containing actin, several actin-binding proteins (including ADF/cofilin), and tau. The mechanism of formation of these inclusions is unknown. ADF/cofilin-actin rods are bundles of filaments that form smaller inclusions and are mainly present in axons and dendrites. Members of the ADF/cofilin family are important regulators of actin dynamics. Active (dephosphorylated) cofilin binds with higher affinity to ADP-actin, twisting actin filaments and severing them. It is still unknown if an exacerbated accumulation of F-actin in AD brains can trigger the formation of ADF-cofilin-actin rods, that could recruit additional proteins and give rise, over time, to Hirano bodies[49,53,54].

In hippocampal neurons, ATP depletion works as a mediator of neurodegeneration, inducing a reorganization of actin, ADF and cofilin that form rod-like inclusions containing in dendrites and axons[54,55]. Neurites with ADF/cofilin-actin rods exhibit a disrupted microtubule network, causing degeneration of the distal neurite without neuronal death. This suggests that ADF/cofilin-actin inclusions in the brain can account for the pruning and loss of synapses without neuronal loss[55]. Moreover, treatment of hippocampal neurons with $A\beta_{42}$ also induces ADF/cofilin-actin rods in a subpopulation of neurons[54], and inhibits fast axonal transport[56]. Therefore, rod formation, initiated by amyloid toxicity, may occlude neurites causing a defective transport of material needed to maintain synaptic function, and leading to distal neurite atrophy[54,55]. In addition, Maloney *et al.* reported that neurites where ADF/cofilin accumulated presented a vesicular punctate staining for APP, BACE1, PS-1 and β-cleaved APP (βCTF and/or Aβ)[54]. Thus, defects in neuronal transport may also promote the accumulation of APP and its proteolytic machinery within stalled endosomes, leading to the continued generation of Aβ.

1.3 Late-onset AD genetic risk factors: BIN1 and CD2AP

Late-onset AD has not been related to a familial inheritance. However, GWAS have identified several susceptibility genes that, along with APOEε4, contribute to an increased risk to develop the disease, and thus are putative genetic risk factors[8,57]. GWAS are large scale meta-analysis methods to identify single nucleotide polymorphisms (SNPs), in the genome of lat-onset AD patients, with increased statistical power[8]. One of the first major GWAS identified the most frequent SNP in AD patients after APOEε4, which is adjacent to the bridging integrator 1 (*BIN1*) gene, or amphiphysin 2 (*AMPH2*), located on chromosome 2[58]. The second set of large GWAS identified SNPs adjacent to the CD2-associated protein (CD2AP), located on chromosome 6, which encodes a scaffolding protein that regulates the actin cytoskeleton[59]. Whether Bin1 and CD2AP are AD risk factors remains to be validated.

1.3.1 BIN1 (Amphiphysin 2)

Bin1 belongs to the BAR family of proteins which include the mammalian bridging-integrators (Bin1 and Bin2), amphiphysins, and the yeast proteins Rvs161p and Rvs167p[60,61]. All members of this family share an N-terminal BAR domain, with predicted coiled-coil structure and essential for membrane association, and a C-terminal Src homology 3 (SH3) domain. The central insert domain is more variable among isoforms (Fig. 1.5)[57,61]. Amphiphysin 1 (Amph1) was the first to be identified, enriched in presynaptic terminals of mammalian brains and associated with synaptic vesicles[60,62]. Amphiphysin 2 (Amph2), an homologous of Amph1 yet ubiquitously expressed, exists in vertebrates and is commonly called Bin1[60–62]. BIN1 transcripts are subjected to extensive differential splicing (Fig. 1.6) which leads to a vast diversity of Bin1 isoforms, though the most important isoforms are: the neuronal isoform of Bin1 (Amph2 or Bramp2); the muscle isoform of Bin1; and two broadly expressed Bin1 isoforms, SH3P9 and ALP1[57,61]. Amph1 and Amph2 can oligomerize and form a complex of homo- or heterodimers, through their N-terminal domains[61,63]. The heterodimer is the predominant form in the brain[64]. This work is focused on the neuronal isoform of Bin1.

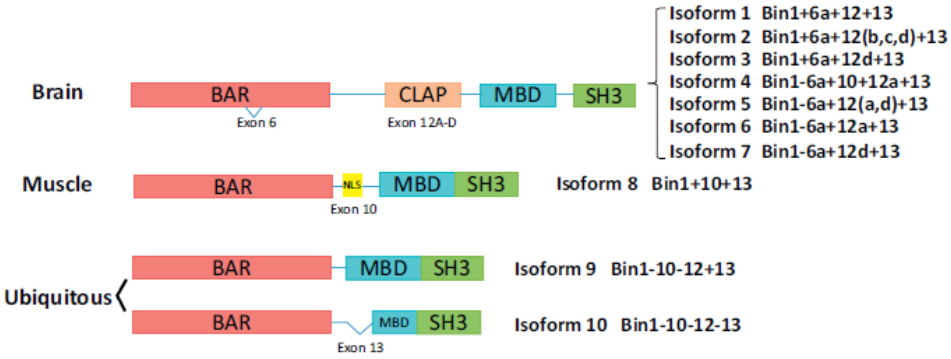

Figure 1.6 Schematic domain structure and alternative splicing of Bin1. The main tissue-specific splice variants are the neuronal (brain) variant, which includes exons 6a, 12 and 13; and the muscle variant that contains exons 10 and 13. The neuronal isoform undergoes further differential splicing in the main four exons (6a, 10, 12 and 13). There are also two broadly expressed Bin1 isoforms, SH3PO or isoform 9, with exons 12, 13 and without exon 10; and ALP1 or isoform 10 that does not have any of the previous exons. Abbreviations: BAR, BIN1/Amphiphysin/RVS; CLAP, Clathrin-AP2 binding region; MBD, Myc-binding domain; SH3, Src homology 3 domain; NLS, Nuclear localization sequence. *Adapted from Tan et al., 2013*

1.3.1.1 Bin1 molecular and cellular function

Initially, Bin1 was identified as tumor suppressor protein, due to its binding domain to the oncoprotein Myc[57,61]. With growing research, interactions of Bin1 and amphiphysins with several other proteins allowed to infer on its different cellular functions.

Amphiphysins are enriched at nerve terminals in the brain, and interact with proteins from the endocytosis machinery, in particular clathrin-mediated endocytosis, therefore being involved in synaptic vesicle endocytosis[62,64,65]. Amphiphysin heterodimers interact with the adaptor protein-2 complex (AP-2), which recruits clathrin to the plasma membrane[63,64], and with clathrin heavy chains and endophilin A1, a key molecule in the formation of endocytic

vesicles. This allows the polymerization of clathrin into a lattice that forms the clathrin-coated pit[62–64]. The SH3 domain of Amph1 can also interact with dynamin 1, that severs the clathrin-coated pit neck forming a vesicle, or synaptojanin, crucial for uncoating clathrin of the vesicles[61,62,65]. Thus it is believed that Bin1, as a member of the amphiphysin family, may play a major role in clathrin-mediated endocytosis at nerve terminals, through its interaction with several adaptor proteins associated with this mechanism[61,63,64].

In PC12 cells, Bin1 associates with dynamin in a greater extent when cells have been stimulated with nerve growth factor (NGF), suggesting that this interaction is dependent on a signaling event and that Bin1 may be connected to receptor-dependent signaling pathways[62].

Additionally, Bin1 localizes to axon initial segments and nodes of Ranvier, both exhibiting a dense submembranous cytoskeleton matrix which contains actin[61]. This subcellular localization suggests a role for Bin1 in the organization and/or function of the actin cytoskeleton, which will be further explored.

1.3.1.2 The role of Bin1 in endocytosis and trafficking

Bin1 has a particular key role in clathrin-mediated endocytosis. Amphiphysin heterodimers stimulate GTPase activity of several dynamin molecules and promote its assembly into a ring-like structure on the collar of an invaginated clathrin-coated pit[62–64]. In fact, overexpression of the SH3 domain of Amph1 or Bin1 inhibits clathrin-mediated endocytosis, either in nerve terminals or in fibroblasts[64,66], through prevention of dynamin multimerization and ring formation, essential for the fission step of this process[60].

In the brain, Bin1 is critically dependent on Amph1 expression. Brain extracts that lack *AMPH1* have normal levels of *BIN1* transcript but have reduced levels of the protein, which suggests that, in the brain, only Amph1/Bin1 heterodimers are stable. Perhaps only these heterodimers are able to functionally interact with dynamin 1, required for endocytosis of both synaptic vesicles and receptors[66]. Knockout mice for Bin1 present a slight reduction in the kinetics of synaptic vesicle endocytosis, and an impaired association of clathrin and AP-2 with the membrane and with dynamin. Besides, mice lacking Bin1 exhibit learning and memory deficits[60].

Additional data proposes that Bin1 may also participate in endocytic trafficking. Sorting nexin 4 (SNX4), a regulator of intracellular trafficking, associates with Bin1 in HeLa and 3T3 cells. Expression of the SH3 domain of Bin1 inhibited transferrin receptor endocytosis, suggesting Bin1 may be important to control endosome fate, after the formation of the endocytic vesicle[67]. Moreover, the N-terminal BAR domain of Bin1 binds lipid membranes and induces membrane curvature in T-tubules (muscle cells) and endocytic pits (neuronal and non-neuronal cells)[57,67]. It has been previously shown that Amph1 can transform spherical liposomes into narrow tubules, as well as its binding partners dynamin 1 and endophilin. This particular function of the amphiphysin proteins indicates its potential role in membrane

deformation and vesicle budding[65,68]. Therefore, Bin1 seems to be involved not only in endocytosis, but also in endocytic trafficking mechanisms.

1.3.1.3 Impact of Bin1 in the actin cytoskeleton

As stated above, the subcellular localization of Bin1 suggests it may have a function in the regulation of the actin cytoskeleton. In hippocampal neurons, Amph1 and F-actin colocalize to growth cones. Suppressing Amph1 expression led to a collapse of growth cones, inhibition of neurite outgrowth and axon formation, and a breakdown of F-actin into tangles mainly concentrated at one pole of the cell[60,69]. The budding yeast homologues of mammalian amphiphysins – *rvs161* and *rvs167* – code for BAR domain proteins that also form heterodimers. Mutant strains of these proteins present mislocalization of cortical actin patches on the plasma membrane, abnormal polarity and uneven cell size[64,70,71]. Besides, they exhibit endocytic defects that can be due to a disruption of the peripheral cytoskeleton, indicating that Rvs167p and Rvs161p are required for normal cortical actin organization[64].

Recently, it was discovered that the muscle isoform of Bin1 interacts with the actin nucleation factor N-WASP that activates the Arp2/3 complex, in myofibers[72]. Mutations in Bin1 led to a disruption of this interaction and of N-WASP distribution. Furthermore, knockdown of N-WASP or Bin1, in myotubes, altered the normal position of the nucleus and decreased myofiber thickness and organization. The same phenotype was observed when myofibers were treated with latrunculin B. Thereby, Bin1 may regulate the actin cytoskeleton in muscle cells, through recruitment of N-WASP[72]. As well as in myofibers and skeletal muscle, the muscle isoform of Bin1 is also found at cardiomyocytes. In fact, Bin1 is downregulated in falling hearts and its deletion leads to disruption of membranes and extracellular diffusion of calcium and potassium ions. Rescuing Bin1 expression promotes actin polymerization through N-WASP which creates a diffusion barrier to extracellular ions by stabilizing membranes in cardiomyocytes[73].

As a member of the amphiphysin family, and likewise its homologues and different isoforms, neuronal Bin1 may also play an important role in the dynamics of the actin cytoskeleton.

1.3.1.4 BIN1 pathological function in AD

BIN1 is the most important genetic risk locus in LOAD, after the *APOE* gene. The main associated SNPs are in the 5' region adjacent to *BIN1*: rs744373 and rs7561528[57]. SNPs upstream of *BIN1* correlate with a higher risk to develop LOAD and to increased *BIN1* transcripts[57,74,75]. However, the mechanisms that underlie the contribution of this risk factor to AD pathogenesis are still unknown.

The Bin1 homologue in drosophila was reported to interact with tau protein and its loss suppressed tau-induced neurotoxicity, using drosophila eye as a model[75]. Additionally, mice lacking Amph1 or Bin1 in the brain are deficient in endocytic recycling mechanisms, which correlate with major learning deficits[57]. As mentioned before, muscle Bin1 seems to regulate intracellular calcium levels in cardiomyocites[73]. Aβ accumulation can lead to dysregulation of intracellular calcium levels, through alterations in the expression of calcium channels and calcium influx. Intracellular calcium is crucial for neuronal function, synaptic transmission, and neuronal plasticity mechanisms that underlie memory and learning[57,76]. Thus, Bin1 could be related to AD pathological mechanisms through its modulation of calcium levels[57].

Bin1 function on endocytosis and trafficking is of most importance for AD, since alterations in APP and/or BACE1 intracellular trafficking can directly influence whether APP undergoes the amyloidogenic or nonamyloidogenic pathway. Bin1, through its interaction with dynamin and/or through its regulation of actin-binding proteins, may lead to changes in APP or BACE1 endocytosis at the plasma membrane, or to alterations in tubulation mechanisms that are essential for BACE1 recycling.

1.3.2 CD2AP

CD2AP is a 80 kDa protein expressed mainly in epithelial and lymphoid cells[77]. The protein has three SH3 domains at the N-terminus, critical for protein, followed by a proline-rich region and a coiled-coil domain, with actin-binding sites, at the C-terminus (Fig. 1.6)[78–80].

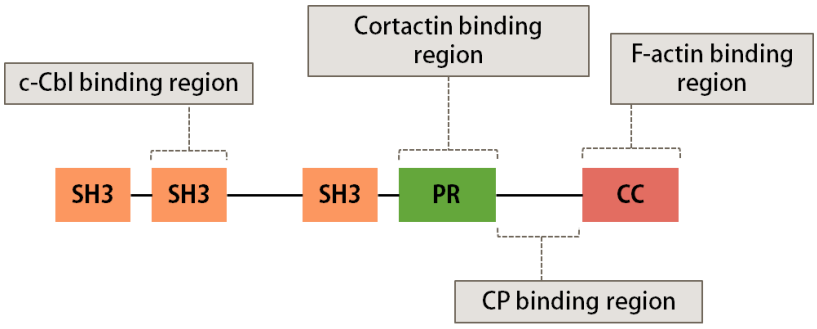

Figure 1.7 Schematic domain structure of CD2AP. CD2AP presents three Src homology 3 (SH3) domains at the N-terminus, a proline-rich region (PR) and a coiled-coil domain (CC) with an actin-binding site, at the C-terminus. The second SH3 domain of CD2AP binds to the proto-oncoprotein c-Cbl[80]. The proline-rich region of CD2AP binds the SH3 domain of cortactin[81]. The region of CD2AP between the proline-rich

sequences and the coiled-coil domain is the putative capping protein (CP) binding site[79]. The C-terminal coiled-coil domain of CD2AP is known to interact with F-actin[82]. Figure b*ased on Cormont et al., 2003.*

1.3.2.1 CD2AP molecular and cellular function

CD2AP was first identified as a molecular scaffold that binds and clusters the transmembrane protein CD2 in T-cells, playing a crucial role for cytoskeletal polarization at sites of cell contact, such as in the formation of an effective T-cell-antigen-presenting cell junction[78,83]. Later it was discovered that CD2AP-deficient mice die at a young age from renal failure[77,78,80]. CD2AP functions in podocytes of the kidney, as an adaptor protein binding to nephrin and podocin, anchoring these proteins to actin filaments of podocyte cytoskeleton, and in signal transduction[78,84]. Independently, it was characterized in humans as a partner of p130Cas, a member of the Cas family of adaptor proteins and docking protein for several signaling cascades, named CMS (Cas ligand with multiple SH3 domains).

CD2AP interacts with the proto-oncogene c-Cbl, an E3 ubiquitin-protein ligase, implicated in receptor-mediated signaling and endocytosis[77,80]. Moreover, CD2AP also interacts with endophilin, synaptojanin, clathrin-adaptor protein 2, capping protein and cortactin[79], suggesting a role in endocytosis and actin cytoskeleton regulation, which will be further discussed.

1.3.2.2 The role of CD2AP in endocytosis and trafficking

CD2AP self-associates through its C-terminal portion, likely forming a complex[80]. A previous study reported that, in CHO cells, this CD2AP dimer was present at the plasma membrane and in punctate structures within the cell that did not colocalize with the early endosomal marker EEA1. Yet, when coexpressed with Rab4 or c-Cbl the distribution of CD2AP changed dramatically and both proteins could be localized to large vesicles, along with EEA1. This suggested that CD2AP must interact with both Rab4 and c-Cbl, inducing a modification in endosomes' morphology[80]. Additionally, expression of a truncated form of CD2AP, that inhibits the interaction with c-Cbl, prevented ligand-induced degradation of the platelet-derived growth factor (PDGF) receptor. Thus CD2AP may not only control early endosome morphology, but it may also play a role in trafficking between early and late endosomes[80].

Indeed, other studies reported the likely role of CD2AP in the degradative pathway. Electron microscopy analysis of CD2AP heterozygous podocytes revealed defects in the formation of MVBs. This suggested that CD2AP may play a role in vesicular trafficking to the lysosome, mediated by MVB formation[77]. In 2004, CD2AP was found to be part of a complex with c-Cbl and Flt-1, a vascular endothelial growth factor (VEGF) receptor, upon VEGF stimulation. In NIH3T3 cells with overexpression of CD2AP and Flt1, VEGF stimulated the colocalization of these proteins in endocytic vesicles, and the internalization and degradation of Flt-1, which was inhibited by a mutant form of CD2AP. Additionally, coexpression of c-Cbl

and CD2AP led to the formation of enlarged vesicles in cells, suggesting once again a role in the control of endosome morphology[85].

Gauthier *et al.* studied the role of CD2AP in the trafficking of VacA-containing vesicles, a bacterial toxin that is transported form the cell surface to late endosomes where it induces the formation of large vacuoles. Expression of a truncated form of CD2AP, or depletion of the protein in HeLa cells blocked the arrival of VacA into late endosomes and the formation of large vacuoles. Therefore, CD2AP is implicated in the sorting and transport of VacA to late endosomes[86].

CD2AP also interacts with cortactin's SH3 domain. In MDA-MB-231 cells, this interaction was induced by epidermal growth factor (EGF). After 5 min of EGF stimulation, EGF receptors accumulated in membrane ruffles, colocalizing with CD2AP and cortactin. Colocalization was transiently and after 15 min the receptors were concentrated into vesicular structures within the cytosol. Hence, it is possible that a complex of CD2AP and cortactin may regulate trafficking of internalized EGF receptors[81]. These interactions between CD2AP and actin-regulatory proteins may link endocytic vesicles to actin polymerization-based trafficking, hence making it a critical regulator of the endocytic and degradative pathways.

1.3.2.3 Impact of CD2AP in the actin cytoskeleton

CD2AP interacts directly with filamentous actin, through its C-terminus, supporting its role as a regulator of the actin cytoskeleton[82]. In mouse M-1 kidney epithelial cells, CD2AP was enriched in the perinuclear region and along the leading edge of the cells, where it colocalized with F-actin. Upon treatment with CytoD to disrupt the actin cytoskeleton, or with jasplakinolide, which stabilizes F-actin and promotes actin polymerization, there was a redistribution of CD2AP to aggregates that colocalized with the collapsed actin at the cell periphery. This suggested that CD2AP distribution depends on an intact actin cytoskeleton[82].

As previously mentioned, CD2AP also interacts with cortactin[81]. In immortalized mouse podocytes, transfected CD2AP was diffusely expressed in the cytoplasm and it was also present in highly motile spots where it colocalized with F-actin and cortactin. These spots, which were frequently associated with Rab4-positive vesicles, had a limited lifetime, a delayed uptake of fluorescent dextran, and an inhomogeneous luminal distribution consistent with a membranous suborganization in the vesicle interior, typical of MVBs. The motility of CD2AP spots depended on actin polymerization, evidenced by their rapid accumulation of G-actin and by abrogation of their motility by jasplakinolide. These results suggested that CD2AP is associated with dynamic actin in later endosomal compartments, likely playing a role in sorting and/or trafficking via regulation of actin assembly in vesicles[87].

As stated above, CD2AP controls the late endosomal trafficking of VacA, a process that seems to be regulated by the formation of actin structures at the tip of early endosomes[86]. In VacA-containing vesicles, CD2AP colocalized with cortactin and appeared to make a bridge

between the surface of the vesicles and F-actin structures. Overexpression of full-length CD2AP increased actin polymerization in EEA1-positive vesicles containing VacA. However, expression of a truncated form of CD2AP, with just the first two SH3 domains, completely blocked the formation of the F-actin structures and led to greater levels of cortical F-actin. Depletion of CD2AP, on the other hand, induced a massive remodeling of the actin cytoskeleton, with several stress fibers and a decrease in cortical actin. Thus, the presence of these actin structures on early endosomes depends on CD2AP, which may act along with cortactin[86].

Besides cortactin, CD2AP also binds capping protein (CP), a protein enriched in lamellipodia that associates with the barbed end of actin filaments, limiting their growth and enhacing new actin filament branching through the Arp2/3 complex[79]. CD2AP can partially inhibit CP and/or promote its uncapping from the filament. The balance between filopodia and lamellipodia is dependent on CP, so it is likely that distinct pools of CP exist bound to different CP-binding proteins. Recruitment of CD2AP to the plasma membrane might inhibit CP activity and thereby promote filopodia formation or decrease the density of branched filaments, although researchers could not find an effect in the actin cytoskeleton in CD2AP-deficient or overexpressing HEK293T cells[79].

More recently, CD2AP was found to drive shape changes at the cell periphery, where it colocalized with CP and cortactin, during the initial phases of cell spreading in podocytes. CD2AP knockdown cells had a deficient recruitment of CP to the cell periphery, with increased filopodia and ruffling appearance, a phenotype similar to CP-deficient cells. A CD2AP mutant, lacking cortactin-binding domain localized poorly to the cell periphery, which was rescued by wild type cortactin. Using superresolution microscopy, it was possible to determine that, in CD2AP wild-type podocytes, CD2AP links CP and cortactin at the cell periphery, where there was significant colocalization of these proteins, compared to CD2AP knockdown cells. Thus, CD2AP may play a crucial scaffolding role to enhance CP- and cortactin-mediated actin assembly, likely via the Arp2/3 complex[88].

In fact CD2AP was identified as a capping protein itself. Using a rhodamine-labeled actin assay, researchers discovered that CD2AP blocked the addition of monomeric actin to filaments, and that it prevented depolymerization of actin. A truncated form of CD2AP, that still binds to F-actin, failed to inhibit actin addition, which means its capping activity requires the full-length protein[89]. All these data support the crucial role of CD2AP in the regulation of different actin-associated structures within the cell.

1.3.2.4 CD2AP pathological function in AD

In 2011, *CD2AP* was identified as a susceptibility gene related to AD[59]. It was recently discovered two of the associated SNPs, rs9296559 and rs9349407, which are correlated with increased LOAD risk[28] and rs9349407, in particular, correlates with neuritic plaque burden[90], although CD2AP mRNA expression has not been found altered in brains with AD[91]. However, the putative functional impact of these SNPs is still unknown and the functional role of CD2AP in the brain, and its role in AD are still elusive.

A functional screening using a *Drosophila* model of AD implicated *cindr*, the fly ortholog of the human *CD2AP*, as a modulator of tau-dependent eye toxicity, exhibiting a moderately reduced eye size and roughened surface[92]. In yeast and *C. elegans*, homologs of CIN85 (c-Cbl interacting protein of 85 kDa), which behaves similarly to CD2AP, have been identified as suppressors of Aβ toxicity[93]. Additional studies are needed to understand the underlying mechanism of CD2AP as a genetic risk factor for Alzheimer's disease, and in more relevant models of the disease.

1.4 Aim of the current work

AD has been widely studied in the past decades. However an effective treatment to the disease is still missing. Bin1 and CD2AP were identified as putative risk factors for late-onset AD, although it is not known how they contribute to the disease. Actin dynamics is involved in several trafficking mechanisms within the cell. At the endosome, a actin is associated with recycling tubules and is functionally required for endosomal maturation [45,46]. Branched actin networks are involved in the stabilization and organization of specific endosomal domains, to which different actin-binding partners are recruited and assist in cargo sorting and membrane remodeling [40,43]. APP and BACE1 meet at the endosome, where Aβ is generated. Previous data from the lab have implicated Bin1 and CD2AP in the control of the endocytic trafficking pathways of these proteins. Since Bin1 and CD2AP have been described to control actin dynamics, we decided to investigate if the mechanism whereby Bin1 and CD2AP impact APP and BACE1 trafficking is through the regulation of the actin cytoskeleton associated with early endosomes. Thus, we will focus on three main objectives:

1) Study the role of Bin1 and CD2AP as regulators of endosomal actin dynamics;
2) Investigate if actin dynamics controls APP and BACE1 endocytic trafficking and Aβ generation;
3) Determine if and how Bin1 and CD2AP control the association of actin with endosomes.

We will use a neuron-like cell line and mouse primary neurons, as experimental models, to test our hypothesis that Bin1 and CD2AP control Aβ generation by regulating the actin-dependent endocytic trafficking of APP and BACE1.

Chapter 2

Previous Data

In order to understand the context of this work, I will briefly describe the previous results obtained in the Neuronal Trafficking in Aging Laboratory, which are being prepared for publication. These results were the starting point for this thesis project and led to the hypothesis that the AD risk factors Bin1 and CD2AP impact the neuronal trafficking associated with AD, through an actin-mediated mechanism. The data below was done mainly by Cláudia Almeida, Florent Ubelmann, Tatiana Burrinha, Ricardo Gomes and Cláudio Ferreira.

Initially, it was verified that both Bin1 and CD2AP are expressed in the working cellular models, which are N2a cells, a mouse neuroblastoma cell line, and mouse primary neurons. This was performed by western blot and immunofluorescence. The proteins exhibited a polarized distribution in primary neurons (PN), with Bin1 being particularly enriched in axons, whereas CD2AP was mainly present in the somatodendritic compartment. To validate their roles as AD genetic risk factors, the impact of Bin1 and CD2AP loss of function on Aβ accumulation was investigated. Bin1 and CD2AP were efficiently knockdown in both N2a cells and PN and immunostained for $A\beta_{42}$ (Fig. 2.1A and B).

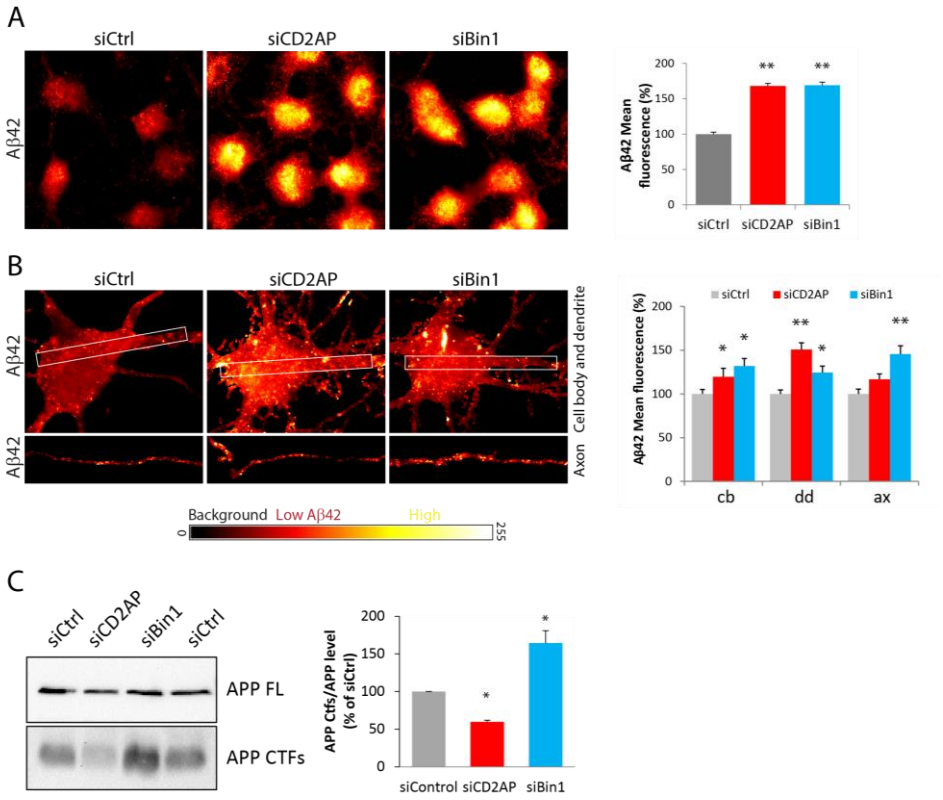

Figure 2.1 Loss of Bin1 and CD2AP impact APP processing and increase Aβ levels in N2a cells and PN. **A.** Immunofluorescence of N2a cells, transfected with non-targeting siRNA (siCtrl), or siRNA against CD2AP (siCD2AP) or Bin1 (siBin1), with an antibody specific for $A\beta_{42}$. Levels of $A\beta_{42}$ mean fluorescence in the different conditions are represented in the graph, as a percentage of siRNA control cells. **B.** Representative images of the cell body, dendrites and axon of primary neurons transfected and immunostained as in A. The graph represents the mean fluorescence of $A\beta_{42}$ in the different conditions and neuronal compartments, as a percentage of siRNA control cells. Images in A and B are presented with the "red hot" LUT, in which dark colors indicate low levels of $A\beta_{42}$ and bright colors indicate high levels of $A\beta_{42}$. **C.** Western blot analysis of

cell lysates from PN transfected with siCtrl, siCD2AP or siBin1 and blotted with an antibody against APP C-terminus. Levels of APP C-terminal fragments (APP CTFs) were normalized to the levels of APP full lenght (APP FL), and represented in the graph as a percentage of siRNA control cells. * $p<0.05$ vs siCtrl; ** $p<0.01$ vs. siCtrl.

In N2a cells, Bin1 and CD2AP depletion increased the levels of intracellular $A\beta_{42}$, compared to N2a cells treated with non-targeting siRNA (siControl). Interestingly in PN, although both Bin1 and CD2AP increased $A\beta_{42}$ accumulation in the cell body, in Bin1 knockdown $A\beta_{42}$ was particularly increased in axons, while in CD2AP knockdown this increase was more significant in dendrites. This polarized effect of Bin1 and CD2AP is consistent with the differential localization of these proteins in neurons.

Given these results, it was crucial to understand how these risk factors impact Aβ levels. Since they are both regulators of endocytic trafficking, it was considered if they could control APP and/or BACE1 endocytosis, thereby promoting Aβ production. In order to test this hypothesis, it was performed pulse-chase experiments to analyze APP and BACE1 endocytosis, recycling and degradation in N2a cells and PN knockdown for Bin1 and CD2AP. CD2AP and Bin1 knockdown did not significantly affect the internalization of APP or BACE1 (not shown).

Previous studies reported that, after internalization, most BACE1 is recycled back to the plasma membrane. Thus, analyses of BACE1 recycling upon Bin1 and CD2AP knockdown, by immunofluorescence, revealed that Bin1-depleted N2a cells had lower levels of recycled Bin1, compared to siRNA and CD2AP knockdown cells (not shown). Looking at the pool of BACE1 that remained in the cell, indeed it was observed that BACE1 accumulates intracellularly when Bin1 is knockdown (Fig. 2.2A and B). CD2AP had no significant effect in BACE1 endocytic trafficking. Similar results were obtained in PN, where there was a polarized decrease in BACE1 recycling in the cell body and axon, suggesting Bin1 controls BACE1 recycling to the axonal plasma membrane.

This prompted the question: where does BACE1 accumulates within the cell? In N2a cells there was a marked increase in the overlap between internalized BACE1 and the early endosomal marker EEA1 (Fig. 2.2A, arrows). There was also an increase in colocalization between BACE1 and Rab5 in the axon of primary neurons, indicating that BACE1 accumulates in axonal early endosomes (not shown). In addition, loss of Bin1 produced an enlargement of EEA1-positive endosomes, in primary neurons. Additionally, by imaging live neurons expressing BACE1-GFP and Rab5-RFP, it was seen that depletion of Bin1 led to an increase in BACE1 tubules extruding from Rab5 early endosomes, compared to the control knockdown (Fig. 2.2C and D). Interestingly, unlike the control, these tubules were not severed, preventing the formation of a BACE1 carrier that could be transported to the cell surface (Fig. 2.2C). This may explain the impairment in BACE1 recycling and its consequent accumulation in early endosomes, when Bin1 is knockdown.

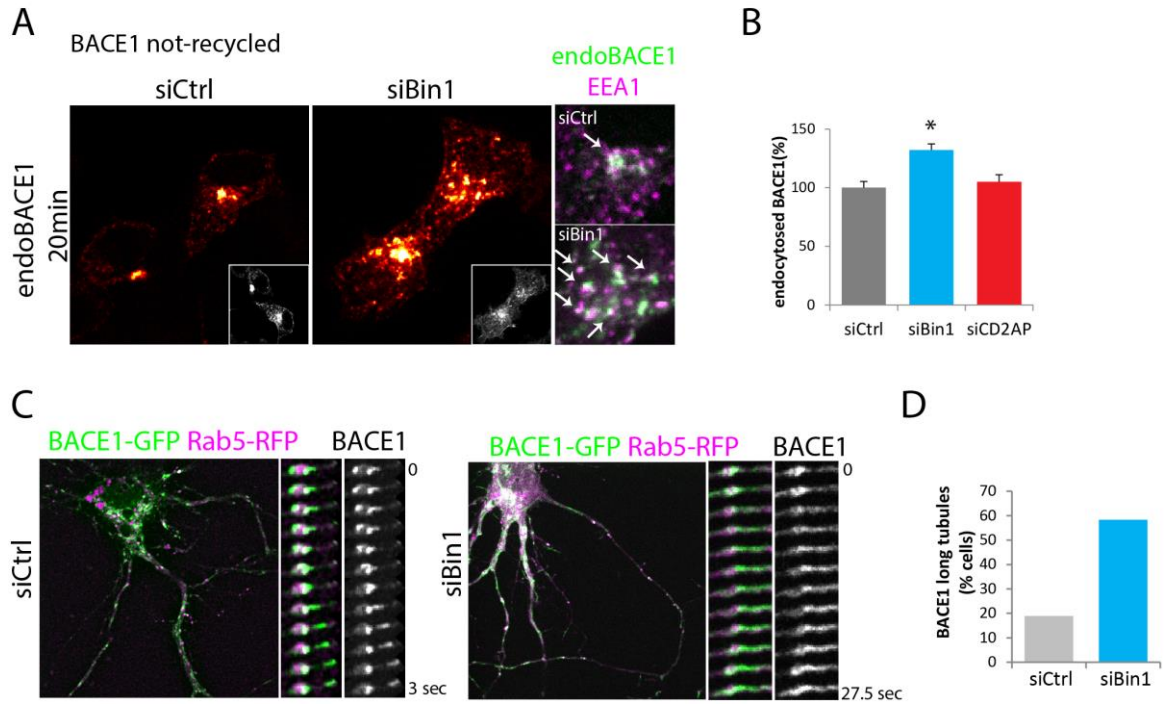

Figure 2.2 Bin1 controls BACE1 recycling via endocytic recycling tubules. **A.** Immunofluorescence images of N2a cells transfected with non-targeting siRNA or with siRNA against Bin1, and with Flag-BACE1-GFP. Flag antibody was pulsed for 10 min and chased for 20 min. Alexa555 was added after surface stripping and permeabilization (internalized anti-Flag; grey). "Red hot" LUT was applied to images. Right panels are magnification of the perinuclear region, showing higher colocalization of internalized BACE1 (green) with EEA1 (purple) in siBin1 than in siCtrl cells. **B.** Quantification of endocytosed BACE1 (not-recycled), represented in A. **C.** Live cell imaging of siCtrl and siBin1 PN, transfected with Flag-BACE1-GFP and Rab5-RFP to label early endosomes. The right panels are frames of a representative time lapse series showing rab5-positive early endosomes (purple) containing BACE1 (green). Scission of endosomal tubules containing BACE1 occurs in siCtrl but not in siBin1 neurons. **D.** Percentage of long BACE1-containing tubules is increased in siBin1 neurons. *<0.05 vs. siCtrl

Next, we investigated the endocytic trafficking of APP. Interestingly, when looking at APP degradation, there was an increase in the remaining APP within the cells, after 60 min, in CD2AP depleted N2a cells, compared to the control and to Bin1 knockdown (Fig. 2.3A and B). APP was retained in early endosomes stained with EEA1, suggesting CD2AP prevents APP degradation (Fig. 2.3A arrows). In primary neurons the result was identical, with APP accumulating mainly in the cell body and in dendrites (not shown).

To visualize APP sorting within endosomes, wild-type neurons were transfected with APP-RFP and Rab5QL-GFP, a constitutively active mutant Rab5 that produces giant endosomes (Fig. 2.3C). In control neurons APP was localized inside the enlarged endosomes, instead, upon CD2AP knockdown, endosomes were almost completely devoid of APP (Fig. 2.3C and D). This loss of APP signal could indicate the release of the RFP-tagged APP C-terminal due to β- and γ-cleavage of APP by BACE1 and g-secretase. To verify this hypothesis, neurons were treated with DAPT, a γ-secretase inhibitor that inhibited APP disappearance from localization to Rab5QL endosomes.

This data indicates that APP is cleaved at a higher rate in early endosomes, in the absence of CD2AP than in control neurons (Fig. 2.3C and D). Rab5QL allows to distinguish in detail the endosomal membrane from the lumen. In control cells, APP was usually at the lumen of the endosomes, yet in CD2AP knockdown cells treated with DAPT, APP was restored at the membrane of the endosome (Fig. 2.3C magnifications and E). Therefore, this data indicates that loss of CD2AP increases the localization of APP to the endosomal membrane thus facilitating APP processing.

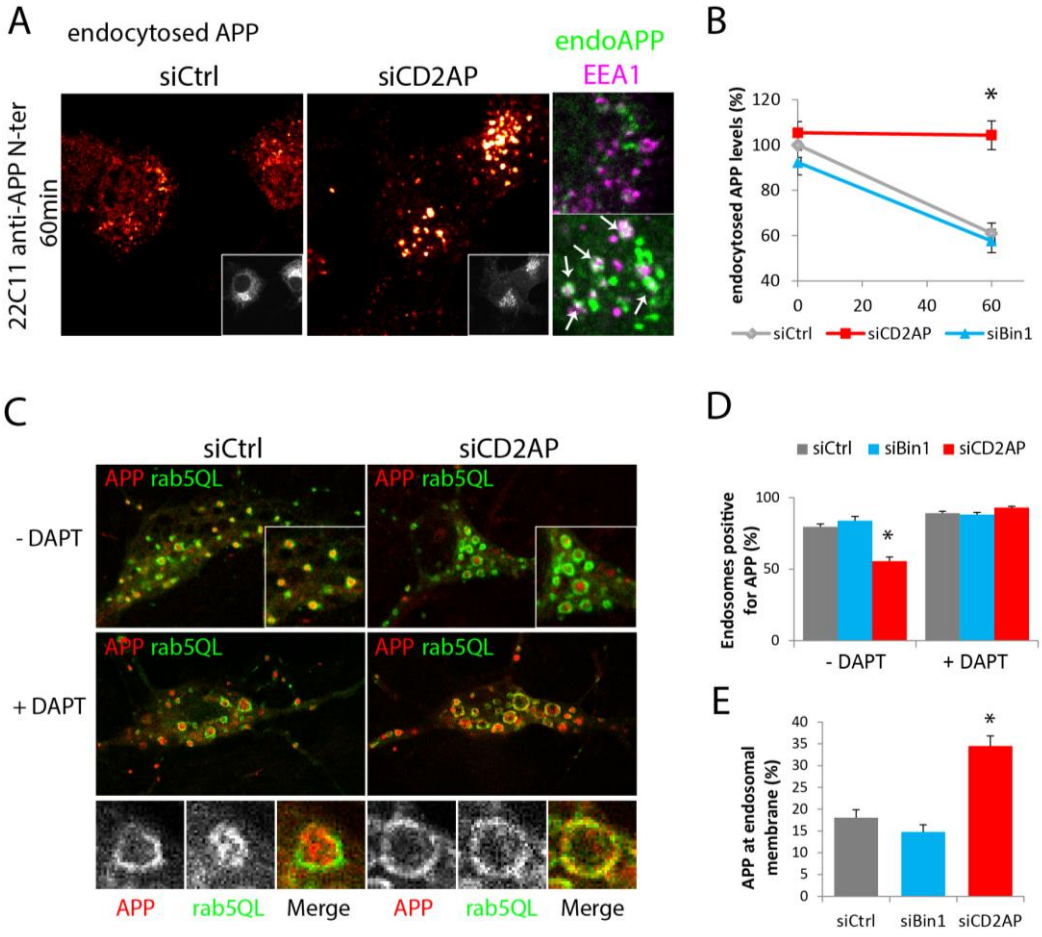

Figure 2.3 CD2AP controls APP sorting to the lumen of endosomes. **A.** Immunofluorescence images of N2a cells transfected with non-targeting siRNA or with siRNA against CD2AP, and with APP-RFP. APP was labeled with a specific antibody (22c11) for 10 min and chased for 60 min (internalized anti-APP; grey). "Red hot" LUT was applied to images. Right panels are magnification of the perinuclear region, showing higher colocalization of internalized APP (green) with EEA1 (purple) in siCD2AP than in siCtrl cells. **B.** Quantification of endocytosed APP (endoAPP) levels in siCtrl and siCD2AP N2a cells at 0 min and 60 min chase period. **C.** Immunofluorescence images of siCtrl and siCD2AP PN transfected with APP-RFP and the mutant rab5QL, and treated or not with DAPT. Magnifications on the bottom show that APP is not sorted to the endosomal lumen of rab5QL endosomes when CD2AP is depleted and APP γ-processing is blocked by DAPT of PN. **D.** Quantification of the number of endosomes containing APP in the lumen. **E.** Quantification of the number of endosomes with APP at the endosomal membrane. *<0.05 vs. siCtrl

In conclusion, Bin1 and CD2AP differentially control the endocytic generation of Aβ by two different mechanisms (Fig. 2.4). First, Bin1 enriched in axons controls BACE1 recycling to

the axonal plasma membrane. In the absence of Bin1, endocytosed BACE1 accumulates in early endosomes, likely due to impaired scission of recycling tubules. Second, CD2AP enriched in dendrites controls APP degradative pathway in the somatodendritic compartment. In the absence of CD2AP, endocytosed APP accumulates in early endosomes, likely due to impaired sorting of APP to the inner luminal vesicles during endosomal maturation.

Thus, these risk factors control different cargo and different intracellular trafficking mechanisms at spatially distinct compartments. Their loss of function promotes BACE1 and APP encounter in early endosomes, leading to the overproduction of $A\beta_{42}$ that triggers synaptic dysfunction, ultimately leading to AD.

Besides their role in intracellular trafficking, Bin1 and CD2AP are also critical regulators of actin dynamics. Therefore, we hypothesize that actin is required for Bin1-dependent tubulation of endosomal membranes, hence allowing BACE1 recycling; and for CD2AP-dependent invagination of endosomal membranes, assisting in multivesicular body sorting of APP for degradation.

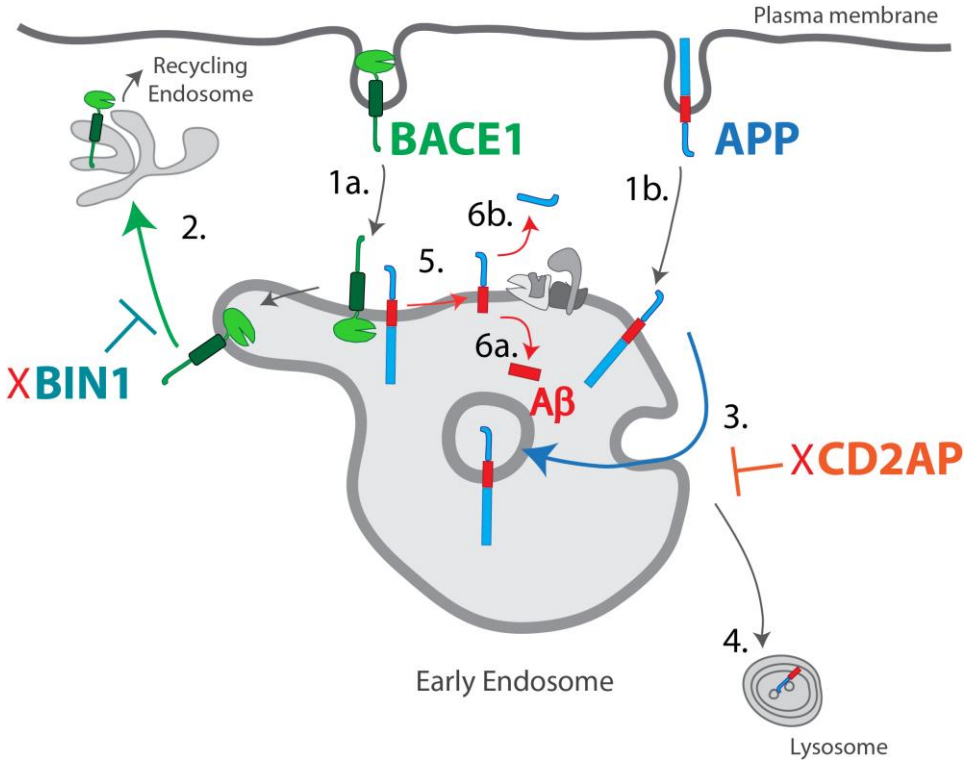

Figure 2.4 Bin1 and CD2AP differentially control the endocytic generation of Aβ (working model). BACE1 and APP at the plasma membrane are endocytosed to early endosomes (1a,1b respectively). BACE1 is recycled back to the plasma membrane through endosomal tubules (2), whereas APP is sorted to inner luminal vesicles during endosomal maturation and MVB formation (3), ultimately being degraded in the lysosome (4). At the endosomal membrane, APP is cleaved by BACE1, generating an APP β-CTF (5), which is then cleaved by γ-secretase complex, releasing Aβ (6a) and an APP γ-CTF (6b). Bin1 knockdown (red cross) prevents BACE1 recycling, likely via impaired endosomal tubule scission. CD2AP knockdown prevents endosomal sorting of APP and its degradation, retaining it at the limiting membrane of the endosome, where it is cleaved by BACE1 and γ-secretase, increasing Aβ generation.

Chapter 3

Materials and Methods

3.1 Antibodies and Constructs

Table 3.1 Antibodies and probes used in this study, with respective dilutions and suppliers.

Primary antibodies	IF dilution	WB dilution	Supplier
α-tubulin	-	1:20000	Sigma-Aldrich
Aβ42	1:50	-	Genetex
Actin	-	1:1000	abcam
Bin1	1:100	1:1000	EMD Millipore
Cd2ap	1:100	1:1000	Santa Cruz Biotechnology
EEA1	1:50	-	Santa Cruz Biotechnology
Flag M1	1:300	-	Sigma-Aldrich
PSD-95	-	1:1000	Cell Signaling Technology
WASH	1:250	1:1000	Gift from E. Derivery
Secondary antibodies	IF dilution	WB dilution	Supplier
Alexa-555 anti-goat	1:500	-	Invitrogen
Alexa-647 anti-goat	1:250	-	Invitrogen
Alexa-647 anti-mouse	1:500	-	Invitrogen
Alexa-647 anti-rabbit	1:500	-	Invitrogen
HRP anti-mouse	-	1:5000	Bio-Rad
HRP anti-rabbit	-	1:5000	Bio-Rad
Probes	IF dilution	-	Supplier
Phalloidin-488	1:200	-	Life Technologies
Phalloidin-555	1:200	-	Life Technologies
Phalloidin-568	1:100	-	Life Technologies

Table 3.2 Constructs used in this study, with respective concentrations used and suppliers.

Construct	Concentration (μg/μL)	Supplier
APP-mRFP	0.5	Gift from S. Kins
Flag-BACE1-GFP	0.5	Gift from S. Miserey-Lenkei
Lifeact-mCherry	0.5	Gift from G. Montagnac
Rab5-GFP	0.5	Gift from M. Arpin and D. Chirivino

3.2 DNA amplification

E.coli DH5α Transformation

Competent bacteria (*E.coli* DH5α) (Life Technologies) was slowly thawed on ice, and subsequently 0.5 μg of DNA was added to 50 μL of bacteria and mixed. Bacteria were incubated on ice 30 min and then exposed to a heat shock (an increase in temperature) at 42ºC for 20 sec, inducing the formation of pores through which plasmidic DNA can enter. Returning the cells to a lower temperature (2 min on ice) allows the cell wall to self-heal. Once cells had taken up the plasmid, Luria Bertani (LB) (Sigma-Aldrich) medium was added and they were put to grow on a shaker for 1h at 37ºC. After this, the medium with bacteria was spread on LB-agar plates containing 100 μg/mL of antibiotics, according to the antibiotic resistance of the construct used (ampicillin 50 mg/mL; kanamycin 5 mg/mL) (VWR). Cells grew overnight at 37ºC.

Plasmid DNA preparation

A single colony of transformed bacteria, grown in LB-agar plate or from a glycerol stock was picked with a sterile pipette tip. The pipette tip was deposited in 5 mL of LB medium containing either ampicillin (100 μg/mL) or kanamycin (100 μg/mL). Bacteria were incubated for 8h at 37ºC in an orbital shaker (189 rpm). After this, starter culture was used to inoculate an erlenmeyer containing LB medium supplemented with antibiotic, depending on the antibiotic resistance of the construct used. The culture was incubated overnight at 37ºC in an orbital shaker (189 rpm). Plasmid DNA purification from *E.coli* cells was performed using the NZYMidiprep (NZYTech), following their protocol. The precipitated DNA was dissolved in ultraPure DNase/RNase free distilled water (Invitrogen, Life Technologies) and the DNA concentration was determined by absorbance at 260 nm, using NanoDrop 2000 UV-Vis spectrophotometer (Thermo Scientific).

After transformed and grown in LB medium overnight at 37ºC, *E.coli* cells in exponential phase of growth were added to 50% glycerol in a cryovial (Thermo Scientific) and then stored at -80ºC.

3.3 Tissue Culture

Cell lines

N2a cells are a mouse neuroblastoma cell line (Mouse Neuro 2a or N2a). These cells are like neural precursors that have the ability to differentiate into neurons, and are able of unlimited proliferation *in vitro*[94]. N2a cells were cultured in Dulbecco's Modified Eagle Medium (DMEM) (DMEM+GlutaMAX, Gibco, Life Tecnhologies) supplemented with 10%

fetal bovine serum (FBS) (Sigma-Aldrich) in a humidified incubator at 37ºC with 5% CO_2. Once the cells reached 80%-90% confluence, they were washed once with phosphate buffered saline (PBS pH 7.4) (Gibco, Life Technologies) and trypsin (Life Technologies) was added to dissociate adherent cells from the dish. After trypsin addition, cells were incubated 5 minutes at 37ºC with 5% CO_2. Trypsin activity was stopped by adding complete medium (DMEM+FBS). The resulting cell suspension was split, in a dilution of 1:10, to another dish to maintain culture. According to each experiment, cells were plated in different amounts.

Mouse primary neuronal cultures

Mouse primary neuronal cultures were prepared from cerebral cortices of mice embryos with 16 days of gestation (E16). Brains were dissected in ice-cold Hanks balanced salt solution (HBSS; Gibco, Life Technologies) with 0.45% glucose (from 50% D-glucose stock in water) (Sigma-Aldrich) and 0.5% HEPES 10mM (Gibco, Life Technologies). Under magnifier, cortices were separated from brains and digested with 0.1% trypsin (Life Technologies) in HBSS/Glucose/HEPES solution at 37ºC for 15 min. Then, trypsin was removed and cortices were washed 3 times with HBSS/Glucose/HEPES solution to inhibit trypsin activity. To dissociate neurons from the cortices, DMEM was supplemented with 10% FBS and 1% Penicillin/Streptomycin (10 000 units/mL of penicillin; 10 000 µg/ml of streptomycin) (Gibco, Life technologies) was added, and by pipetting up and down with a glass pipette the cortices were triturated. A centrifugation step was performed to remove the supernatant and ressuspend the pellet in DMEM/FBS/Pen/Strep solution. After counting, the cells were plated on Poly-D-lysine hydrobromide (2mg/ml) (Sigma-Aldrich) coated 6-well plates (used for Western blot) (VWR) and glass coverslips (Menzel) on 24-well plates (used for immunofluorescence) (VWR), diluted in complete medium for PN, and incubated at 37ºC with 5% CO_2. The day after, medium was substituted to Neurobasal (Gibco, Life Technologies) containing 0.1% GlutaMAX supplement, 1% Pen/Strep and 2% B-27 supplement (GibcoTM, Life Technologies).

The dissection process was always performed by Florent Ubelmann, and the coating of coverslips (addition of poly-D-lysine), preparation of Neurobasal/GlutaMAX/Pen/Strep/B-27 solution, complete medium for PN and HBSS/D-Glucose/HEPES solution was mainly done by Tatiana Burrinha. I occasionally helped her with these tasks.

Counting and plating cells

After trypsinization and dilution in complete medium, trypan blue (Amresco), a dye that colors intact cell membranes, was added to cell suspension in a 1:2 dilution. This mix was added to the Neubauer Chamber (or Haemacytometer) and cells not stained with trypan blue (viable) were counted. Then, cell average of the four grid squares in the haemacytometer was

multiplied by the dilution factor and the conversion factor for neubauer, 10^4. Cell were plated according to Table 4.3.

Table 3.3 Number of cells per mL that were plated according to each method.

Transfection	Cell type	Number of cells per well	Method
None or overexpression	N2a	80 000 100 000	Immunofluorescence Western blot
	PN	100 000	Immunofluorescence
siRNA Control	N2a	40 000 120 000	Immunofluorescence Western blot
	PN	100 000	Immunofluorescence Western blot
siRNA Bin1	N2a	45 000 135 000	Immunofluorescence Western blot
	PN	100 000	Immunofluorescence Western blot
siRNA Cd2ap	N2a	30 000 90 000	Immunofluorescence Western blot
	PN	100 000	Immunofluorescence Western blot

Plasmid transiently transfection

N2a cells were plated in glass coverslips in a 24-well plate or in a 6-well plate and cultured in complete medium in 5% CO_2 at 37°C. After 24h of culture, the confluence was about 80%-90% and cells were transiently transfected with the cDNA of interest (Table 3.2), using Lipofectamine 2000 (Invitrogen). For each plasmid transfection, it was prepared a mix with 0.5 µg DNA in 12.5 µL of Opti-MEM (Gibco, Life Technologies) medium and another with 0.5 µL Lipofectamine 2000 in 12.5 µL of Opti-MEM (volumes per well). Mixes were combined and incubated for 20 min at room temperature and then added to each well and incubated with the cells, at 37°C in a 5% CO_2 incubator. After approximately 3 hours, the medium was changed to complete medium and cells stayed in the incubator until the next day, when assays were performed.

PN were transfected at 7-12 *DIV* when the confluence was about 90%-95% and neurons were completely developed, having somatodendritic polarity and mature synapses[95].

siRNA transfection

N2a cells and PN were transfected with 10 µM of non-targeting control siRNA (10 nM) (Life Technologies), 20 µM of siRNA specific for BIN1 (20 nM) (Life Technologies), or 10nM of siRNA targeting CD2AP (10uM) (Santa Cruz Biotechnology). For each siRNA transfection, two separate mixes were prepared, one with 0.5 µL non-targeting siRNA, or 1 µL siRNA

against BIN1, or 0.5 µL siRNA against CD2AP, in 25 µL of Opti-MEM medium, and the other with 0.8 µL Lipofectamine RNAiMAX transfection reagent (Invitrogen, Life Technologies) in 25 µL of Opti-MEM medium (volumes per well). Mixes were combined and incubated for 20 min at room temperature. The cell culture medium was removed from 24-well plates and complete growth medium without Pen/Strep was added. The mix was then added to each well and incubated with the cells at 37°C in a 5% CO_2 incubator for 72 h.

In experimental procedures that included siRNA transfection plus the transient transfection of another plasmid, cells were first transfected with siRNA and after 48h the cell culture medium (containing the siRNA) was removed and stored. New medium (DMEM+FBS) was added and the transient transfection of the plasmid was done as previously described. After approximately 3 hours, the cell culture medium was removed and substituted with the stored medium containing the siRNA. Cells were then incubated at 37°C in a 5% CO_2 incubator until the next day, completing the 72h with the siRNA. This procedure was only done in N2a cells.

Latrunculin A treatment

N2a cells were treated with 10 nM of dimethyl sulfoxide (DMSO) or with 10 nM of latrunculin A (Sigma-Aldrich) overnight, at 37°C in a 5% CO_2 incubator. In the morning of the next day, cells were fixed with 4% paraformaldehyde (PFA) (Sigma-Aldrich) with 0.1 mM Ca^{2+} (Sigma-Aldrich) and Mg^{2+} (Merck) in PBS for 20 minutes at room temperature, and stored at 4ºC until the afternoon, when the immunofluorescence procedure was performed.

3.4 Fluorescence microscopy

Standard Immunofluorescence

After transfection, N2a cells were washed in PBS 1X with 0.1 mM Ca^{2+} and Mg^{2+} and fixed in 4% PFA (Sigma-Aldrich) with 0.1 mM Ca^{2+} and Mg^{2+} in PBS for 20 minutes at room temperature. Thereafter, cells were washed 2 times in PBS 1X and permeabilized in 0.1% saponin in PBS 1X for 1 hour at room temperature. Cells were washed twice again in PBS 1X and then blocked in 3% FBS in PBS 1X for 1 hour at room temperature. After blocking, cells were incubated for 1 hour at room temperature with primary antibodies in blocking solution. Cells were then washed four times with PBS 1X to remove the excess of primary antibody. Appropriate secondary antibodies diluted in blocking solution were used for 1 hour at room temperature. After washing four times with PBS 1X, coverslips were mounted on slides with Fluoromount-G (SouthernBiotech).

PN immunofluorescence assays were performed as described for N2a cells, except for the fixation step that was performed in 4% PFA plus 4% sucrose (Fisher Scientific) diluted in PBS

1X for 20 minutes at room temperature, and the blocking step that was done in 3% FBS plus 1% BSA in PBS 1X for 1 hour at room temperature.

Exceptionally, N2a cells stained with Aβ or EEA1 were incubated with primary antibodies in blocking solution overnight at 4ºC. PN stained with EEA1 were incubated with primary antibodies in blocking solution (3% FBS and 1% BSA) plus 0.1% saponin in PBS 1X, overnight at 4ºC. Additionally, N2a cells used for super-resolution microscopy were fixed and permeabilized as previously, and the blocking solution used contained 3% FBS, 1% BSA and 0.1% saponin in PBS 1X. Primary antibodies were diluted in this solution and incubated overnight at 4ºC. After staining with secondary antibodies (diluted in blocking solution), cells were again fixed with 4% PFA for 5 minutes. Coverslips were embedded in an oxygen scavenger buffer, as previously described[96], imaged on the same day of labeling, and kept in the dark until imaged.

Immunofluorescence and pre-permeabilization

For imaging endogenous bin1 and cd2ap along with APP and BACE1 in the perinuclear region, N2a cells were pre-permeabilized as in *Almeida et al., 2011* with minor alterations. Briefly, 24 hours post-transfection cells were washed in PBS 1X with 0.1 mM Ca^{2+} and Mg^{2+} and were pre-extracted with 4% PFA plus 0.3% Triton X-100 (Acros Organics) in PBS 1X for 30 seconds. Then, they were fixed with 4% (v/v) PFA with 0.1mM Ca^{2+} and Mg^{2+} in PBS 1X for 20 minutes. Cells were washed in PBS 1X three times and blocked in 3% FBS in PBS 1X for 1 hour at room temperature. After blocking, the procedure was the same as described in *Standard immunofluorescence.*

BACE1 internalization

After siRNA and Flag-BACE1-GFP transfection, N2a cells were placed with DMEM without FBS (starvation) at 37ºC for 1h, to improve flag antibody uptake. Then, cells were incubated with Flag M1 primary antibody (Sigma-Aldrich), diluted in DMEM/FBS plus 10 mM HEPES (Gibco, Life Technologies), for 10 min at 37ºC, allowing the antibody to bind to Flag-BACE1-GFP (pulse). Cells were then incubated with DMEM/FBS/HEPES, for 20 min at 37ºC, so that BACE1 would be internalized (chase). After this, cells were washed twice with PBS 1X, fixed with 4% PFA for 20 min and again washed 3 times with PBS 1X. The subsequent steps are the same as described in *Standard immunofluorescence.*

Image acquisition

Most images were acquired on a Zeiss Z2 upright widefield microscope, equipped with an AxioCam 506 mono, using the 63x/1.4NA Plan-Apochromat Oil immersion objective, Alexa fluor 488 (517 nm) + Alexa fluor 647 (668 nm) + Alexa fluor 594 (618 nm) fluorescence filtersets and DIC optics, controlled with the ZEN Imaging software.

Exceptionally, some images were acquired on different microscopes. Images from figures 4.10B, 4.11 and 4.12 were acquired on a Leica DMRA2 upright microscope, equipped with a CoolSNAP HQ CCD camera, using the 100x/1.4NA Oil immersion objective, FITC (519 nm) + Cy5 (665 nm) fluorescence filtersets and DIC optics, controlled with the MetaMorph software. Images from figures 4.1B, 4.2 and 4.6 were acquired on an Andor Spinning-disk confocal microscope, using the 100x/1.4NA Oil immersion objective and a Andor iXon+ EMCCD camera to acquire images for the emission of the Alexa 488 and Alexa 555 flurochromes.

Images from figure 4.1D were acquired on a super-resolution dSTORM microscope. Briefly, for each coverslip, 4-5 area fields were pre-selected on the microscope for imaging, based on EEA1 signal. This enabled to determine the proper localization and expression levels of the proteins of interest in the analyzed cells. Then, the objective was refocused on the surface of the coverslip, TIRF illumination was switched and a dSTORM image-stream acquisition was performed for the Cy5 channel (635 nm laser-excitation at 1.7 kW/cm^2, 662–690 nm emission) and then for the Alexa Fluor 568 channel (561 nm laser-excitation at 2.4 kW/cm^2, 589–625 nm emission), each composed of 30.000 images acquired at 30 Hz. Imaging parameters were set using the Manager freeware running on a desktop PC. Single-molecule detection and localization was carried by a custom algorithm using the ThunderSTORM Fiji plugin[97]. Potential sample drifting was automatically corrected. I did the immunofluorescence procedure; Nuno Pimpão Martins (from the Advanced Imaging Unit at Instituto Gulbenkian de Ciência) acquired the images, and Florent Ubelmann analyzed them.

Single cell and perinuclear quantitative analysis

All images were analyzed with Fiji (ImageJ) software. To assess the average fluorescence on cell lines, cells were outlined using the "polygon selection" tool. First, the average fluorescence of a region of the background was measured and after this, the average fluorescence of a cell was quantified with the "measure" function. The average fluorescence of the background was then subtracted to the average cellular fluorescence. The results were presented in percentage of the average fluorescence of cells expressing siRNA Control or treated with DMSO (100%, control).

To quantify the average fluorescence of the perinuclear region, the area adjacent to the cell nucleus where there was a concentration of staining was considered as perinuclear. This region was outlined using the "polygon selection" tool and its average fluorescence was measured, as for the single cell measurement. The total intensities of the cell and the perinuclear region were calculated, multiplying their mean fluorescence intensity (after subtraction of the background average fluorescence) by the respective area. Then, the total intensity of the perinuclear region was divided by the cell's total intensity and presented as the ratio perinuclear:cell fluorescence in percentage.

Line profile analysis

In images of N2a cells with labeled F-actin, a line with 80 μm width was drawn, using Fiji software, across the cell, from the cortical region in one side of the cell, through the perinuclear region, to the cortical region on the other side. Then, the "plot profile" tool from Fiji was used and the results were copied to Excel and normalized to the mean F-actin fluorescence of cells treated with control siRNA. The graphs depicting the normalized F-actin fluorescence according to distance were then made, for each condition, in Excel.

Colocalization analysis

To analyze colocalization on dendrites of PN, a portion of a dendrite, with approximately 20 μm was selected in the F-actin channel using the "rectangular selection" tool and that region of interest (ROI) was transferred to the EEA1 channel (Fig. 3.1-1). Then, images were processed with the "subtract background" tool with the rolling ball radius set to NaN pixels. When setting background pixels to NaN it gives an image in which the foreground pixels retain their original value, while the background pixels are not turned to 0 but to Not A Number (NaN), which is a special value that ImageJ ignores when measuring. Thus, it is used to mask out regions. Background subtraction to NaN was used to present colocalization figures, since it facilitated its observation, and in order to do a clear threshold of the region of interest to be analyzed. To measure fluorescence intensity, the resulting threshold must be applied to the original image (without background subtraction). After background subtraction, the "polygon selection" tool was used to outline the dendrite and with the "clear outside" tool it was possible to have just the section delimitated (Fig. 3.1-2). Afterwards, the "threshold" tool was used in the EEA1 channel to delimitate EEA1-positive endosomes, which were then selected with the "Create selection" tool (Fig. 3.1-3). This selection was transferred to the F-actin channel and cleared outside (Fig. 3.1-4). Then the threshold of this selection was done in the F-actin channel, determining the F-actin puncta overlapping with the EEA1-positive endosomes (Fig. 3.1-5). Both thresholds (in F-actin and EEA1 channels) were analyzed using the "analyze particles" tool (Fig. 3.1-6). The amount of EEA1 vesicles associated with F-actin was determined doing the ratio of F-actin-positive EEA1 particles by the total EEA1 particles, and presented as a percentage.

In N2a cells, the procedure was as described above, but outlining the cell or a region of interest in it. When examining the colocalization between F-actin and other proteins, the same procedure was done but instead of the EEA1 channel it was used the channel of the protein of interest. Exceptionally, images acquired on the Spinning-disk confocal microscope did not require the background subtraction step, since the resolution of the images allowed the correct threshold of the particles.

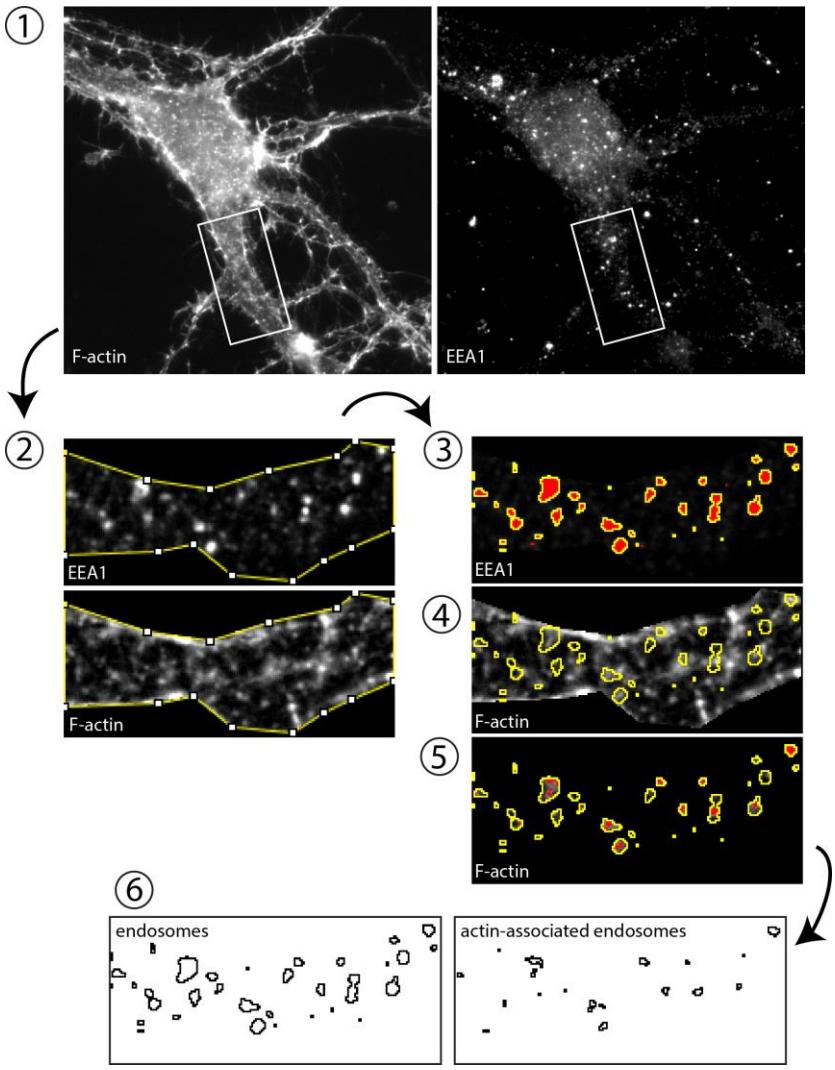

Figure 3.1 Scheme of the colocalization method used in dendrites of primary neurons, using Fiji software. **1.** A portion of a dendrite, with approximately 20 µm, is selected in the F-actin channel and transferred to the EEA1 channel. **2.** Images are processed with the "subtract background" tool and the dendrite is delineated and cleared outside, in both channels. **3.** The EEA1 channel is thresholded and a selection is created, in order to get a mask of the early endosomes. **4.** The EEA1 mask is transferred to the F-actin channel. **5.** The F-actin channel image, with the applied EEA1 mask, is cleared outside and a second threshold is done to obtain the F-actin puncta in early endosomes. **6.** The number of particles in both channels is counted with the "analyze particles" tool and the ratio between the number of endosomes with associated F-actin and the total number of endosomes, in that portion of the dendrite, is calculated.

3.5 Immunobloting

Preparation of cell lysates

N2a cells and PN, after transfection, were placed on ice and washed with ice-cold PBS 1X. Lysis buffer, also known as RIPA buffer (Radio-Immunoprecipitation Assay) was added to cells to enable a rapid and efficient cell lysis. RIPA buffer was composed by 50nM Tris-HCl pH 7.4 (Sigma-Aldrich), 1% NP-40 (Sigma-Aldrich), 0.25% sodium deoxycholate (Sigma-Aldrich), 150mM NaCl (NZYTech), 1mM EGTA (Sigma-Aldrich) supplemented with

protease inhibitor cocktail (Roche Diagnostics). After RIPA buffer addition, cells were lysed by scraping with a rubber policeman to ensure the complete rupture of cell membranes. Lysates were placed on ice for 15 min and after this were centrifuged for 10 min at 12 000 x g at 4ºC. Supernatants were frozen and stored at -80ºC until used.

Western Blot

Proteins from cell lysates were denatured by the addition of sample buffer (Tris 0.25M pH 6.8, 40% glycerol (Sigma-Aldrich), 8% sodium dodecyl sulfate (SDS) (Sigma-Aldrich), Bromophenol blue 0.015% (GE Healthcare) and 10% β-mercaptoethanol (Sigma-Aldrich)) and by heating to 95ºC for 5 min. Proteins were separated by using Tris-Glycine SDS-PAGE (running buffer: 25 mM Tris, 192 mM glycine (NZYTech) and 0.1% SDS) at 120 V for 2-3h, using BioRad Mini-PROTEAN. Electrophoretic transfer (transfer buffer: 150mM glycine, 20mM Tris, 0.037% SDS, 20% ethanol 96% (VWR)) to nitrocellulose membranes (GE Healthcare Life sciences) was performed at 10 V for 1h, using Bolt Mini Blot Module. The percentage of acrylamide (NZYTech) gels was 7.5%.

After transfer, membranes were blocked in PBS containing 0.01% Tween 20 (PBST) (Sigma-Aldrich) and 5% non-fat dry milk for 30 min at room temperature, so that milk proteins prevent non-specific antibody binding to the membrane after antibody addition. Incubation with primary antibody diluted in 1% non-fat dry milk in 0.01% PBST was done for 1h at room temperature or overnight at 4ºC, always under stirring. Membranes were rinsed three times with 0.01% PBST, during 5 min, to remove the non-specifically bound primary antibody. The, membranes were incubated with secondary antibody, conjugated to the reporter enzyme Horseradish peroxidase (HRP), diluted in 0.01% PBST with 1% non-fat dry milk, for 1h at room temperature. Membranes were further rinsed three times with 0.01% PBST, during 5 min, to remove the non-specifically bound secondary antibody. To detect target proteins, membranes were incubated with equal amounts of luminol and peroxide solution, for 1 min, in a process called enhanced chemiluminescent (Amersham ECL Prime Western Blotting Detection Reagent, GE Healthcare). Horseradish peroxidase catalyzes the oxidation of luminol, emitting light in the same proportion of protein quantity. The protein immunoreactive bands were visualized by ChemiDoc XRS+ system. Exposure times varied depending on the target proteins. Analysis of protein band intensities was performed using Fiji software and band intensities of the proteins of interest were normalized to the corresponding band intensity for α-tubulin.

3.6 Statistical analysis

Experiments done with sets of neurons prepared from sibling embryos from different mothers were considered independent experiments. Experiments done with cells plated in different days were considered independent experiments. The statistical analysis was

performed using the SPSS statistical package version 20 (IBM). Due to sample size, the Shapiro-Wilk test was used to verify the data for normality. Since an absence of a Gaussian distribution was observed in continuous variables, a non-parametric approach was used to analyse the data. Statistical comparisons, to check significant differences between two groups of independent variables, were performed using *t*-test and the Mann-Whitney test, with significance placed at $p < 0.05$. Data is presented as mean ± SEM (standard error of the mean)

Chapter 4

Results

4.1 Characterization of the actin pool associated with early endosomes

We started by studying the pool of actin associated with early endosomes in a neuronal-like cell line (N2a cells). To visualize filamentous actin (F-actin) associated with early endosomes we used fluorescent phalloidin, an F-actin binding probe, and EEA1, an early endosome protein to label N2a cells. In N2a cells (Fig. 4.1), we observed by epifluorescence microscopy F-actin concentrated at the cortex and enriched in filopodia, finger-like membrane protrusions (Fig. 4.1A a). In the perinuclear region (Fig. 4.1A d, inset) there is a concentration of discrete actin puncta. In this same region we observed a concentration of EEA1-positive endosomes (Fig. 4.1A b). In higher magnification (Fig. 4.1A d-f) we observed an F-actin puncta often juxtaposed or overlapping early endosomes. In fact, 63% of endosomes in the perinuclear region were associated with actin puncta (Fig. 4.1A f).

Next, in order to image early endosomes and F-actin with a better resolution, spinning-disk confocal microscopy was used (Fig. 4.1B a-c). At higher resolution EEA1 endosomes were found more frequently associated with F-actin (86% overlap) (Fig. 4.1B d-f). To complement these results, N2a cells were transfected with Lifeact-mCherry that binds F-actin, allowing for its indirect visualization, and with Rab5-GFP, a small GTPase that localizes to early endosomes (Fig. 4.1C a-c). Cells expressing Lifeact-mCherry and Rab5-GFP exhibited a perinuclear concentration of F-actin and Rab5-positive endosomes (Fig. 4.1C a, b), with 56% of endosomes being associated with actin in the perinuclear region (Fig. 4.1C d-f). Additionally, we used dSTORM microscopy, to reach 100 nm resolution, in order to resolve the association of F-actin with early endosomes at super resolution (Fig. 4.1D). N2a cells imaged by dSTORM exhibit phalloidin-labeled F-actin structures often adjacent to endosomes labeled with EEA1 (Fig. 4.1D b-e). In conclusion, actin is frequently associated with early endosomes in N2a cells, as previously described in non-polarized cells [86].

Next, we investigated the association of F-actin with early endosomes in polarized cortical and hippocampal primary neurons prepared from wild-type mice (PN). In PN at 9-12 DIV, EEA1-positive endosomes are scattered throughout the soma and dendrites (Fig. 4.2 b) but absent from axons, consistent with the previously described polarized distribution of EEA1 to somatodendritic endosomes [23]. The absence of a concentration in the perinuclear region reflects the complex and bidirectional organization of the microtubule network in neurons[9]. We observed F-actin organized in discrete puncta and in patches (Fig. 4.2 a), consistent with *D'Este et al.,* F-actin puncta were often associated with EEA1-positive endosomes in neuronal cell bodies and throughout dendrites, in contrary to N2a cells where F-actin puncta are concentrated in the perinuclear region (Fig. 4.2 c-f).

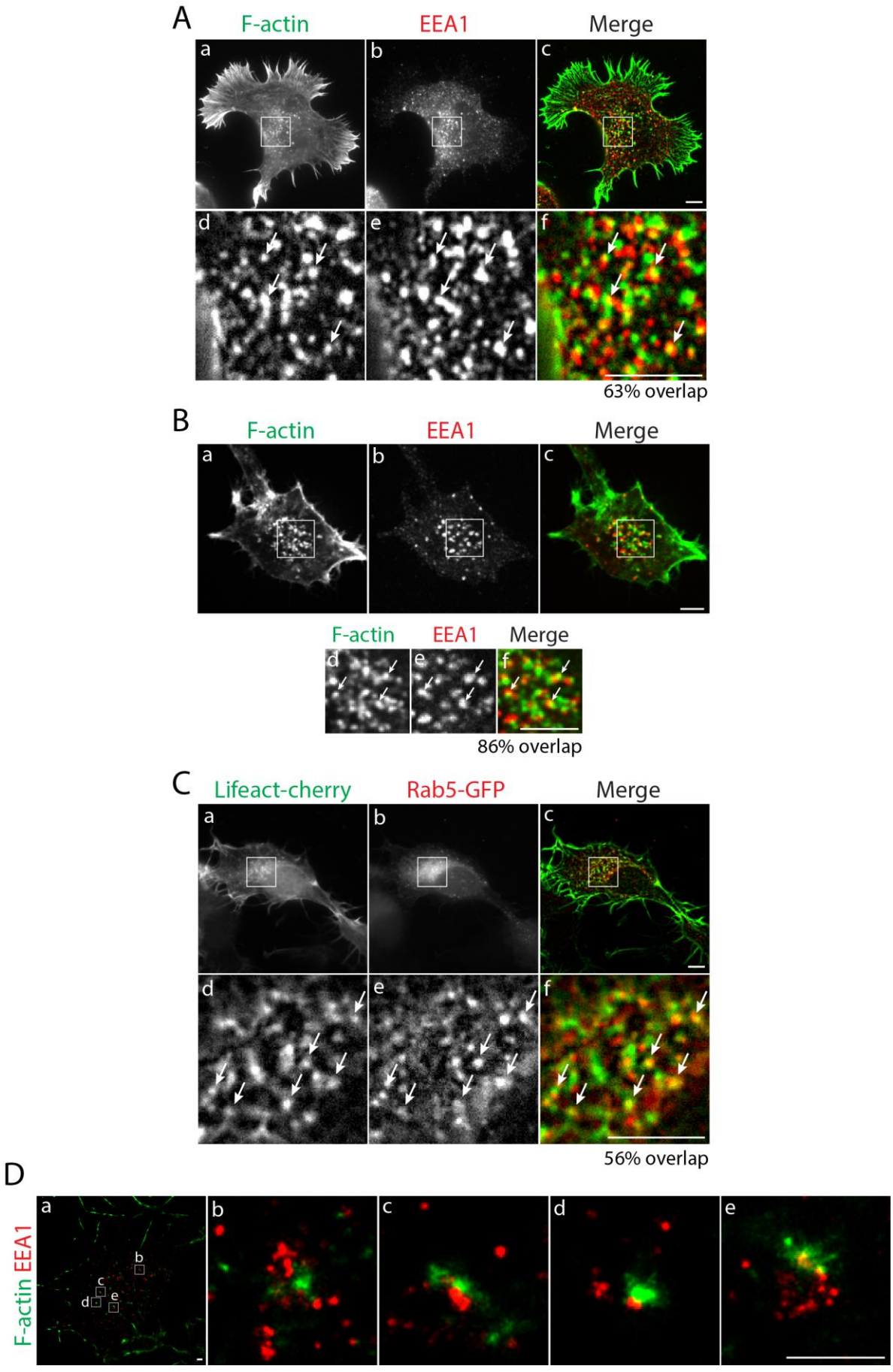
A
F-actin
EEA1
Merge
63% overlap
B
F-actin
EEA1
Merge
86% overlap
C
Lifeact-cherry
Rab5-GFP
Merge
56% overlap
D
F-actin EEA1

Figure 4.1 F-actin associates with early endossomes in N2a cells. Representative images of N2a cells with labeled F-actin and early endosomes. **A.** Epifluorescence images phalloidin-labeled F-actin and EEA1-labeled early endosomes (a, b). Note EEA1 and F-actin puncta accumulated in the perinuclear region. Merged images of F-actin (green) and EEA1 (red) (c). White boxes in (a, b, c) correspond to magnifications in (d, e, f), respectively. **B.** Spinning-disk confocal images stained as in A. (d, e, f) are magnifications from (a, b, c - boxes) respectively. **C.** Epifluorescence images of cells transiently transfected with Lifeact-mCherry, to visualize F-actin (a), and with Rab5-GFP, a protein present in early endosomes (b); (c) represents the merge of F-actin and rab5; (d, e, f) are magnifications from (a, b, c - boxes) respectively. **D.** Super-resolution images of an N2a cell exhibiting F-actin and EEA1 structures throughout the cytoplasm (a). Boxes in (a) are magnified in (b, c, d, e). Arrows indicate colocalization. Merged images and magnifications in A, B and C were background subtracted. Scale in A, B and C, 5 µm. Scale in D, 1 µm.

Discrete F-actin puncta were often associated with EEA1-positive endosomes, either overlapping or juxtaposed, in both N2a cells (Fig. 4.1) and PN (Fig. 4.2), despite early endosomes being polarized and spread out in dendrites in PN. Thus, we observed for the first time that a pool of F-actin associates with dendritic early endosomes in PN, indicating a possible role for actin in endosomal membrane remodeling in neurons.

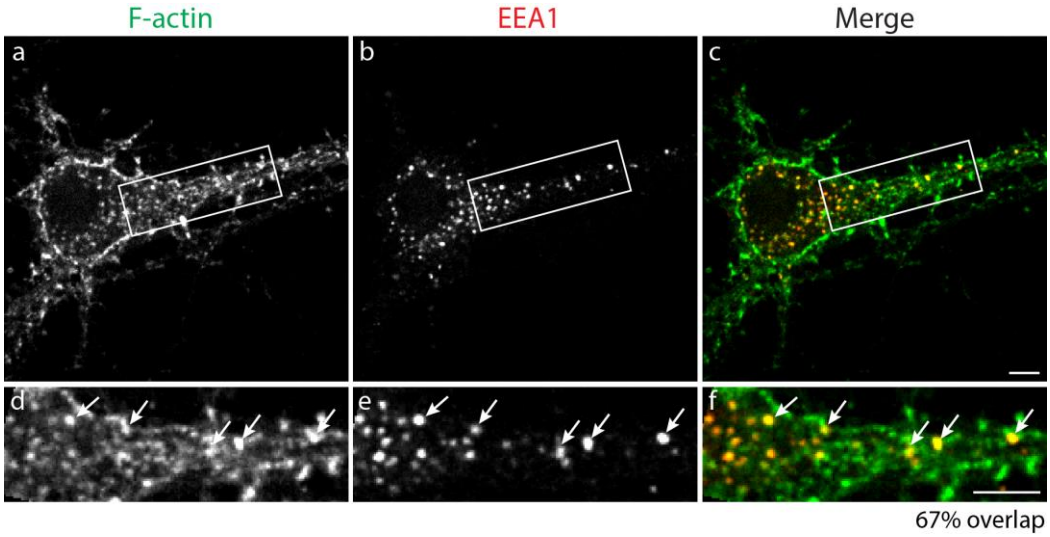

Figure 4.2 F-actin associates with early endosomes in the cell body and dendrites of primary neurons. Spinning-disk confocal image of a neuron, at 9-12 DIV, exhibiting F-actin patches and puncta, labeled with phalloidin (a), and early endosomes labeled with EEA1 (b). Merged images of F-actin (green) and EEA1-positive endosomes (red) are represented in (c). (d, e, f) are magnifications of boxes in (a, b, c) respectively. Colocalization appears in yellow and pointed with arrows. Scale, 5 µm.

4.2 Bin1 and CD2AP localization to actin-positive early endosomes

Bin1 and CD2AP have been reported to localize to endosomes[80,86] and to work as actin-regulatory proteins, thus we investigated if they localized to actin-positive-early endosomes. To confirm the association of Bin1 and CD2AP with early endosomes and with F-actin, we labeled filamentous actin and early endosomes as previously, and used specific antibodies to label endogenous Bin1 and CD2AP in N2a cells. Bin1 was evenly distributed within the cell (Fig. 4.3A c), making it difficult to evaluate the previous described endosomal localization or its codistribution with F-actin. The few Bin1 puncta detected were found adjacent to

endosomes associated with actin (Fig. 4.3A e-h, arrows). CD2AP was evenly distributed within the cell, in discrete vesicular puncta (Fig. 4.3B c), in agreement with previous data[80]. A pool of CD2AP puncta could be found juxtaposed with early endosomes and actin, frequently with two or three puncta of endogenous CD2AP surrounding EEA1-positive endosomes associated with F-actin (Fig. 4.3B e-h).

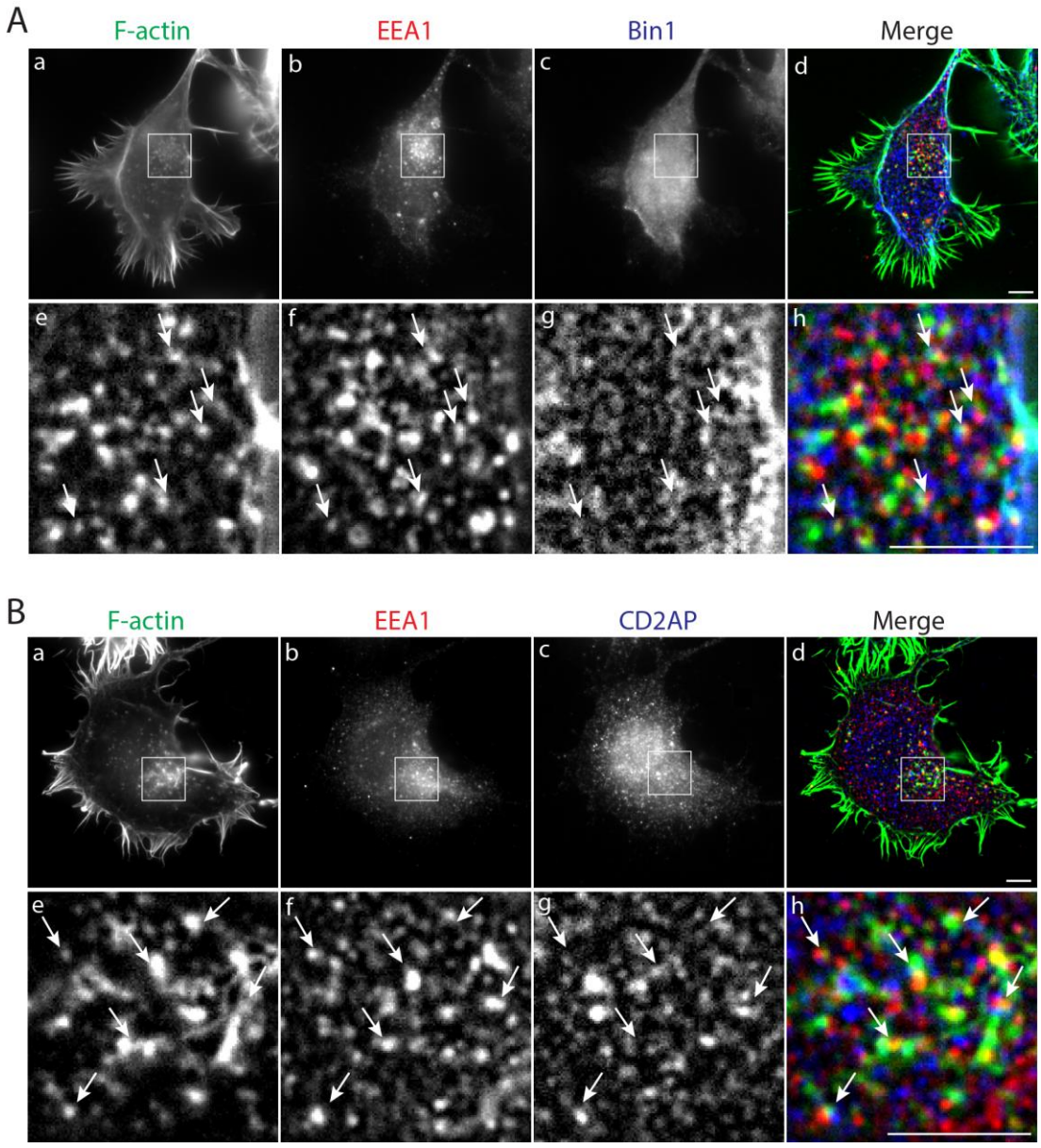

Figure 4.3 Bin1 and CD2AP localization to endosomes associated with F-actin. Representative epifluorescence images of N2a cells with labeled F-actin (phalloidin), early endosomes (EEA1) and endogenous Bin1 or CD2AP. **A.** N2a cell showing F-actin puncta (a) and EEA1-positive endosomes (b), concentrated in the perinuclear region, and immunolabeled with Bin1 (c). Images are merged in (d). White boxes in (a, b, c, d) correspond to magnifications in (e, f, g, h). **B.** Cell labeled as in A (a, b), but stained for CD2AP (c). (d) represents the merged images, and (e, f, g, h) are magnifications of boxes in (a, b, c, d) respectively. Arrows in A and B indicate Bin1 or CD2AP puncta juxtaposed to actin-positive endosomes. Merged images and magnifications were background subtracted. Scale, 5 µm.

Therefore, we can conceive that Bin1 and CD2AP play a role in the regulation of the actin pool associated with early endosomes, since both proteins localize nearby EEA1-vesicular structures containing F-actin.

4.3 Impact of Bin1 and CD2AP loss of function on the actin cytoskeleton

We hypothesized that Bin1 and CD2AP function as actin regulators to remodel the actin pool associated with endosomal membranes. In order to assess the impact of their loss of function on the actin cytoskeleton, we analyzed total actin levels in Bin1 and CD2AP depleted N2a cells and PN.

Bin1 and CD2AP were knockdown using specific interference RNA, and quantitative immunoblotting was used to evaluate the efficiency of the knockdown. Bin1 has several isoforms as a result of alternative splicing[57]. In neurons two isoforms are mainly expressed, a neuronal isoform at 80 kDa and a ubiquitous isoform at 60 kDa (Fig. 4.4B)[98]. In N2a cells, Bin1 Western blot revealed three bands (Fig. 4.4A), with the upper band likely being non-specific, since its intensity was not significantly altered by the Bin1 siRNA treatment. The other two bands most likely correspond to Bin1 since they virtually disappear upon treatment with siRNA specific to exon 3, common to all Bin1 isoforms[99]. The upper band of about 80 kDa has the predicted size of the longer neuronal isoform and the lower band of about 60 kDa has the predicted size of the smaller ubiquitous isoform[74] (Fig. 4.4A). N2a cells treated with siRNA against Bin1 showed a decrease in expression of Bin1 (neuronal and ubiquitous isoform) of 74%, compared to the non-targeting control siRNA (Fig. 4.4A). Bin1 knockdown in PN caused a decrease in protein level by 55% (neuronal and ubiquitous isoform), compared to control siRNA (Fig. 4.4B).

CD2AP appeared as a single band above 75 kDa in both N2a cells (Fig. 4.4C) and PN (Fig. 4.4D), consistent with its predicted size of 80 kDa [80]. In N2a cells transfected with CD2AP siRNA there was a decrease of 91% in CD2AP levels (Fig. 4.4C), and in PN CD2AP levels decreased nearly 70%, compared to the control siRNA (Fig. 4.4D). These results confirm the efficiency of the knockdown upon treatment of N2a cells or PN with Bin1 and CD2AP siRNA.

To analyze global actin levels in the cells, we performed an immunoblot analysis of N2a cells and PN upon siRNA treatment against Bin1 and CD2AP. We performed this experiment twice and observed some variability. At this point the data points to a decrease in actin levels by 54% and 22% upon knockdown of Bin1 and CD2AP, respectively, compared to control siRNA treated N2a cells (Fig. 4.4E). In PN, actin levels increased 19% in Bin1-depleted neurons, whereas in CD2AP-depleted neurons it decreased by 20%, relative to the control siRNA (Fig. 4.4F). Thus, CD2AP knockdown leads to a decrease in actin levels in both N2a cells and PN. Bin1 knockdown, on the other hand, induces different effects in actin levels, which may reflect distinct roles for Bin1-mediated actin regulation in neuronal and non-neuronal cells, or experimental variability.

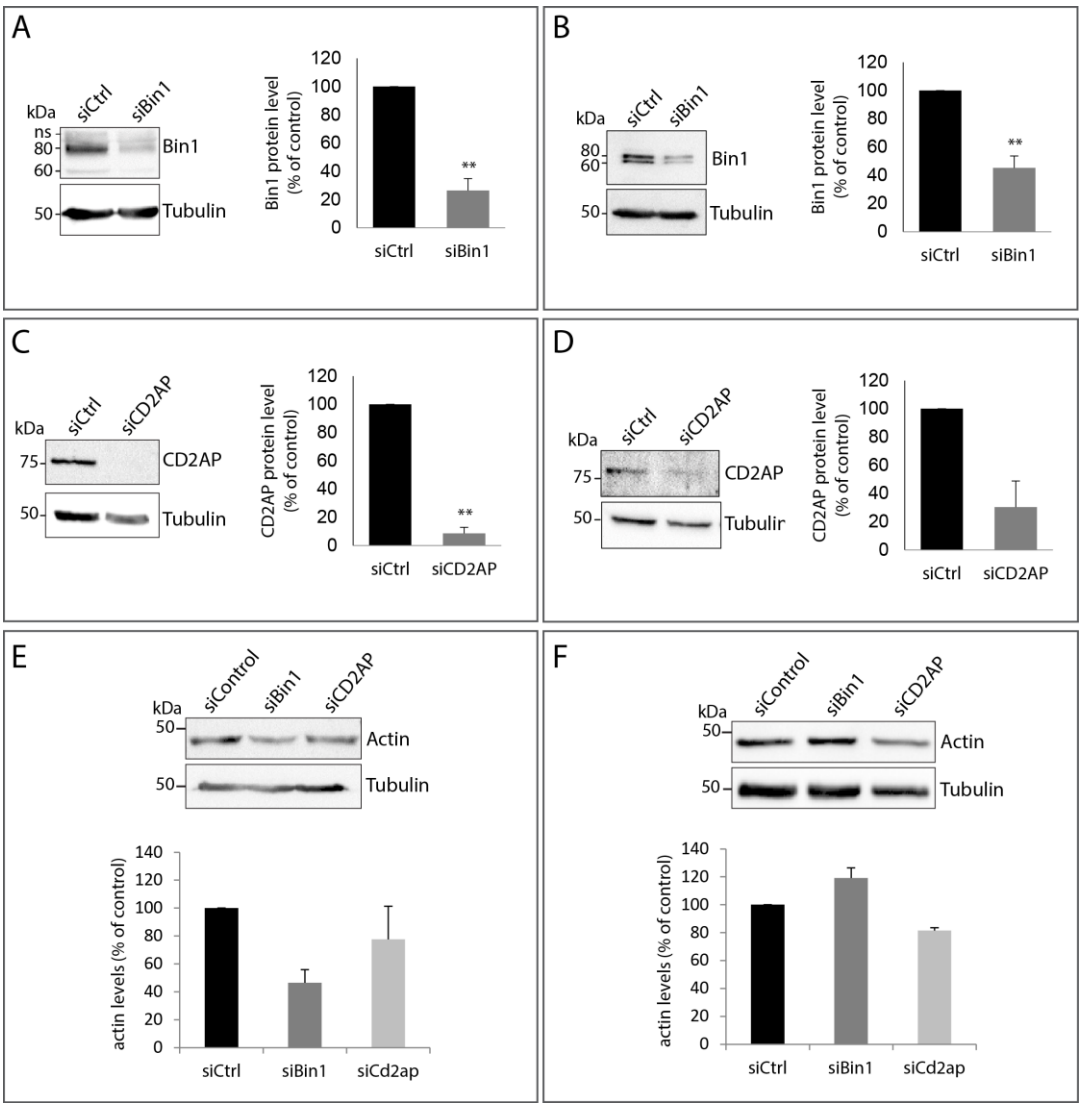

Figure 4.4 Bin1 and CD2AP downregulation impact actin levels in N2a cells and primary neurons. Western blot analysis of cell lysates from N2a cells and PN transfected with non-targeting siRNA (siCtrl), or siRNA against Bin1 (siBin1) or CD2AP (siCD2AP) for 72h. **A.** Western blot of N2a cells transfected with siCtrl and siBin1 and blotted with antibodies against Bin1 and α-tubulin (n=3). **B.** Western blot of PN transfected with siCtrl and siBin1 and blotted as in A. (n=5). Graphs in A and B represent the quantification of band intensities of total Bin1 (neuronal and ubiquitous), normalized by total α-tubulin. Levels of Bin1 are represented as a percentage of Bin1 levels in siCtrl cells. **C.** Western blot of N2a cells transfected with siCtrl and siCD2AP and blotted for CD2AP and α-tubulin (n=3). **D.** Western blot of PN transfected with siCtrl and siCD2AP and blotted as in C (n=3). Graphs in C and D represent the quantification of band intensities of CD2AP, normalized by α-tubulin and represented as a percentage of CD2AP levels in siCtrl cells (p=0.06 vs. siCtrl). **E.** Western blot of N2a cells transfected with siCtrl, siBin1 or siCD2AP and blotted with an antibody against actin and α-tubulin (n=2). **F.** Western blot of PN transfected with siCtrl, siBin1 and siCD2AP and blotted as in E (n=2). Graphs in E and F represent the quantification of the respective blots, normalized by α-tubulin and represented as a percentage of siCtrl cells. ** $p<0.01$ vs. siCtrl

Taken together, these results indicate that Bin1 and CD2AP expression impact actin levels in N2a cells and PN, validating their role as actin regulatory proteins.

4.4 Impact of Bin1 and CD2AP loss of function on actin associated with early endosomes

In order to assess the impact of Bin1 and CD2AP loss of function on the actin cytoskeleton pool that localizes in the perinuclear region, we analyzed F-Actin with fluorescently-labeled phalloidin in N2a cells depleted for Bin1 and CD2AP.

In fig 4.5A, we can compare the distribution of F-actin between the two main pools of actin in N2a cells, the cortical actin and perinuclear actin. The perinuclear actin puncta are condensed and appear as bright F-actin puncta (Fig. 4.5A a-inset) that were shown above to be associated with early endosomes (see Fig. 4.1). We observed a reduction in the amount of bright perinuclear actin structures by comparing the perinuclear actin distribution in N2a cells depleted with Bin1 (Fig. 4.1A b, inset) and CD2AP (Fig. 4.1A c, inset) with control siRNA N2a cells (Fig. 4.1A a, inset).

By appreciating the cellular line profiles (Fig. 4.1A d-f) one can more easily perceive that the perinuclear actin reduction is accompanied by an increase in cortical actin, especially in N2a cells knockdown for CD2AP. To support our observations, we quantified the ratio of F-actin fluorescence intensity levels in the perinuclear region relative to the overall fluorescence in the cell, which reflects mostly the cortical actin, since only 17% of the cellular F-actin is in the perinuclear region in control cells (Fig. 4.5B). We observed that upon Bin1 knockdown, the fraction of F-actin in the perinuclear region decreased to 12% (Fig. 4.5A and B). CD2AP-depleted N2a cells present a clear decrease in perinuclear actin (Fig. 4.5B), with 8% of F-actin in the perinuclear region, a reduction of 54% compared to the control cells.

In addition, we observed that the mean intensity of F-actin in the cell increased, particularly in CD2AP-depleted cells (Fig. 4.5C). N2a cells depleted for Bin1 showed a small increase of 16% in cellular F-actin, compared to control cells (Fig. 4.5C). N2a cells depleted for CD2AP showed an 86% increase in cellular F-actin (Fig 4.5C). This remarkable rise in cellular F-actin is likely due to alterations in CD2AP dependent-actin dynamics, with an increase in number and brightness of filopodia projections (Fig. 4.5A c), as seen by Zhao *et al.* in podocytes. This data indicates that the perinuclear F-actin foci decreased probably due to a disruption in the F-actin filaments' structural organization, and not to a reduction in actin filaments (Fig. 4.5A f; 4.5C). Additionally, downregulation of Bin1 and CD2AP slightly affected the average size of N2a cells (Fig. 4.5D). Bin1 knockdown led to a 10% decrease in cell size, whereas CD2AP-depleted cells were 16% bigger compared to control cells, likely due to the knockdown cells being more spread.

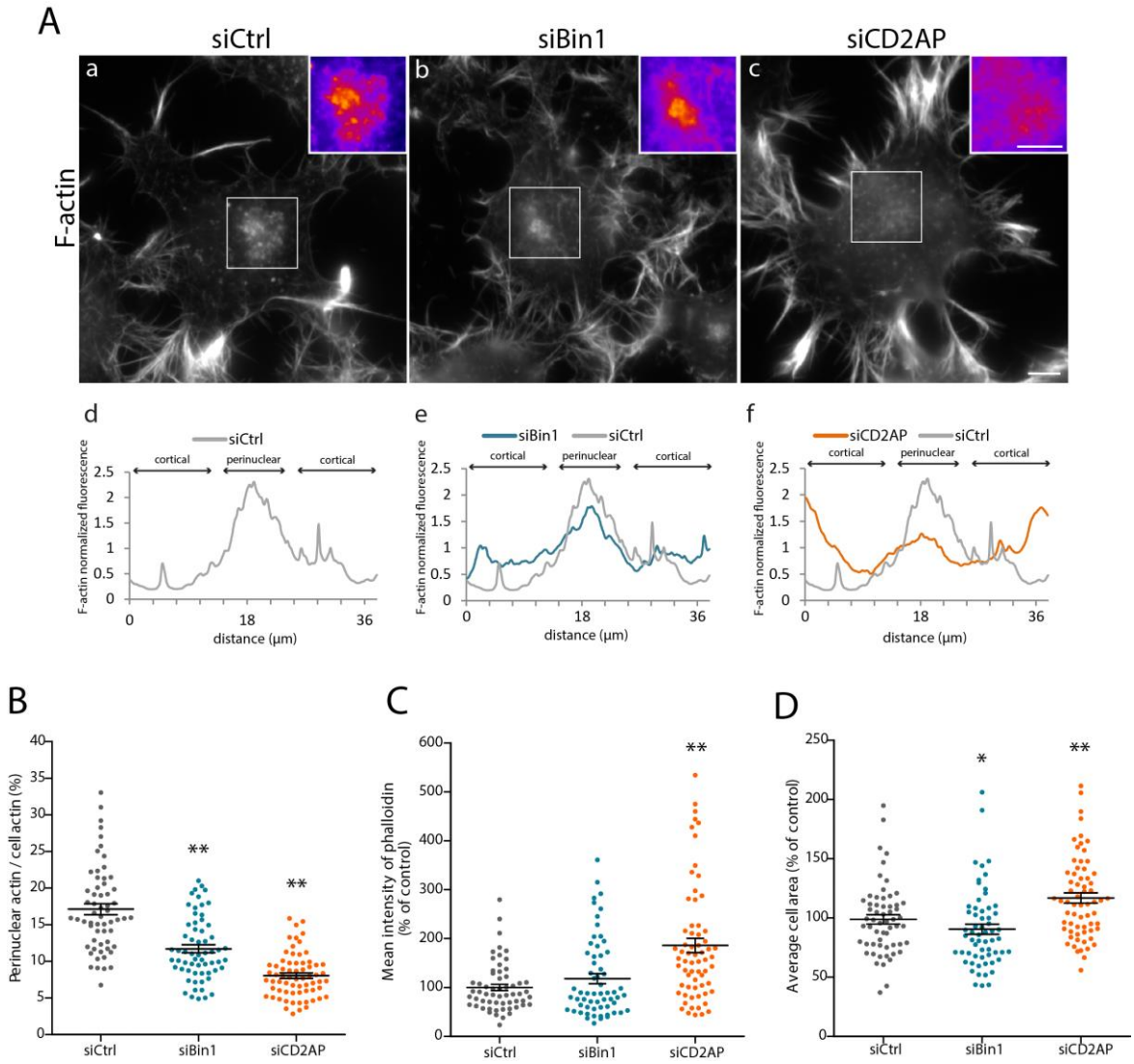

Figure 4.5 Bin1 and CD2AP loss of function impacts the actin cytoskeleton in N2a cells. A. Epifluorescence representative images of N2a cells treated with non-targeting siRNA (siCtrl) (a), or siRNA against Bin1 (siBin1) (b) or CD2AP (siCD2AP) (c), and stained for F-actin with phalloidin. White boxes are magnified in the upper right corner, with the "fire" LUT applied to allow a better visualization of the actin pool in the perinuclear region. (d, e, f) represent line profiles of the normalized F-actin fluorescent across the cells in (a, b, c) respectively. The line profile of the siCtrl cell (grey line) is used as a comparison. **B.** Ratio of perinuclear to cell actin, representing the percentage of F-actin in the perinuclear region of N2a cells in the different conditions. **C.** Quantification of F-actin mean fluorescence overall in the cells, in the different conditions, represented as a percentage of siCtrl cells. **D.** Average cell area in the different conditions, represented as a percentage of siCtrl cells. n=5; * p<005 vs. siCtrl; **p<0.01 vs. siCtrl. Scale, 5 µm.

Considering these results, we can conclude that Bin1 and CD2AP impact the actin cytoskeleton associated with early endosomes in N2a cells. Downregulation of Bin1 or CD2AP leads to a decrease in the percentage of F-actin in the perinuclear region. It remains to be investigated if Bin1 and CD2AP are controlling actin associated with early endosomes by locally controlling F-actin structural organization, or if by controlling actin polymerization at the cortex and indirectly affecting actin puncta at the perinuclear region.

The perinuclear pool of actin is closely associated with early endosomes (Fig. 4.1), thus a reorganization of F-actin in this region may compromise the actin puncta associated with early endosomes. To better understand the impact of Bin1 and CD2AP on the F-actin pool associated with early endosomes, in a preliminary experiment we used spinning-disk confocal microscopy to inspect alterations in the F-actin puncta associated with individual endosomes in N2a cells depleted for Bin1 and CD2AP (Fig. 4.1). Early endosomes were labeled with EEA1 and phalloidin was used to stain F-actin (Fig. 4.6A).

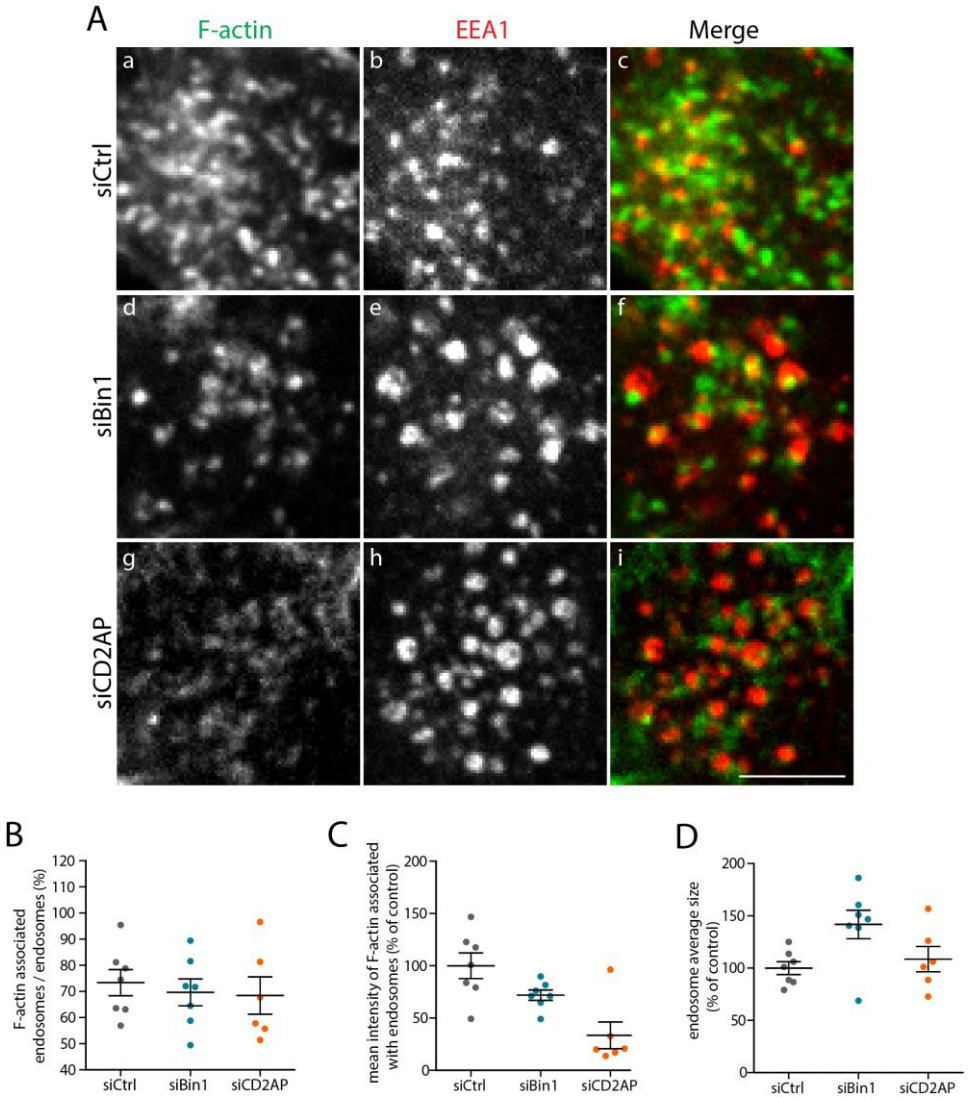

Figure 4.6 Bin1 and CD2AP loss of function impacts the F-actin puncta associated with early endosomes in N2a cells. A. Representative spinning-disk confocal images of the perinuclear region of N2a cells transfected with non-targeting siRNA (siCtrl) (a-c), or siRNA against Bin1 (siBin1) (d-f) or CD2AP (siCD2AP) (g-i). Phalloidin was used to label F-actin puncta (a, d, g) and EEA1 to label early endosomes (b, e, h). Merged images are presented in (c, f, i) with F-actin in green and EEA1-positive endosomes in red. **B.** Ratio between the number of endosomes associated with F-actin and the total number of early endosomes in the perinuclear region, represented as the percentage of F-actin-positive endosomes. **C.** Quantification of the mean fluorescence of F-actin puncta associated with early endosomes in the perinuclear region, represented as a percentage of the mean intensity of siCtrl cells. **D.** Average size of endosomes in the perinuclear region, represented as a percentage of the mean size of endosomes in siCtrl cells. n=1; scale 5 µm.

Loss of Bin1 and CD2AP slightly decreased the number of F-actin puncta associated with early endosomes overlapping with F-actin (Fig. 4.6B). More important was the decrease observed in the mean intensity of each F-actin puncta associated with endosomes (Fig. 4.6C), which was of 28% in Bin1-depleted cells and of 67% in CD2AP-depleted cells, compared with control siRNA treated cells (Fig. 4.6C). Of note early endosomes were 42% larger in Bin1-depleted N2a cells (Fig. 4.6A f) compared to control siRNA treated cells (Fig. 4.6D).

Next, we explored the effect of Bin1 and CD2AP depletion on F-actin puncta associated with early endosomes, in dendrites of primary neurons. Endosomes were labeled with EEA1 that are often widespread in dendrites, thus enabling the segmentation of single endosomes using threshold, even in epifluorescence images. In control dendrites, 64% of early endosomes were associated with actin (Fig. 4.7A g; 4.7B). Bin1 knockdown reduced to 36% the number of early endosomes associated with F-actin puncta in dendrites (Fig. 4.7A h; 4.7B), a decrease of 43% compared to control cells. CD2AP-depleted dendrites had 44% of endosomes associated with F-actin (Fig. 4.7A i; 4.7B), a decrease of 32% compared to control neurons.

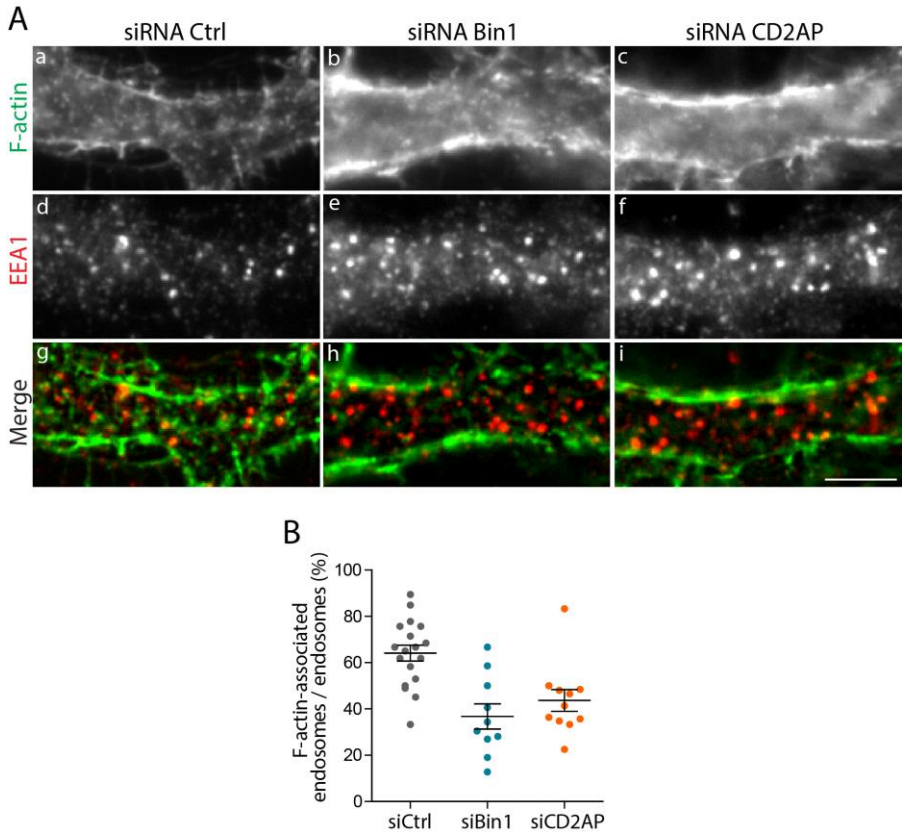

Figure 4.7 Bin1 and CD2AP loss of function impacts the F-actin puncta associated with early endosomes in dendrites of primary neurons. A. Representative epifluorescence images of dendrites' sections (20 µm) from PN, at 9-12 DIV, transfected with non-targeting siRNA (siCtrl) (a, d, g), siRNA againsta Bin1 (siBin1) (b, e, h), or siRNA against CD2AP (siCD2AP) (c, f, i). F-actin was labeled with phalloidin (a-c) and EEA1 was used to stain early endosomes (d-f). Merged images of F-actin puncta (green) and dendritic early endosomes (red) are represented in (g-i). **B.** Ratio between the number of endosomes associated with F-actin and the total number of early endosomes in that section of the dendrite, represented as the percentage of F-actin-positive endosomes. Merged images were background subtracted. n=1; scale 5 µm.

4.5 Actin dynamics and the control of APP and BACE1 endocytic trafficking

So far we found that Bin1 and CD2AP can control the actin pool associated with endosomes in N2a cells and primary neurons. Previously, we had found that these two proteins controlled the endosomal sorting of APP and BACE1. In particular, that Bin1 controls BACE1 recycling to the plasma membrane through endosomal recycling tubules, whereas CD2AP controls the intraluminal sorting of APP that is essential for MVB formation and APP degradation. Both mechanisms involve membrane remodeling for which actin dynamics could be crucial. To understand if Bin1 and CD2AP control the endocytic trafficking of APP and BACE via regulation of endosomal actin, we started by studying the distribution of F-actin, using phalloidin, relative to the distribution of APP or BACE1, and CD2AP or Bin1, by immunofluorescence. N2a cells transfected with APP-RFP or FLAG-BACE1-GFP were pre-permeabilized to remove the cytosol, improving the visualization of membrane proteins. The distribution of APP and BACE1 was compared to that of endogenous CD2AP or Bin1, respectively, and F-actin (Fig. 4.8).

APP was concentrated in the perinuclear region, most likely corresponding to the previous described APP localization to the TGN[9] (Fig. 4.8A b), where F-actin was also present (Fig. 4.8A a). APP and F-actin often co-distributed (Fig. 4.8A e,f). CD2AP appeared as puncta throughout the cell (Fig. 4.8A c), and it was occasionally juxtaposed to actin and APP labeled structures (Fig. 4.8A h, arrows). Often more than one CD2AP puncta appeared to enclose an APP and F-actin puncta (Fig. 4.8A g), as previously (Fig. 4.3B) with EEA1-positive endosomes. BACE1 had a clear vesicular distribution, with a predominant localization in the perinuclear region, previously described to be consistent with BACE1 localization to the perinuclear endocytic recycling compartment[10] (Fig. 4.8B b). Bin1 was diffused through the cell, its high signal in the nucleus was likely due to excessive permeabilization during the pre-extraction (Fig. 4.8B c). BACE1 and F-actin were greatly concentrated in the perinuclear region, which hampers the observation of a possible colocalization between the two. However, in the vicinity of this region, we could see some F-actin puncta associated with BACE1 and Bin1 (Fig. 4.8B e).

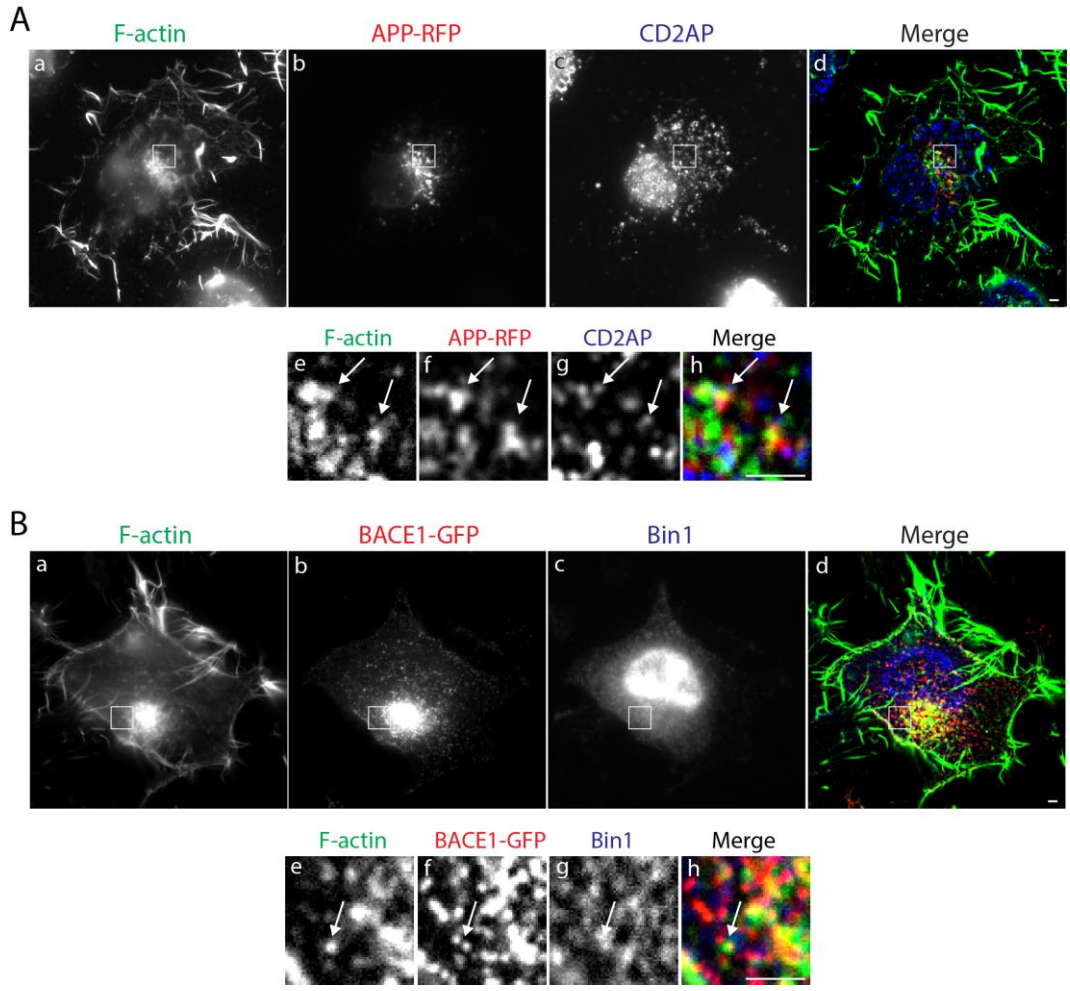

Figure 4.8 Bin1 and CD2AP localization to F-actin puncta and BACE1 or APP in N2a cells. Representative epifluorescence images of N2a cells transfected with BACE1-GFP or APP-RFP, pre-permeabilized, stained for F-actin (phalloidin) and immunolabeled with specific antibodies for endogenous Bin1 or CD2AP. **A.** N2a cell transfected with APP-RFP (b) and with labeled F-actin (a) and endogenous CD2AP (c). Images are merged in (d). Boxes in the perinuclear region (a-d) are magnified in (e-h), respectively. Arrows indicate association of CD2AP and F-actin puncta with APP-positive vesicles. **B.** N2a cell transfected with BACE1-GFP (b) and with labeled F-actin (a) and endogenous Bin1 (c). Images are merged in (d). Boxes in the perinuclear region (a-d) are magnified in (e-h), respectively. Arrow indicates association of Bin1 and F-actin puncta with BACE1-positive vesicles. Magnifications and merged images were background subtracted. Scale, 2 μm.

Thus, in a pool of APP or BACE1 vesicles associated with actin puncta, we could see adjacent CD2AP or Bin1, perhaps reflecting a transient interaction of these proteins with a subpopulation of endosomes containing APP/BACE1, to regulate their endosomal sorting.

To further investigate our hypothesis that Bin1 and CD2AP work to remodel the actin cytoskeleton associated with early endosomes, and for APP and BACE1 endocytic trafficking, we evaluated the impact of Bin1 depletion on actin association to BACE1 in endosomes. N2a cells transfected with FLAG-BACE1-GFP were incubated with anti-FLAG antibody for 20 min, to label endocytosed BACE1 (endoBACE1). In Fig. 4.9A we observed that endoBACE1 colocalized more with F-actin than BACE1-GFP (48% of overlap) (Fig.4.9A d-h), in control siRNA treated cells. On the other hand, in Bin1 depleted cells, endoBACE1 colocalized less

with F-actin, as seen in Fig. 4.9B h that presents 44% BACE1 vesicles associated with F-actin, while control cells show 56% colocalization (Fig. 4.9A h).

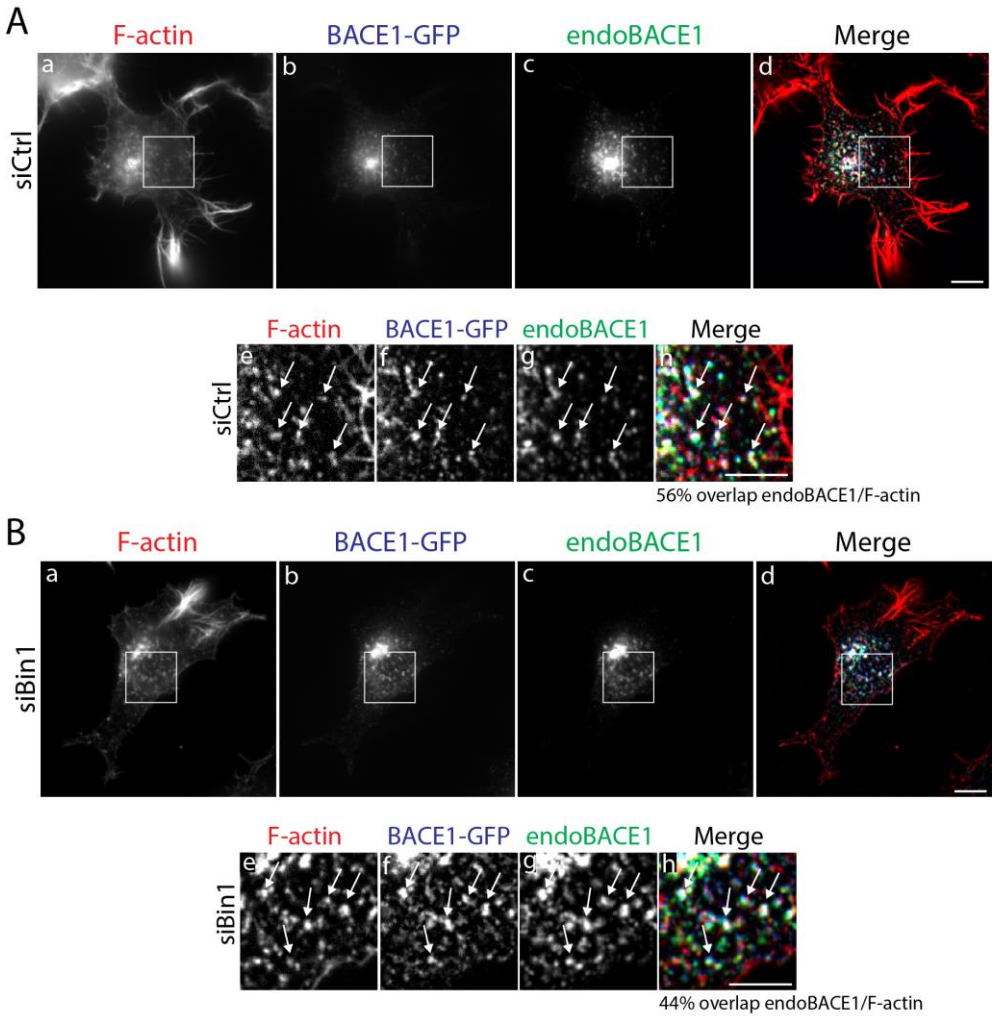

Figure 4.9 Bin1 depletion may impact the association of endocytosed BACE1 with F-actin puncta in N2a cells. Epifluorescence images of N2a cells transfected with non-targeting siRNA (siCtrl) or siRNA against Bin1 (siBin1), and with flag-BACE1-GFP. Flag antibody was pulsed for 10 min and chased for 20 min, and endocytosed BACE1 was labeled along with F-actin (phalloidin). **A.** siRNA control cells with labeled F-actin (a), BACE1-GFP (b) and endocytosed BACE1 (c). Images are merged in (d). Boxes in (a-d) are magnified in (e-h), respectively. **B.** siBin1 cells with labeled F-actin (a), BACE1-GFP (b) and endocytosed BACE1 (c). Images are merged in (d). Boxes in (a-d) are magnified in (e-h), respectively. In A and B, the percentage of overlap between endocytosed BACE1 and F-actin, in the magnified region, is presented below the merged inset (h). Endocytosed BACE1 is often found associated with F-actin puncta (arrows in A and B). Magnifications and merged images were background subtracted. Scale, 5 μm.

Given these results, we can suppose that Bin1 contributes to the control of the association of F-actin to BACE1 vesicles in N2a cells. Lack of Bin1 and, consequently, loss of actin puncta from BACE1-containing endosomes may impact the remodeling and/or scission of recycling tubules, thereby preventing BACE1 recycling. We will investigate in a next experiment the impact of CD2AP on F-actin puncta association with early endosomes containing APP.

4.6 Bin1 and CD2AP-mediated mechanism(s) to control the association of actin with endosomes

Several studies describe mechanisms by which Bin1 and CD2AP control actin remodeling, and most of them report interactions with other actin regulatory proteins. At the endosome, two different NPFs can be found, WASH [40] and WASP [41], that help the recruitment and activation of the Arp2/3 complex. WASH, in particular, was shown to mediate actin assembly on endosomes, along with cortactin and Arp2/3 [43], likely being necessary for tubule scission [40]. Therefore, we decided to investigate the potential role of Bin1 and CD2APin the regulation of endosomal actin dynamics, mediated by WASH.

First, we analyzed WASH distribution by immunofluorescence, in N2a cells with labeled EEA1-positive endosomes.

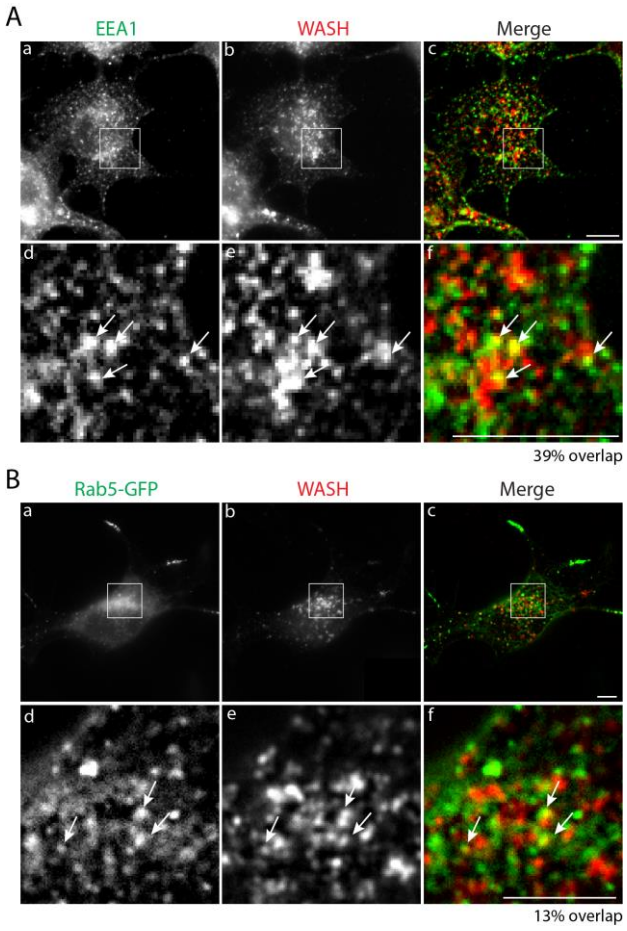

Figure 4.10 WASH associates with early endosomes in N2a cells. Representative epifluorescence images of N2a cells with labeled early endosomes and the nucleation promoting factor WASH. **A.** N2a cell immunostained with EEA1 to label early endosomes (a) and with a WASH specific antibody (b). Images are merged in (c). Boxes in (a, b, c) correspond to magnifications in (d, e, f). **B.** N2a cell transfected with rab5-GFP to label early endosomes (a) and immunostained with a WASH specific antibody (b). Images are merged in (c). Boxes in (a, b, c) correspond to magnifications in (d, e, f). Colocalization appears in yellow and is pointed with arrows. In A and B, the percentage of overlap between WASH and F-actin, in the magnified region, is presented below the merged inset (f). Magnifications and merged images were background subtracted. Scale in A, 5 µm; scale in B, 1 µm.

WASH appeared as bright puncta that accumulated in the perinuclear region (Fig. 4.10A b), where it colocalized with early endosomes (39% overlap) (Fig. 4.10A d-f). In addition, we transfected N2a cells with Rab5-GFP (Fig. 4.10B a) and observed a colocalization of WASH with rab5-early endosomes, although not in a great extent, with just 13% overlap in the perinuclear region (Fig. 4.10B d-f).

In order to understand if Bin1 and CD2AP regulated WASH, thereby controlling the actin puncta associated with early endosomes, we examined WASH levels and distribution upon Bin1 and CD2AP knockdown in N2a cells, by immunofluorescence. Control cells presented WASH vesicular puncta throughout the cell, with nearly 25% concentrated in the perinuclear region (Fig. 4.11A a; 4.11 C). N2a cells lacking Bin1 and CD2AP had roughly the same amount of perinuclear WASH (Fig. 4.11C). Interestingly, the distribution of WASH slightly changed when Bin1 or CD2AP were depleted (Fig. 4.11A b,c). The perinuclear pool of WASH was more condensed and with less vesicular structures scattered through the cell's cytoplasm, which is particularly noticeable in cells lacking CD2AP.

When examining the distribution of WASH relative to F-actin, in the perinuclear region, we could see that WASH colocalized extensively with F-actin, in control cells (Fig. 4.11B a-c arrows). In Bin1 and CD2AP depleted cells we could also detect WASH puncta colocalizing with F-actin in the perinuclear region (Fig. 4.11B d-f, g-i arrows). However, while in control cells we could detect clear F-actin puncta that overlapped with WASH in the vicinity of the perinuclear area, in both Bin1 and CD2AP knockdown cells F-actin was diffuse so although there was still some overlap, WASH puncta were no longer clearly associated with actin (Fig. 4.11B d-f arrowheads; 4.11B g-i arrowheads).

Overall, WASH levels in siRNA-treated cells were similar to control cells, with a small increase of 14% in Bin1 knockdown cells, and a decrease of 18% in CD2AP knockdown cells (Fig. 4.11D). Considering this, we then performed a Western blot to analyze WASH levels. WASH appeared as two bands at 70 kDa (Fig. 4.11F) and, indeed, we could see an increase of 25% in Bin1 knockdown cells, and a decrease of 37% when CD2AP was knockdown (Fig. 4.11G). N2a cells knockdown for Bin1 were practically the same size as the control, whereas CD2AP knockdown cells were nearly 20% larger (Fig. 4.11E), as seen previously (Fig. 4.5D).

Overall, Bin1 and CD2AP regulate WASH levels and its perinuclear distribution in N2a cells. Loss of CD2AP led to a decrease in WASH protein levels, which may explain the decrease in F-actin in the perinuclear region of CD2AP-depleted cells. Bin1 knockdown, on the other hand, caused an increase in WASH levels. Importantly, knockdown of bin and CD2AP caused a redistribution of WASH, which was reduced to the perinuclear region, particularly in cells lacking CD2AP. This phenotype may be a consequence of the reorganization of F-actin in the perinuclear region of Bin1 and CD2AP depleted N2a cells, as seen previously.

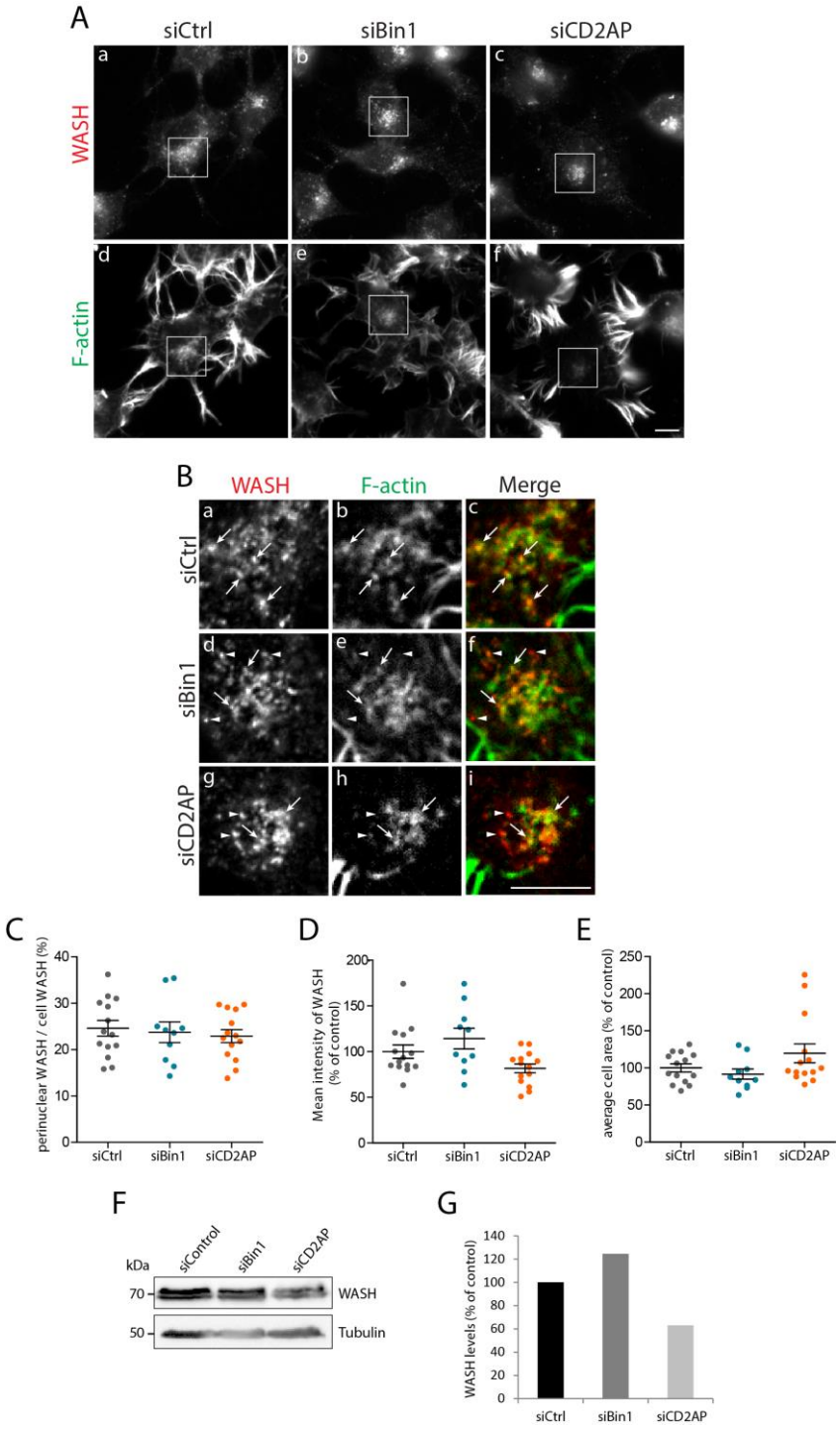

Figure 4.11 Bin1 and CD2AP depletion impact WASH levels and its distribution in N2a cells. A. Epifluorescence images of N2a cells transfected with non-targeting siRNA (siCtrl) or with siRNA against Bin1 (siBin1) or CD2AP (siCD2AP), and stained for WASH (a-c) and F-actin (phalloidin) (d-f). **B.** Magnifications of boxes in A, showing WASH (a, d, g) and F-actin puncta (b, e, h) in the perinuclear region of siRNA-treated cells. (c, f, i) represent merged images. WASH (red) is frequently associated with F-actin puncta (green) (arrows). Arrowheads indicate WASH puncta not associated with F-actin. **C.** Ratio of perinuclear to cell WASH, representing the percentage of WASH in the perinuclear region of siRNA-treated N2a cells. **D.** Quantification of WASH mean fluorescence overall in the cells, represented as a percentage of siCtrl cells. **E.** Average cell area in the different conditions, represented as a percentage of siCtrl cells. **F.** Western blot analysis of cell lysates from siCtrl, siBin1 or siCd2ap N2a cells, and blotted with antibodies against WASH and α-tubulin. **G.** Quantification of band intensities in F, with WASH levels normalized by α-tubulin, and represented as a percentage of WASH levels in siCtrl cells. n=1; scale, 5 µm.

4.7 The effect of actin dynamics on $A\beta_{42}$ levels

Bin1 and CD2AP appear to disrupt the actin cytoskeleton associated with early endosomes in N2a cells and PN. Additionally, we have previous results indicating that Bin1 and CD2AP knockdown increase $A\beta_{42}$ levels in both cellular models. Therefore, we decided to use latrunculin A (LatA), a toxin that binds actin monomers and prevents their association to filaments, resulting in actin depolymerization (ref), and examine its effect on the perinuclear actin of N2a cells, which is closely associated with early endosomes, and in $A\beta_{42}$ levels.

N2a cells were treated overnight with 10 nM of DMSO, as a control, or LatA and labeled for F-actin, with phalloidin, and for $A\beta_{42}$, using an antibody that recognizes the C-terminal of $A\beta_{42}$. Cells treated with LatA exhibited a 20% decrease in the amount of F-actin, compared to control cells (Fig. 4.12A a,b insets; 4.12C). LatA-treated cells had almost no filopodia or presented retracting cables.

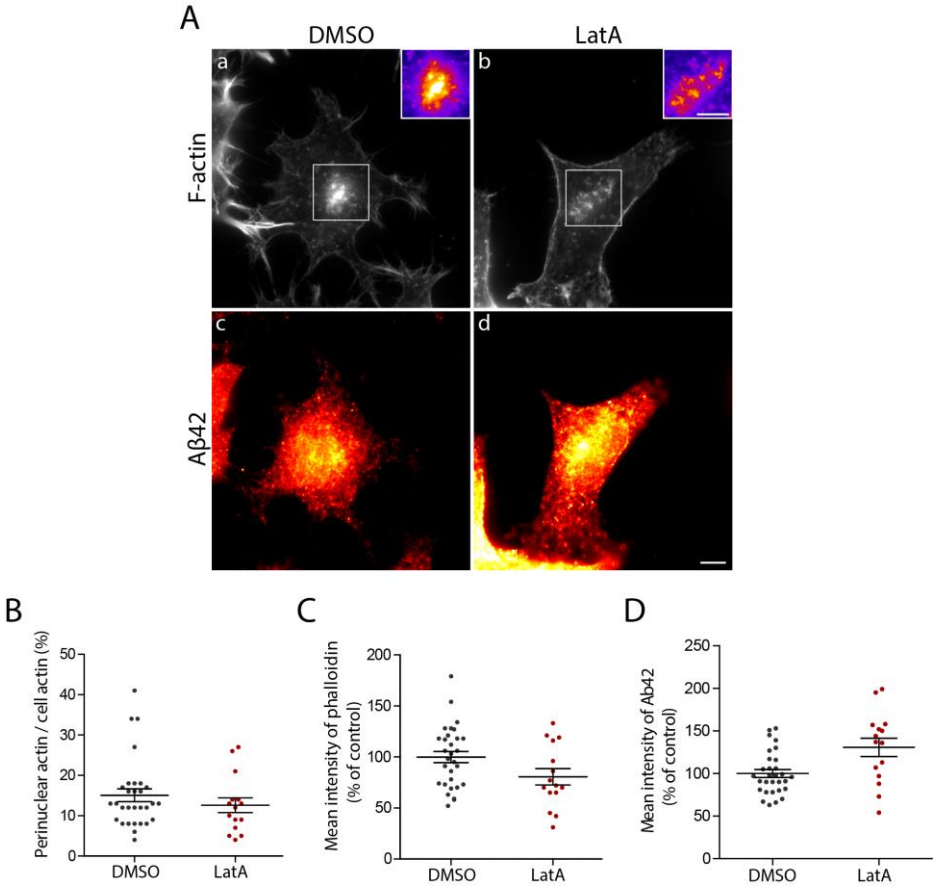

Figure 4.12 Actin depolymerization induces an increase in $A\beta_{42}$ levels. A. Epifluorescence images of N2a cells treated with 10 nM of DMSO, as a control, or with 10 nM of latrunculin A (LatA), and labeled for F-actin (phalloidin) (a, b) and $A\beta_{42}$, using a specific antibody (c, d). Boxes in (a, b) are magnified in the upper right corner and with "fire" LUT, to visualize the perinuclear pool of F-actin. (c, d) are presented with the "red hot" LUT, in which the yellow color indicate higher levels of $A\beta_{42}$. **B.** Ratio of perinuclear to cell actin, representing the percentage of F-actin in the perinuclear region of cells treated with DMSO or LatA. **C.** Overall mean fluorescence intensity of F-actin in cells treated with DMSO or LatA, represented as a percentage of DMSO-treated cells. **D.** Quantification of $A\beta_{42}$ mean fluorescence in cells treated with DMSO or LatA, and represented as a percentage of DMSO-treated cells. n=1; scale, 5 µm.

When examining the perinuclear pool of F-actin, we could see that cells treated with LatA had 17% less of perinuclear F-actin compared to control cells (Fig. 4.12B). Importantly, cells incubated with LatA showed increased levels of $A\beta_{42}$ (Fig. 4.12 c,d), with an increase of 31%, relative to control cells (Fig. 4.12 D).

Taken together, these preliminary results indicate a role for actin dynamics in Aβ generation. Disruption of the actin cytoskeleton led to reduced F-actin at the cortex and perinuclear region of N2a cells. In addition, LatA induced an increase in $A\beta_{42}$ levels, perhaps revealing that a stable actin cytoskeleton is required for the proper sorting of APP and BACE1 involved in Aβ production.

4.8 The impact of Bin1 and CD2AP loss of function in PSD-95 levels

Spine dynamics is greatly dependent on the actin cytoskeleton that works as a structural scaffold at the synapse [50]. At post-synaptic regions Aβ is responsible for decreasing PSD-95 and thus affecting the anchoring of glutamate receptor subunits [22], contributing to the dysfunction of the glutamatergic synapse, hence to neuronal function [50]. Because Bin1 and CD2AP depletion had an impact on Aβ generation and on the levels of F-actin in PN, we wondered if this would cause an effect in PSD-95 levels.

By quantitative immunoblotting, we could see PSD-95 as a single band at the expected 95 kDa (Fig. 4.13A). Knockdown of CD2AP caused a reduction of 35% in PSD-95 levels, while Bin1 depletion had no significant effect (Fig. 4.13B). Previously, it was reported a decrease in PSD-95 levels in neurons of AD transgenic mouse models [22].

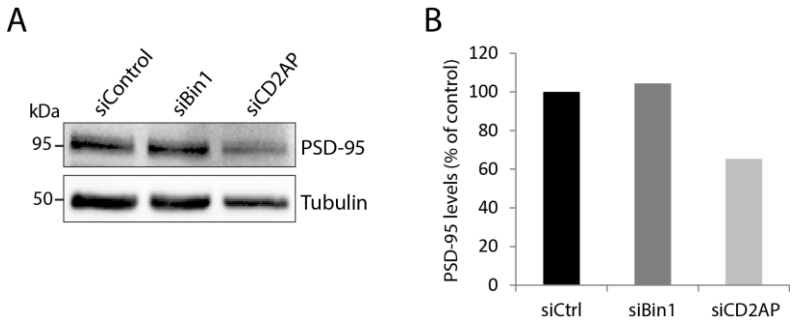

Figure 4.13 CD2AP depletion reduces PSD-95 levels in primary neurons. A. Western blot analysis of cell lysates from primary neurons transfected with non-targeting siRNA (siCtrl), siRNA against Bin1 (siBin1) or siRNA against CD2AP (siCD2AP), and blotted with antibodies against PSD-95 and α-tubulin. **B.** Quantification of band intensities in A, with PSD-95 levels normalized by α-tubulin and presented as a percentage of PSD-95 levels in siCtrl neurons.

Thus, CD2AP may impact the actin cytoskeleton involved in dendritic spines, causing a decrease in PSD-95 and impairing synaptic function, ultimately leading to synapse loss and AD. Further studies are needed to unravel the role of Bin1 and CD2AP in dendritic spine morphology and function.

Chapter 5

Discussion and Future Perspectives

Bin1 and CD2AP are two known risk factors for late-onset Alzheimer's disease, although it is still unknown how they confer a higher probability to develop AD. Previously we have discovered that loss of function of Bin1 and CD2AP increase ab generation. We found a role for Bin1 as regulator of BACE1 recycling, whereas CD2AP controls APP sorting for degradation via the MVB pathway. This might be the mechanism by which Bin1 and CD2AP increase Aβ levels. These risk factors control endocytic trafficking[67,80] but they are also regulators of actin dynamics[72,81], which is implicated in distinct membrane shape events, as recycling tubule formation[43] and endosomal maturation[45]. Therefore, we hypothesize that Bin1 and CD2AP regulate the convergence of APP and BACE1 in early endosomes in a novel actin-dependent mechanism, hence increasing Aβ production and the risk for AD.

First, we characterized the actin pool associated with early endosomes in N2a cells and mouse primary neurons. N2a cells presented an enrichment of F-actin in the perinuclear region where actin was organized in discrete puncta (Fig. 4.1A a), consistent with other studies in non-polarized cells[48]. This perinuclear F-actin pool was often found associated with EEA1-positive endosomes, which concentrate in the perinuclear region (Fig. 4.1A), the typical distribution of early endosomes in non-polarized cells[23]. Similar results were obtained using a high resolution spinning-disk confocal microscope and a super-resolution microscope (Fig. 4.1B and D), and in N2a cells transfected with Lifeact-mCherry and Rab5-GFP (Fig. 4.1C). In PN, F-actin was observed in patches and discrete puncta, frequently overlapping with EEA1-positive endosomes, which were scattered throughout dendrites (Fig. 4.2). This evenly distribution of endosomes likely serves the spatial demands of neurons[23].

Thus, a perinuclear pool of F-actin associates with EEA1-positive endosomes in N2a cells, as previously reported in other non-polarized cell types[86]. Additionally, we describe for the first time the presence of F-actin puncta associated with dendritic endosomes in primary neurons. These results point to a putative role of F-actin in the regulation of endosomal shape remodeling. In the future, we will examine the localization of actin puncta in axonal early endosomes labeled with rab5, as well as endosomal shape changes by super resolution microscopy.

Bin1 and CD2AP localize to early endosomes[80,86] and several studies report their role as actin-regulatory proteins. Bin1 contains a BAR domain that induces membrane curvature, required for tubule formation in the recycling pathway[100], and it may control actin polymerization by interacting with the Arp2/3 activator N-WASP [72]. CD2AP can regulate actin dynamics directly, through its capping activity[89], and/or indirectly, via interaction with cortactin and with capping protein[88]. CD2AP has been reported to control endosomal maturation through regulation of actin assembly at endosomes[87].

Thereafter, we validated Bin1 and CD2AP localization to early endosomes associated with F-actin in N2a cells. Bin1 was diffused throughout the cell (Fig. 4.3A c), whereas CD2AP was evenly distributed in discrete puncta (Fig. 4.3B c), in agreement with *Cormont et al.* The few Bin1 puncta observed were adjacent to EEA1-positive endosomes associated with F-actin (Fig. 4.3A). CD2AP was also codistributed with actin-positive endosomes (Fig. 4.3B), usually with more than one CD2AP puncta nearby early endosomes with F-actin. Overall, Bin1 and CD2AP appear to be associated with the endosomal actin pool that is concentrated in the perinuclear region of N2a cells. Pre-permeabilization of N2a cells, in order to remove the cytosol, would improve the visualization of Bin1 and CD2AP puncta and allow a better evaluation of their codistribution along actin-positive early endosomes.

To study the role of Bin1 and CD2AP as regulators of the actin cytoskeleton, we analyzed F-actin levels in Bin1 and CD2AP depleted N2a cells and PN, by Western blot. Bin1 and CD2AP were efficiently knockdown in both N2a cells (Fig. 4.4A and C) and PN (Fig. 4.4B and D), using specific interference RNA. Upon CD2AP depletion, actin levels decreased in both cellular models, particularly in N2a cells. Bin1 knockdown led to a decrease in actin levels in N2a cells, although the levels of actin increased in PN (Fig. 4.4E and F). This may account for distinct roles of Bin1 in the regulation of the actin cytoskeleton in neuronal and non-neuronal cells. Therefore, we confirm that Bin1 and CD2AP function as actin regulatory proteins, controlling actin levels in N2a cells and primary neurons. Analyzing endogenous Bin1 and CD2AP distribution in neurons, relative to F-actin, would give further insights on how these proteins regulate actin dynamics, and if they control a specific pool of actin in specialized neuronal compartments.

Bin1 and CD2AP have been described as regulators of the actin cytoskeleton[72,86] and endocytic trafficking[67,80], thus we investigated the F-actin pool associated with early endosomes in N2a cells and PN lacking Bin1 and CD2AP. In N2a cells, we observed a decrease in the perinuclear F-actin pool, where we had previously observed an accumulation of EEA1-positive endosomes, in both Bin1 and CD2AP knockdown cells. Importantly, CD2AP-depleted cells exhibited a major rise in cortical F-actin, which could be observed by a marked increase in finger-like filopodia projections at the cell periphery, consistent with what Zhao *et al.* had observed in podocytes.

In order to evaluate Bin1 and CD2AP impact on actin-positive endosomes, we quantified the overlap between EEA1-labeled endosomes and F-actin puncta in N2a cells and dendrites of PN. In N2a cells, knockdown of Bin1 or CD2AP led to a slight decrease in EEA1-positive endosomes associated with F-actin (Fig. 4.6). Gauthier *et al.* had also seen a loss of F-actin structures on EEA1-positive endosomes, upon CD2AP depletion in HeLa cells. Remarkably, the fluorescence intensity of these actin puncta associated with early endosomes was significantly reduced upon Bin1 and CD2AP knockdown. Moreover, N2a cells lacking Bin1

and CD2AP exhibited larger EEA1-positive endosomes, compared to control cells (Fig. 4.6). Others have previously reported enlarged endosomes and altered endocytic function in neurons of individuals with early stage AD[4,101]. The enlargment in early endosomes is likely due to the accumulation of proteins within them, which may reflect defects in endosomal sorting. Similarly, in PN, knockdown of Bin1 and CD2AP led to a decrease in EEA1-positive endosomes associated with F-actin (Fig. 4.7), particularly in Bin1-depleted neurons.

Taken together, these results suggest that Bin1 and CD2AP differentially regulate the localization and/or organization of F-actin in N2a cell. Loss of Bin1 and CD2AP appears to induce a reorganization of the perinuclear F-actin pool, which may impact early endosomes in this region, likely compromising endocytic sorting mechanisms.

Previous data from the lab showed that CD2AP knockdown significantly increased $A\beta_{42}$ levels in the cell body and dendrites of PN. Additionally, previous studies reported that hippocampal neurons treated with fibrillar Aβ exhibit greater F-actin polymerization, with a marked increase in the formation of filopodia and lamellipodia[53,56]. To complement our results, we will examine F-actin levels in PN by immunofluorescence, and investigate if CD2AP depletion recapitulates the cortical F-actin rise observed in N2a cells. Bin1 knockdown, on the other hand, increases $A\beta_{42}$ levels in the cell body and axons of PN, thus we will analyze axonal rab5-positive endosomes associated with F-actin in Bin1 and CD2AP knockdown PN, in order to understand if there is a polarized impact in actin associated with early endosomes in neurons.

Overall, these results demonstrate that Bin1 and CD2AP can regulate the F-actin pool associated with early endosomes in N2a cells and PN. Therefore, loss of these proteins may impair the F-actin pool associated with early endosomes, leading to endocytic trafficking defects and promoting Aβ production, likely through regulation of APP and BACE1 endocytic trafficking.

Actin is required to remodel the shape of endosomal membranes, essential for endocytic recycling and MVB sorting mechanisms[43,45]. Bin1 and CD2AP appear to regulate the actin pool associated with early endosomes. However, to understand if this is the mechanism by which they impact APP and BACE1 trafficking, we first analyzed the distribution of Bin1 and CD2AP relative to endosomal F-actin, APP and BACE1 in N2a cells. Since Bin1 controls BACE1 recycling to the plasma membrane, we studied the distribution of transfected BACE1-GFP along with Bin1 and F-actin. CD2AP controls the intraluminal sorting of APP, hence we analyzed the distribution of transfected APP-RFP along with CD2AP and F-actin. Both APP and BACE1 were concentrated in the perinuclear region, along with F-actin. We could see some APP/BACE1-vesicles associated with F-actin and occasionally with CD2AP or Bin1 puncta, respectively (Fig. 4.8). Although it is not possible to conclude if in fact these proteins interact, we can conceive that CD2AP and Bin1 control a pool of APP and/or BACE1

endosomes, by regulating their associated actin. Hereafter, we will examine the distribution of actin-positive endosomes containing APP and BACE1, relative to endogenous Bin1 and CD2AP, in dendrites and axons of primary neurons. Additionally, we will analyze if APP interacts with CD2AP and BACE1 interacts with Bin1, by immunoprecipitation assays.

We then examined the localization of internalized BACE1 relative to F-actin, in Bin1 depleted N2a cells (Fig. 4.9). BACE1 was often associated with F-actin puncta in control cells. Loss of Bin1 appeared to reduce the number of BACE1 vesicles with associated F-actin, which may impact endosomal shape remodeling required for recycling tubule formation and/or scission. A quantitative analysis of the overlap between BACE1 and F-actin is needed to draw more consistent conclusions. In the future we will perform this experiment in primary neurons, taking into account dendrites vs. axon. Additional experiments will investigate the distribution of internalized APP relative to actin-positive endosomes, in CD2AP knockdown N2a cells and PN. To explore if Bin1 and CD2AP control two different actin pools at endosomes, since they control two different endosomal sorting events, we will use conventional electron microscopy to visualize actin filaments associated with endosomal tubules and/or endosomal invaginations.

It is still elusive whether Bin1 and CD2AP regulate actin dynamics directly or mediated by the interaction with other actin-binding partners. Several studies report interactions of Bin1 and CD2AP with actin-regulatory proteins. CD2AP interacts with cortactin[81,86,88] and with capping protein[79,88], both promoting filament branching through the Arp2/3 complex. Bin1 is known to interact with the actin nucleation promoting factor N-WASP, in myofibers[72]. In order to understand if Bin1 and CD2AP regulate endosomal F-actin in N2a cells through an indirect mechanism, we started by analyzing WASH protein. WASH is found at the base of endosomal recycling tubules, along with cortactin and the Arp2/3 complex[40].

WASH was concentrated in the perinuclear region of N2a cells, and appeared as vesicular punctate structures that occasionally were found associated with EEA1- and rab5-positive endosomes (Fig. 4.10). To study the potential role of WASH in Bin1- and CD2AP-mediated regulation of actin, we examined WASH levels and distribution in N2a cells knockdown for Bin1 and CD2AP (Fig. 4.11). We could see that, while there was no significant alteration in the percentage of WASH in the perinuclear region, its distribution changed compared to control cells. In both Bin1 and CD2AP depleted cells, WASH was greatly condensed in the perinuclear region, presenting less vesicular puncta in the cytoplasm as compared to control knockdown cells. This phenotype was particularly observed in CD2AP-depleted N2a cells. The overall WASH levels, examined by immunofluorescence, were slightly increased upon Bin1 knockdown and decreased in CD2AP knockdown cells, consistent with the results obtained by Western blot.

Additionally, we analyzed WASH localization and observed that it colocalized significantly with F-actin puncta, in the perinuclear region of N2a cells (Fig. 4.11). Cells

lacking bin and CD2AP still exhibit some perinuclear association between WASH and actin. However, due to the diffusion of F-actin puncta, we could not see WASH structures associated actin as clearly. Accordingly, we can conclude that Bin1 and CD2AP regulate WASH levels and its perinuclear distribution in N2a cells. WASH promotes actin polymerization through the recruitment and activation of Arp2/3[36]. Thus, the decrease in WASH levels induced by CD2AP knockdown may explain the diffusion of F-actin in the perinuclear region of these cells. WASH has been localized to restricted domains of sorting and recycling endosomes[40,43]. *Derivery et al.* observed that WASH knockdown gave rise to long transferrin-containing tubules pulled out from the endosome, impairing transferrin recycling. We have seen previously that Bin1 knockdown also promotes the formation of BACE1 tubules and impairs BACE1 recycling to the plasma membrane. This suggests a possible role for WASH in tubule scission, supported by the fact that both WASH and Bin1 interact with dynamin. Additional experiments are needed to eliminate experimental variability and draw reliable conclusions about WASH involvement in the mechanism by which Bin1 and CD2AP regulate BACE1 and APP endosomal sorting. We still have to investigate the potential role of WASH in APP endosomal sorting, and dynamin function in endosomal tubule scission.

We aim to investigate as well other actin regulatory proteins that interact with Bin1 or CD2AP. For instance, N-WASP is also found at early endosomes[41] and it interacts with Bin1 (ref). Thus, we will knockdown N-WASP and expect to recapitulate the effect of Bin1 depletion on BACE1 recycling. If indeed loss of N-WASP impairs BACE1 trafficking, we will then perform co-immunoprecipitation assays to unravel if N-WASP interacts with APP and/or BACE1. If so, a Bin1 mutant that does not interact with N-WASP will be used, in Bin1-depleted cells, to confirm that its interaction with N-WASP is required for its effect on BACE1 trafficking. To determine if CD2AP regulates the trafficking of APP directly or through interaction with cortactin, we will delete CD2AP SH3 domains (described to mediate its capping activity[89] and analyze the impact on APP degradation and Aβ production. Alternatively, we can knockdown cortactin and see if it recapitulates the effect of CD2AP depletion. Using a similar approach as for Bin1, we will express a CD2AP mutant that does not interact with cortactin, in CD2AP knockdown cells, to confirm that CD2AP interaction with cortactin is required for its effect on APP trafficking.

We have now evidence that Bin1 and CD2AP regulate actin dynamics associated with early endosomes, likely disturbing actin structural organization. Therefore we chemically disrupted the actin cytoskeleton in N2a cells, using latrunculin A (LatA), and analyzed if it recapitulated the impact of Bin1 and CD2AP loss of function in the perinuclear pool of F-actin and in Aβ42 levels (Fig. 4.12). LatA reduced F-actin and the fraction of F-actin in the perinuclear region of N2a cells. Importantly, cells treated with LatA exhibited an increase in Aβ42 levels. These results suggest that the actin cytoskeleton may be important for the

mechanisms involved in Aβ production. In the future, we will study if APP and BACE1 trafficking depends on endosomal actin, treating cells with LatA or other drugs that depolymerize actin (cytochalasin D), or that stabilize actin filaments (jasplakinolide). To more specifically interfere with the actin pool associated with endosomes we will use inhibitors of the Arp2/3 complex or siRNA against the Arp2/3 complex, since it is the main actin polymerizing machinery in endosomes.

Previous studies describe alterations in the actin cytoskeleton during the neurodegenerative process induced by Aβ[49]. One of the most common defects in AD is the loss of synapses, which correlates with cognitive defects and that ultimately leads to neuronal death[50]. Synaptic strength is greatly influenced by dendritic spines, where the actin cytoskeleton is crucial to anchor neurotransmitter receptors, and to contribute to synaptic plasticity through spine remodeling[50,51]. PSD-95 is present at post-synaptic sites where it recruits glutamate receptor subunits, ensuring the correct functioning of glutamatergic synapses[22].

Since Bin1 and CD2AP play an important role in regulating actin dynamics, we are interested in investigating their function beyond endosomal actin remodeling. As a preliminary result, we examined the levels of PSD-95 in PN knockdown for Bin1 and CD2AP (Fig. 4.13). While Bin1 loss of function had no significant impact in PSD-95 levels, CD2AP depletion caused a decrease in PSD-95. Previous studies have reported decreased levels of PSD-95 and cortactin in hippocampal neurons of AD transgenic mice[22,52]. Additionally, hippocampal regions with high levels of Aβ displayed a decrease in F-actin at post-synaptic regions[52]. CD2AP interacts with F-actin and with cortactin, and we have seen that CD2AP knockdown induces a decrease in neuronal actin levels (Fig. 4.4F). Thus it is possible that CD2AP depletion impairs the recruitment of F-actin and cortactin, causing a decrease in PSD-95 levels and disrupting the structure of the synapse. We will further explore this issue by analyzing VGLUT levels, a marker of glutamatergic pre-synaptic terminals, and by characterizing PSD-95 and VGLUT distribution in Bin1 and CD2AP knockdown neurons. Additionally, we will examine the size of dendritic spines in PN knockdown for Bin1 and CD2AP, since it is reported that AD mouse models exhibit larger spines[50].

In conclusion, we hypothesize that actin-dependent shaping of the endosomal membrane is the mechanism whereby Bin1 and CD2AP control the endosomal sorting of BACE1 and APP, hence regulating Aβ generation (Fig. 5.1).

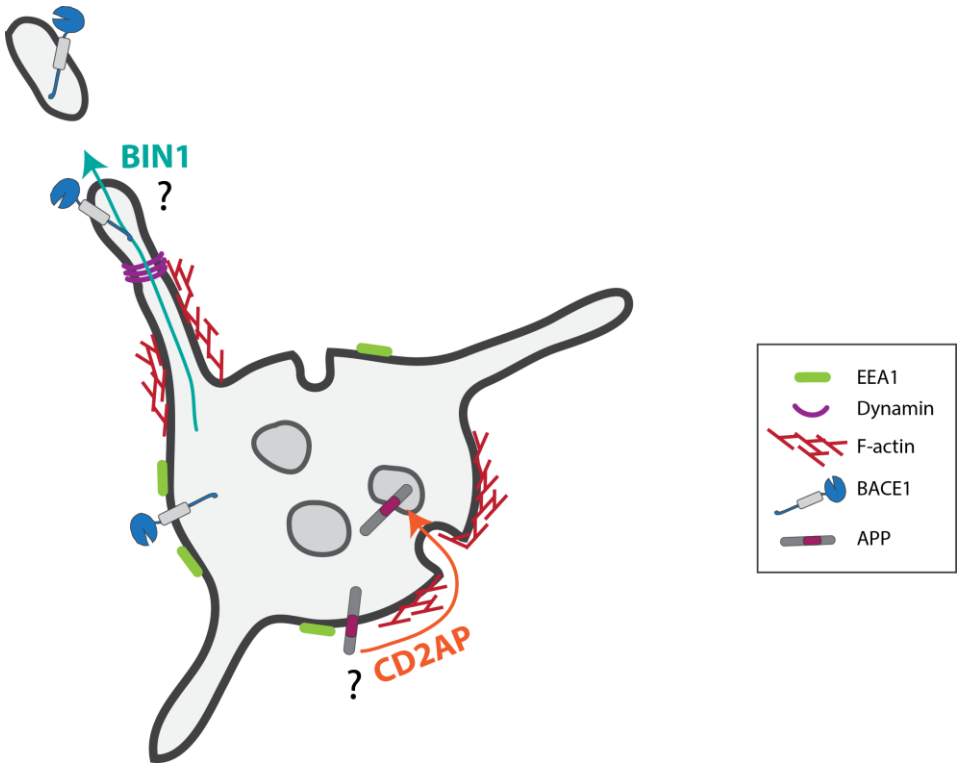

Figure 5.1 Bin1 and CD2AP regulate BACE1 and APP endocytic trafficking via an actin-mediated mechanism. Bin1 may regulate actin dynamics at EEA1-positive early endosomes, promoting recycling tubule formation and/or scission (through interaction with dynamin), thus controlling BACE1 recycling to the plama membrane. CD2AP may have a role in regulating actin dynamics associated with endosomal membrane invagination and MVB formation, hence controlling APP intraluminal sorting and consequent degradation.

Chapter 6

References

1. Blennow, K., de Leon, M. J. & Zetterberg, H. Alzheimer's disease. *Lancet* **368,** 387–403 (2006).

2. Cipriani, G., Dolciotti, C., Picchi, L. & Bonuccelli, U. Alzheimer and his disease: a brief history. *Neurol. Sci.* **32,** 275–9 (2011).

3. World Health Organization. Dementia. *Fact sheet N°362* (2012). at <http://www.who.int/mediacentre/factsheets/fs362/en/>

4. Peric, A. & Annaert, W. Early etiology of Alzheimer's disease: tipping the balance toward autophagy or endosomal dysfunction? *Acta Neuropathol.* (2015).

5. Reitz, C. & Mayeux, R. Alzheimer disease: epidemiology, diagnostic criteria, risk factors and biomarkers. *Biochem. Pharmacol.* **88,** 640–51 (2014).

6. Mucke, L. Neuroscience: Alzheimer's disease. *Nature* **461,** 895–7 (2009).

7. LaFerla, F. M., Green, K. N. & Oddo, S. Intracellular amyloid-beta in Alzheimer's disease. *Nat. Rev. Neurosci.* **8,** 499–509 (2007).

8. Lambert, J. C. *et al.* Meta-analysis of 74,046 individuals identifies 11 new susceptibility loci for Alzheimer's disease. *Nat. Genet.* **45,** 1452–8 (2013).

9. Brunholz, S. *et al.* Axonal transport of APP and the spatial regulation of APP cleavage and function in neuronal cells. *Exp. Brain Res.* **217,** 353–364 (2011).

10. Rajendran, L. & Annaert, W. Membrane trafficking pathways in Alzheimer's disease. *Traffic* **13,** 759–70 (2012).

11. Carey, R. M., Balcz, B. A., Lopez-Coviella, I. & Slack, B. E. Inhibition of dynamin-dependent endocytosis increases shedding of the amyloid precursor protein ectodomain and reduces generation of amyloid beta protein. *BMC Cell Biol.* **6,** 30 (2005).

12. Das, U. *et al.* Activity-induced convergence of APP and BACE-1 in acidic microdomains via an endocytosis-dependent pathway. *Neuron* **79,** 447–60 (2013).

13. Takahashi, R. H. *et al.* Intraneuronal Alzheimer abeta42 accumulates in multivesicular bodies and is associated with synaptic pathology. *Am. J. Pathol.* **161,** 1869–1879 (2002).

14. Almeida, C. G., Takahashi, R. H. & Gouras, G. K. Beta-amyloid accumulation impairs multivesicular body sorting by inhibiting the ubiquitin-proteasome system. *J. Neurosci.* **26,** 4277–88 (2006).

15. Morel, E. *et al.* Phosphatidylinositol-3-phosphate regulates sorting and processing of amyloid precursor protein through the endosomal system. *Nat. Commun.* **4,** 2250 (2013).

16. Karran, E., Mercken, M. & De Strooper, B. The amyloid cascade hypothesis for Alzheimer's disease: an appraisal for the development of therapeutics. *Nat. Rev. Drug Discov.* **10,** 698–712 (2011).

17. Haass, C. & Selkoe, D. J. Soluble protein oligomers in neurodegeneration: lessons from the Alzheimer's amyloid beta-peptide. *Nat. Rev. Mol. Cell Biol.* **8,** 101–12 (2007).

18. Walsh, D. M. *et al.* Naturally secreted oligomers of amyloid beta protein potently inhibit hippocampal long-term potentiation in vivo. *Nature* **416,** 535–9 (2002).

19. Gómez-Isla, T. *et al.* Neuronal loss correlates with but exceeds neurofibrillary tangles in Alzheimer's disease. *Ann. Neurol.* **41,** 17–24 (1997).

20. Gouras, G. K. *et al.* Intraneuronal Ab42 Accumulation in Human Brain. *Am. J. Pathol.* **156,** 15–20 (2000).

21. Cataldo, A. M. *et al.* Abeta localization in abnormal endosomes: association with earliest Abeta elevations in AD and Down syndrome. *Neurobiol. Aging* **25,** 1263–72 (2004).

22. Almeida, C. G. *et al.* Beta-amyloid accumulation in APP mutant neurons reduces PSD-95 and GluR1 in synapses. *Neurobiol. Dis.* **20,** 187–98 (2005).

23. Lasiecka, Z. M. & Winckler, B. Mechanisms of polarized membrane trafficking in neurons - Focusing in on endosomes. *Mol. Cell. Neurosci.* **48,** 278–287 (2011).

24. Tang, B. L. Neuronal protein trafficking associated with Alzheimer disease: from APP and BACE1 to glutamate receptors. *Cell Adh. Migr.* **3,** 118–28 (2009).

25. Buggia-Prévot, V. *et al.* A function for EHD family proteins in unidirectional retrograde dendritic transport of BACE1 and Alzheimer's disease Aβ production. *Cell Rep.* **5,** 1552–63 (2013).

26. Chia, P. Z. C. *et al.* Intracellular itinerary of internalised β-secretase, BACE1, and its potential impact on β-amyloid peptide biogenesis. *Traffic* **14,** 997–1013 (2013).

27. Sannerud, R. *et al.* ADP ribosylation factor 6 (ARF6) controls amyloid precursor protein (APP) processing by mediating the endosomal sorting of BACE1. *Proc. Natl. Acad. Sci. U. S. A.* **108,** E559–E568 (2011).

28. Karch, C. M. & Goate, A. M. Alzheimer's Disease Risk Genes and Mechanisms of Disease Pathogenesis. *Biol. Psychiatry* (2014). doi:10.1016/j.biopsych.2014.05.006

29. Xiao, Q. *et al.* Role of phosphatidylinositol clathrin assembly lymphoid-myeloid leukemia (PICALM) in intracellular amyloid precursor protein (APP) processing and amyloid plaque pathogenesis. *J. Biol. Chem.* **287,** 21279–89 (2012).

30. Willnow, T. E. & Andersen, O. M. Sorting receptor SORLA--a trafficking path to avoid Alzheimer disease. *J. Cell Sci.* **126,** 2751–60 (2013).

31. Offe, K. *et al.* The lipoprotein receptor LR11 regulates amyloid beta production and amyloid precursor protein traffic in endosomal compartments. *J. Neurosci.* **26,** 1596–603 (2006).

32. Cirrito, J. R. *et al.* Endocytosis is required for synaptic activity-dependent release of amyloid-beta in vivo. *Neuron* **58,** 42–51 (2008).

33. Tampellini, D. *et al.* Synaptic activity reduces intraneuronal Abeta, promotes APP transport to synapses, and protects against Abeta-related synaptic alterations. *J. Neurosci.* **29,** 9704–13 (2009).

34. Lodish, H. *et al.* in *Molecular Cell Biology* 779–789 (Freeman, W. H. & Company, 2003).

35. Alberts, B. *et al.* in *Essential Cell Biology* 590 (Garland Science, Taylor & Francis Group, 2009).

36. Anitei, M. & Hoflack, B. Bridging membrane and cytoskeleton dynamics in the secretory and endocytic pathways. *Nat. Cell Biol.* **14,** 11–9 (2012).

37. Granger, E., McNee, G., Allan, V. & Woodman, P. The role of the cytoskeleton and molecular motors in endosomal dynamics. *Semin. Cell Dev. Biol.* **31,** 20–29 (2014).

38. Lanzetti, L. Actin in membrane trafficking. *Curr. Opin. Cell Biol.* **19,** 453–458 (2007).

39. Boulant, S., Kural, C., Zeeh, J.-C., Ubelmann, F. & Kirchhausen, T. Actin dynamics counteract membrane tension during clathrin-mediated endocytosis. *Nat. Cell Biol.* **13,** 1124–31 (2011).

40. Derivery, E. *et al.* The Arp2/3 activator WASH controls the fission of endosomes through a large multiprotein complex. *Dev. Cell* **17,** 712–23 (2009).

41. Taunton, J. *et al.* Actin-dependent Propulsion of Endosomes and Lysosomes by Recruitment of N-WASP 7. **148,** 519–530 (2000).

42. Zech, T., Calaminus, S. D. J. & Machesky, L. M. Actin on trafficking: could actin guide directed receptor transport? *Cell Adh. Migr.* **6,** 476–81 (2012).

43. Puthenveedu, M. a *et al.* Sequence-dependent sorting of recycling proteins by actin-stabilized endosomal microdomains. *Cell* **143,** 761–73 (2010).

44. Derivery, E., Helfer, E., Henriot, V. & Gautreau, A. Actin polymerization controls the organization of WASH domains at the surface of endosomes. *PLoS One* **7,** e39774 (2012).

45. Morel, E., Parton, R. G. & Gruenberg, J. Annexin A2-dependent polymerization of actin mediates endosome biogenesis. *Dev. Cell* **16,** 445–57 (2009).

46. Kirkbride, K. C. *et al.* Regulation of late endosomal/lysosomal maturation and trafficking by cortactin affects Golgi morphology. *Cytoskeleton* **69,** 625–643 (2012).

47. Salas-Cortes, L. *et al.* Myosin Ib modulates the morphology and the protein transport within multi-vesicular sorting endosomes. *J. Cell Sci.* **118,** 4823–32 (2005).

48. Almeida, C. G. *et al.* Myosin 1b promotes the formation of post-Golgi carriers by regulating actin assembly and membrane remodelling at the trans-Golgi network. *Nat. Cell Biol.* **13,** 779–89 (2011).

49. Bamburg, J. R. & Bloom, G. S. Cytoskeletal pathologies of Alzheimer disease. *Cell Motil. Cytoskeleton* **66,** 635–49 (2009).

50. Penzes, P. & Vanleeuwen, J.-E. Impaired regulation of synaptic actin cytoskeleton in Alzheimer's disease. *Brain Res. Rev.* **67,** 184–92 (2011).

51. Knobloch, M. & Mansuy, I. M. Dendritic spine loss and synaptic alterations in Alzheimer's disease. *Mol. Neurobiol.* **37,** 73–82 (2008).

52. Mota, S. I. *et al.* Impaired Src signaling and post-synaptic actin polymerization in Alzheimer's disease mice hippocampus — Linking NMDA receptors and the reelin pathway. *Exp. Neurol.* **261,** 698–709 (2014).

53. Mendoza-Naranjo, A., Gonzalez-Billault, C. & Maccioni, R. B. Abeta1-42 stimulates actin polymerization in hippocampal neurons through Rac1 and Cdc42 Rho GTPases. *J. Cell Sci.* **120,** 279–288 (2007).

54. Maloney, M. T., Minamide, L. S., Kinley, A. W., Boyle, J. a & Bamburg, J. R. Beta-secretase-cleaved amyloid precursor protein accumulates at actin inclusions induced in neurons by stress or amyloid beta: a feedforward mechanism for Alzheimer's disease. *J. Neurosci.* **25,** 11313–11321 (2005).

55. Minamide, L. S., Striegl, A. M., Boyle, J. A., Meberg, P. J. & Bamburg, J. R. Neurodegenerative stimuli induce persistent ADF/cofilin-actin rods that disrupt distal neurite function. *Nat. Cell Biol.* **2,** 628–636 (2000).

56. Hiruma, H., Katakura, T., Takahashi, S., Ichikawa, T. & Kawakami, T. Glutamate and amyloid beta-protein rapidly inhibit fast axonal transport in cultured rat hippocampal neurons by different mechanisms. *J. Neurosci.* **23,** 8967–8977 (2003).

57. Tan, M.-S., Yu, J.-T. & Tan, L. Bridging integrator 1 (BIN1): form, function, and Alzheimer's disease. *Trends Mol. Med.* **19,** 594–603 (2013).

58. Seshadri, S. *et al.* Genome-wide analysis of genetic loci associated with Alzheimer disease. *JAMA* **303,** 1832–40 (2010).

59. Hollingworth, P. *et al.* Common variants at ABCA7, MS4A6A/MS4A4E, EPHA1, CD33 and CD2AP are associated with Alzheimer's disease. *Nat. Genet.* **43,** 429–35 (2011).

60. Zhang, B. & Zelhof, A. C. Amphiphysins: Raising the BAR for Synaptic Vesicle Recycling and Membrane Dynamics. *Traffic* **3,** 452–460 (2002).

61. Ren, G., Vajjhala, P., Lee, J. S., Winsor, B. & Munn, A. L. The BAR domain proteins: molding membranes in fission, fusion, and phagy. *Microbiol. Mol. Biol. Rev.* **70,** 37–120 (2006).

62. Leprince, C. *et al.* A New Member of the Amphiphysin Family Connecting Endocytosis and Signal Transduction Pathways. *J. Biol. Chem.* **272,** 15101–15105 (1997).

63. Wigge, P. *et al.* Amphiphysin heterodimers: potential role in clathrin-mediated endocytosis. *Mol. Biol. Cell* **8,** 2003–15 (1997).

64. Wigge, P. & McMahon, H. T. The amphiphysin family of proteins and their role in endocytosis at the synapse. *Trends Neurosci.* **21,** 339–344 (1998).

65. Takei, K., Slepnev, V. I., Haucke, V. & De Camilli, P. Functional partnership between amphiphysin and dynamin in clathrin-mediated endocytosis. *Nat. Cell Biol.* **1,** 33–9 (1999).

66. Ren, G., Vajjhala, P., Lee, J. S., Winsor, B. & Munn, A. L. The BAR Domain Proteins : Molding Membranes in Fission , Fusion , and Phagy The BAR Domain Proteins : Molding Membranes in Fission , Fusion , and Phagy. **70,** 37–120 (2006).

67. Leprince, C. *et al.* Sorting nexin 4 and amphiphysin 2, a new partnership between endocytosis and intracellular trafficking. *J. Cell Sci.* **116,** 1937–48 (2003).

68. Farsad, K. *et al.* Generation of high curvature membranes mediated by direct endophilin bilayer interactions. *J. Cell Biol.* **155,** 193–200 (2001).

69. Mundigl, O. *et al.* Amphiphysin I antisense oligonucleotides inhibit neurite outgrowth in cultured hippocampal neurons. *J. Neurosci.* **18,** 93–103 (1998).

70. Balguerie, A., Sivadon, P., Bonneu, M. & Aigle, M. Rvs167p , the budding yeast homolog of amphiphysin , colocalizes with actin patches. **2537,** 2529–2537 (1999).

71. Sivadon, P., Bauer, F., Aigle, M. & Crouzet, M. Actin cytoskeleton and budding pattern are altered in the yeast rvs161 mutant: the Rvs161 protein shares common domains with the brain protein amphiphysin. *MGG Mol. Gen. Genet.* **246,** 485–495 (1995).

72. Falcone, S. *et al.* N-WASP is required for Amphiphysin-2/BIN1-dependent nuclear positioning and triad organization in skeletal muscle and is involved in the pathophysiology of centronuclear myopathy. *EMBO Mol. Med.* **6,** 1455–75 (2014).

73. Hong, T. *et al.* Cardiac BIN1 folds T-tubule membrane, controlling ion flux and limiting arrhythmia. *Nat. Med.* **20,** 624–32 (2014).

74. Prokic, I., Cowling, B. S. & Laporte, J. Amphiphysin 2 (BIN1) in physiology and diseases. *J. Mol. Med.* **2,** 1–11 (2014).

75. Chapuis, J. *et al.* Increased expression of BIN1 mediates Alzheimer genetic risk by modulating tau pathology. *Mol. Psychiatry* **18,** 1225–34 (2013).

76. Turner, P. R., O'Connor, K., Tate, W. P. & Abraham, W. C. *Roles of amyloid precursor protein and its fragments in regulating neural activity, plasticity and memory. Progress in Neurobiology* **70,** (2003).

77. Kim, J. M. *et al.* CD2-Associated Protein Haploinsufficiency Is Linked to Glomerular Disease Susceptibility. **300,** 1298–1300 (2003).

78. Wolf, G. & Stahl, R. A. K. CD2-associated protein and glomerular disease. *Lancet* **362,** 1746–8 (2003).

79. Bruck, S. *et al.* Identification of a novel inhibitory actin-capping protein binding motif in CD2-associated protein. *J. Biol. Chem.* **281,** 19196–203 (2006).

80. Cormont, M. *et al.* CD2AP/CMS regulates endosome morphology and traffic to the degradative pathway through its interaction with Rab4 and c-Cbl. *Traffic* **4,** 97–112 (2003).

81. Lynch, D. K. *et al.* A Cortactin-CD2-associated protein (CD2AP) complex provides a novel link between epidermal growth factor receptor endocytosis and the actin cytoskeleton. *J. Biol. Chem.* **278,** 21805–13 (2003).

82. Lehtonen, S., Zhao, F. & Lehtonen, E. CD2-associated protein directly interacts with the actin cytoskeleton. *Am. J. Physiol. Renal Physiol.* **283,** F734–43 (2002).

83. Dustin, M. L. *et al.* A novel adaptor protein orchestrates receptor patterning and cytoskeletal polarity in T-cell contacts. *Cell* **94,** 667–677 (1998).

84. Ha, T.-S., Hong, E.-J. & Han, G.-D. Diabetic conditions downregulate the expression of CD2AP in podocytes via PI3-K/Akt signalling. *Diabetes. Metab. Res. Rev.* **31,** 50–60 (2015).

85. Kobayashi, S., Sawano, A., Nojima, Y., Shibuya, M. & Maru, Y. The c-Cbl/CD2AP complex regulates VEGF-induced endocytosis and degradation of Flt-1 (VEGFR-1). *FASEB J.* **18,** 929–931 (2004).

86. Gauthier, N. C. *et al.* Early endosomes associated with dynamic F-actin structures are required for late trafficking of H. pylori VacA toxin. *J. Cell Biol.* **177,** 343–54 (2007).

87. Welsch, T. *et al.* Association of CD2AP with dynamic actin on vesicles in podocytes. *Am. J. Physiol. Renal Physiol.* **289,** F1134–43 (2005).

88. Zhao, J. *et al.* CD2AP links cortactin and capping protein at the cell periphery to facilitate formation of lamellipodia. *Mol. Cell. Biol.* **33,** 38–47 (2013).

89. Tang, V. W. & Brieher, W. M. FSGS3/CD2AP is a barbed-end capping protein that stabilizes actin and strengthens adherens junctions. *J. Cell Biol.* **203,** 815–33 (2013).

90. Shulman, J. M. *et al.* Genetic susceptibility for Alzheimer disease neuritic plaque pathology. *JAMA Neurol.* **70,** 1150–7 (2013).

91. Karch, C. M. & Goate, A. M. Alzheimer's Disease Risk Genes and Mechanisms of Disease Pathogenesis. *Biol. Psychiatry* **77,** 43–51 (2014).

92. Shulman, J. M. *et al.* Functional screening in Drosophila identifies Alzheimer's disease susceptibility genes and implicates tau-mediated mechanisms. *Hum. Mol. Genet.* **23,** 870–877 (2014).

93. Rosenthal, S. L. & Kamboh, M. I. Late-Onset Alzheimer's Disease Genes and the Potentially Implicated Pathways. *Curr. Genet. Med. Rep.* **2,** 85–101 (2014).

94. Tremblay, R. G. *et al.* Differentiation of mouse Neuro 2A cells into dopamine neurons. *J. Neurosci. Methods* **186,** 60–7 (2010).

95. Pravettoni, E. *et al.* Different localizations and functions of L-type and N-type calcium channels during development of hippocampal neurons. *Dev. Biol.* **227,** 581–94 (2000).

96. Heilemann, M. *et al.* Subdiffraction-resolution fluorescence imaging with conventional fluorescent probes. *Angew. Chem. Int. Ed. Engl.* **47,** 6172–6 (2008).

97. Ovesný, M., Křížek, P., Borkovec, J., Svindrych, Z. & Hagen, G. M. ThunderSTORM: a comprehensive ImageJ plug-in for PALM and STORM data analysis and super-resolution imaging. *Bioinformatics* **30,** 2389–90 (2014).

98. Holler, C. J. *et al.* Bridging Integrator 1 (BIN1) Protein Expression Increases in the Alzheimer's Disease Brain and Correlates with Neurofibrillary Tangle Pathology. *J. Alzheimers. Dis.* **29,** 997–1003 (2014).

99. Falcone, S. *et al.* N-WASP is required for Amphiphysin-2/BIN1-dependent nuclear positioning and triad organization in skeletal muscle and is involved in the pathophysiology of centronuclear myopathy. *EMBO Mol. Med.* **6,** 1455–75 (2014).

100. Pant, S. *et al.* AMPH-1/Amphiphysin/Bin1 functions with RME-1/Ehd1 in endocytic recycling. *Nat. Cell Biol.* **11,** 1399–410 (2009).

101. Cataldo, A. M. *et al.* Endocytic Pathway Abnormalities Precede Amyloid β Deposition in Sporadic Alzheimer's Disease and Down Syndrome. *Am. J. Pathol.* **157,** 277–286 (2000).